GENERAL MOTORS CORPORATION

THE DYNAMICS OF SIMPLE DEEP-SEA BUOY MOORINGS

A Report Submitted to
U.S. NAVY OFFICE OF NAVAL RESEARCH
under
CONTRACT Nonr-4558(00)
PROJECT NR 083-196

GM DEFENSE RESEARCH LABORATORIES
SEA OPERATIONS DEPARTMENT

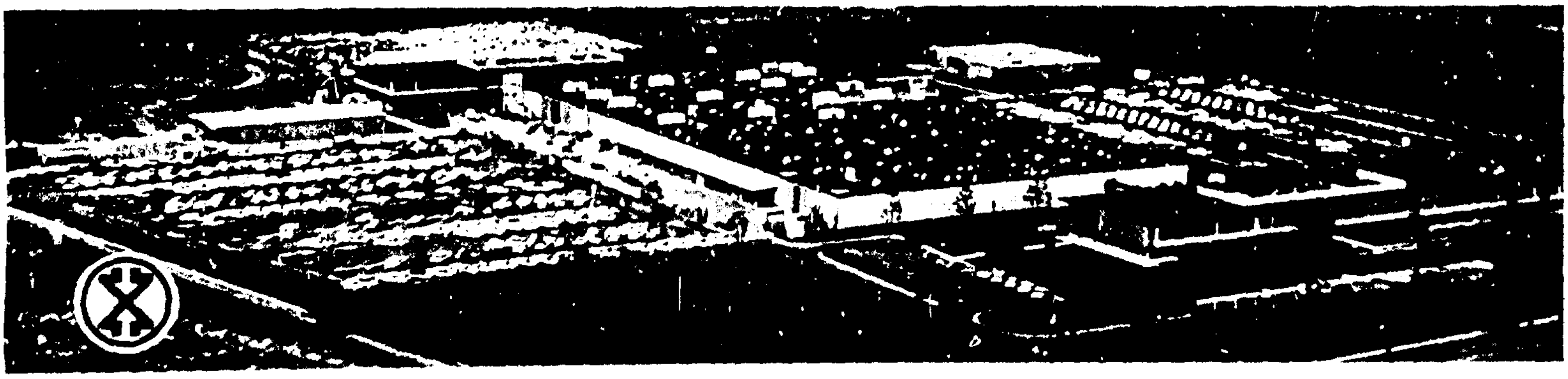

SANTA BARBARA, CALIFORNIA

TR65-79

NOVEMBER 1965

Copy No 49

GENERAL MOTORS CORPORATION

THE DYNAMICS OF SIMPLE DEEP-SEA BUOY MOORINGS

Robert G. Paquette
Bion E. Henderson

A Report Submitted to
U.S. NAVY OFFICE OF NAVAL RESEARCH
under
CONTRACT Nonr-4558(00)
PROJECT NR 083-196

GM DEFENSE RESEARCH LABORATORIES
SANTA BARBARA, CALIFORNIA

SEA OPERATIONS DEPARTMENT

TR65-79

NOVEMBER 1965

ABSTRACT

The dynamics of buoy mooring ropes under conditions typical of the open sea were simulated in an analog computer. Motions sufficient to cause significant errors in current meters were found in the ropes. Dynamic tensions rising to dangerous values were found in short, taut, steel ropes. Lesser tensions were found in nylon ropes. Rope shapes in ocean currents varying with depth also were obtained incidental to the principal study.

CONTENTS

CONTENTS (Continued)

ILLUSTRATIONS

ILLUSTRATIONS (Continued)

TABLES

DEFINITION OF SYMBOLS

A	Effective cross-sectional area of the rope
a_n , b_n , c_n	(See Equation (72))
a^+_{Nn}	Acceleration at Node n normal to Segment s_{n+1}
a^-_{Nn}	Acceleration at Node n normal to Segment s_n
C_D	Normal drag coefficient
d_{CM}	Diameter of current meter
D_B	Horizontal drag force on the buoy
D_n	Water drag normal to the rope on the entire rope segment between Nodes n-1 and n
D'_n	Normal drag on Rope Segment if rope were vertical
$\left[D_n\right]_{TOTAL}$	Total normal drag, including current meters ascribed to Rope Segment s_n
$\left[D'_n\right]_{TOTAL}$	Total normal drag, including current meters ascribed to Rope Segment s_n when the rope is vertical
D^+_{nCM}	Normal drag on lower half of current meter at Node n-1
D^-_{nCM}	Normal drag on upper half of current meter at Node n
$D^{\pm}_{nCM}$	A general expression for either D^+_{nCM} or D^-_{nCM}
$(D^+_{nCM})'$	The equivalent of D^+_{nCM} if the current meter were vertical
D_{Nn}	Water drag concentrated at Node n normal to the mean tangent to the rope at Node n
D_{Tn}	Water drag concentrated at Node n tangential to the mean rope direction at Node n
E	Effective value of Young's Modulus for a rope, units of force/unit area

Q_{xn}	Component in the x-direction of water drag due to current concentrated at Node n
Q'_{xn}	Cyclic portion of Q_{xn}
Q_{yn}	Component in the y-direction of water drag due to current concentrated at Node n
s_n	Length of rope Segment between Nodes n-1 and n
$\bar{s}_n$	Mean value of s_n in the dynamic simulation (same as s_n in the static simulation)
s_{no}	Unstretched reference length of Rope Segment s_n
t	Time
T_n	Tension of the rope immediately above Node n
T'_n	Cyclic portion of T_n
$\bar{T}_n$	Mean value of T_n in the dynamic simulation (same as T_n in the static simulation)
U	Vertical component of rope tension at the anchor
V_c	Water velocity
$V_{c(n-1)}$	Water velocity at Node n-1
$V_c(x)$	Water velocity varying as a function of x
V_{Nn}	Node velocity normal to the mean tangent of the rope at Node n relative to the water
V_{Tn}	Node velocity tangential to the rope at Node n relative to the water
w_n	Rope weight per unit length in water
W_n	Weight forces in water assumed concentrated at Node n
W'_n	Weight in water of an object (current meter) attached to the rope at Node n
x_n	Vertical cartesian coordinate of Node n measured from an origin at the water surface vertically above the anchor

F^{+}_{Nn}	Reaction force at Node n, normal to Segment s_{n+1}, due to entrained water about the half-segment of s_{n+1} nearest Node n
F^{-}_{Nn}	Reaction force at Node n, normal to Segment s_n, due to entrained water about the half-segment of s_n nearest Node n
F^{-}_{xn}	Vertical component of F^{-}_{Nn}
F^{-}_{yn}	Horizontal component of F^{-}_{Nn}
F^{v}_{xn}	$F^{-}_{xn} + F^{+}_{xn}$
F^{v}_{yn}	$F^{-}_{yn} + F^{+}_{yn}$
$\sum F^{x}_{n}$	Sum of all vertical external forces concentrated at Node n except hydrodynamic reaction forces
$\sum F^{y}_{n}$	Sum of all horizontal external forces concentrated at Node n except hydrodynamic reaction forces
h_n	Preassigned depth of Node n
Δh_n	$X_{n-1} - X_n$
H	Horizontal component of rope tension at the anchor
I_n, J_n, K_n I'_n, J'_n, K'_n	Matrix quantities, see Equations (33), (34), (37)
k_{Nn}	See Equation (53)
K_R	An arbitrary rate damping constant multiplying the first order term in the typical differential equation for the static case
ℓ	Length of current meter
m_n	Mass ascribed to Node n
$m^{v}_{n+1/2}$	Virtual mass of water entrained by upper half of Segment s_{n+1}
$m^{v}_{n-1/2}$	Virtual mass of water entrained by lower half of Segment s_n
n	Number of Node counting downward from zero at the buoy to 10 (or 4) at the anchor

x'_n	Cyclic portion of x_n
$\bar{x}_n$	Mean value of x_n in the dynamic simulation (same as x_n in the static simulation)
y_n	Horizontal cartesian coordinate of Node n measured from an origin at the water surface vertically above the anchor
y'_n	Cyclic portion of y_n
$\bar{y}_n$	Mean value of y_n in the dynamic simulation (same as y_n in the static simulation)
α_n	Drag normal to the rope on the upper half of Segment s_n, divided by D_n
γ	Ratio of tangential drag coefficient to normal drag coefficient for a rope
θ_n	The angle measured clockwise from the vertical to the section of rope above Node n
θ'_n	cyclic portion of θ_n
$\bar{\theta}_n$	Mean value of θ_n in the dynamic simulation (same as θ_n in the static simulation)
μ	Dynamic spring constant of nylon rope in units of force/unit extension
ρ	Water density
Ψ_n	Mean of $\bar{\theta}_n$ and $\bar{\theta}_{n+1}$
$\simeq$	Is approximately equal to
$\triangleq$	Is defined as

I. INTRODUCTION

OBJECT

This work had as its object the study of the dynamics of firmly anchored steel and nylon mooring lines attached to a buoy on a sea surface disturbed by simple sinusoidal waves. Interest was especially directed to:

- The motions of current meters attached to the mooring line and the resultant spurious current indications
- The dynamic component of mooring line tension

METHOD

First an analog computer was used to determine rope shapes without wave excitation in typical current profiles. After this the computer was rewired to simulate the dynamic situation as perturbations of typical static cases.

PRIOR WORK

Wilson[(1, 2)*] has recently studied mooring line shapes at some length in both uniform and non-uniform currents. His calculations for non-uniform currents were for 12,000 feet of depth and currents typical of the Gulf Stream. Some of Wilson's methods have been used here, but the necessity of including other depths and weaker currents typical of the greater parts of the ocean prevented any direct use of his results except for checking ours.

Dynamic studies of mooring lines have been made by Whicker,[(3)] by Walton and Polachek,[(4, 5)] and by Polachek, et al.[(6)] Whicker treats the longitudinal oscillations of a steel rope as though it were a straight-stretched, undamped elastic cord, excited longitudinally by sinusoidal displacements; he demonstrates the

* Raised numbers in parentheses indicate references at the end of this report.

probable existence of standing-wave phenomena in long steel ropes. Walton and Polachek made a mathematical analysis of the dynamics of a rope with curvature, water drag, and water inertia, in which they permit components of motion normal to the rope; but they consider the rope inextensible and present results for only a few cases. (Assumption of an inextensible rope is obviously untenable for synthetic fiber ropes and must yield tensions which are substantially too high in long steel ropes at low frequencies.) Polacheck, et al., extended the computational method to provide for elasticity and reported the result of one practical computation. We have made use of some of these authors' methods also.

The authors of References 1, 2, 4, 5, and 6 all used digital computers. (Whicker, who makes no mention of a computer, may have used a desk calculator.) The digital solution of Polachek, et al., was exceedingly time consuming, and Walton[7] estimates 20 hours per case on the IBM 7090 – hence, the choice of an analog computer for the present study.

THE PRESENT STUDY

This study treats curved elastic mooring lines in which all the fixed and oscillatory forces and motions are in the same vertical plane and water and wind velocities have the same direction. Transverse as well as longitudinal motions are permitted, and account is taken of transverse and longitudinal rope drag and of the virtual mass of entrained water. The mooring lines were approximated as a number of unequal, straight spring segments with all the associated masses and forces concentrated at the junctions of the segments (nodes). Mass, weight, and drag, approximating a Richardson current meter, were inserted at each node, except at the buoy and anchor. The buoy was assumed to have no dynamics of its own; the oscillatory excitations were simple elliptical displacements of the top of the mooring line, with the vertical axis of the ellipse four times as great as the horizontal.

The study of line-shape and tension under static conditions was done using a 10-segment approximation. About half of the dynamic study was done with 10 segments also. The complexity of the problem, however, nearly saturated the capabilities of the analog computer, so that component breakdowns were difficult to find and the patch panel was so crowded with wires that scaling changes could be made only with difficulty. Since it appeared economically unjustifiable to proceed, the computer was rewired for a four-segment simulation and the study completed.

VARIABLES STUDIED

One of the limiting factors in this study was the multiplicity of cases. Desirably, the problem should have been solved for several of each of the following:

- rope diameter
- rope type
- current velocity structure
- wind drag
- water depth
- scope (or tension) of mooring line
- wave height
- wave frequency
- current meter distribution

In addition, x and y displacements at, perhaps, 9 points and tensions at from 2 to 11 were required. If each tabulated variable had a multiplicity of, perhaps, 3, there would be 3^9, or 19,683 cases, each requiring roughly 10 minutes of computer time. Evidently a drastic limitation in multiplicity was necessary.

The static solution for rope shape and tensions, therefore, was carried out for 63 of the possible 144 cases derived from the following variables:

- 4 current-profile/surface-drag combinations
- 3 rope materials: steel, nylon, glass
- 2 rope diameters: 1/2 inch and 2 inches
- 3 depths: 1,800, 6,000, and 18,000 feet
- 1–4 rope tensions at the buoy, distributed between breaking strength and a tension at which the rope approached bottom within 10 degrees of horizontal (rescaling about the amplifier representing the length of the bottom rope segment would have been necessary to approach more closely)
- 1 current meter distribution: one meter at each node

The dynamic solution was carried out for:

1 rope diameter: 1/2 inch

2 rope materials: steel and nylon

2 rope shapes at each depth: one resulting from high tension and one from low tension

3 depths: 1,800, 6,000, and 18,000 feet

5 wave periods: 2, 4, 8, 16, and 32 seconds

3 wave heights: 5, 15, and 50 feet (with an occasional substitution of 30 or 40 feet for 50 feet when amplifier limiting demanded)

Ten wave-period/wave-height combinations were used to give a total of 120 separate cases. Displacements of each node were recorded on an x-y recorder; tensions at the top, middle, and bottom of the mooring rope were recorded on a strip-chart recorder. The results were analyzed and are presented as tables and graphs in Section VI. Details of the study are given in the following sections.

II. METHODS

INTRODUCTION

This section treats the general aspects of the computer solutions and details of the philosophy used in setting up the problem and choosing the ranges of variables. Mathematical details are reserved for the appendix.

GENERAL DESCRIPTION OF METHOD

In either a digital- or analog-computer simulation of a mooring rope, the rope is represented as a series of straight segments joined at points called nodes. All forces and masses associated with the rope are assumed to be concentrated at the nodes; sections of rope between nodes are considered to be straight springs without mass. Figure 1 shows this simulation graphically. Any desired degree of accuracy in simulation may be had by increasing the number of segments, but at the cost of increasing the complexity of the problem. For a complete description of its behavior, each node requires two second-order partial differential equations. The resultant equations for the entire rope form a simultaneous set upon which is imposed the requirement that the tension at each end of a between-node segment be the same.

The computer used to solve these equations was the Pace Model 231-R fitted with 150 amplifiers, 40 integrators, 10 servo multipliers, and 4 servo resolvers, plus diode squarers and other analog components. In addition, at one stage a small special computer was brought into play.

As explained earlier, the problem had to be done in two stages, the first a determination of static rope shapes and the second a dynamic simulation calculated as a perturbation of the static condition. This was necessary because the dynamic range of the analog computer was not great enough to show accurately a small perturbation on a background of an already large displacement. *

* Whereas a digital computer conceptually has sufficient dynamic range, the same requirement is found in practice since the static case must be pre-calculated to serve as the initial condition for the dynamic solution.

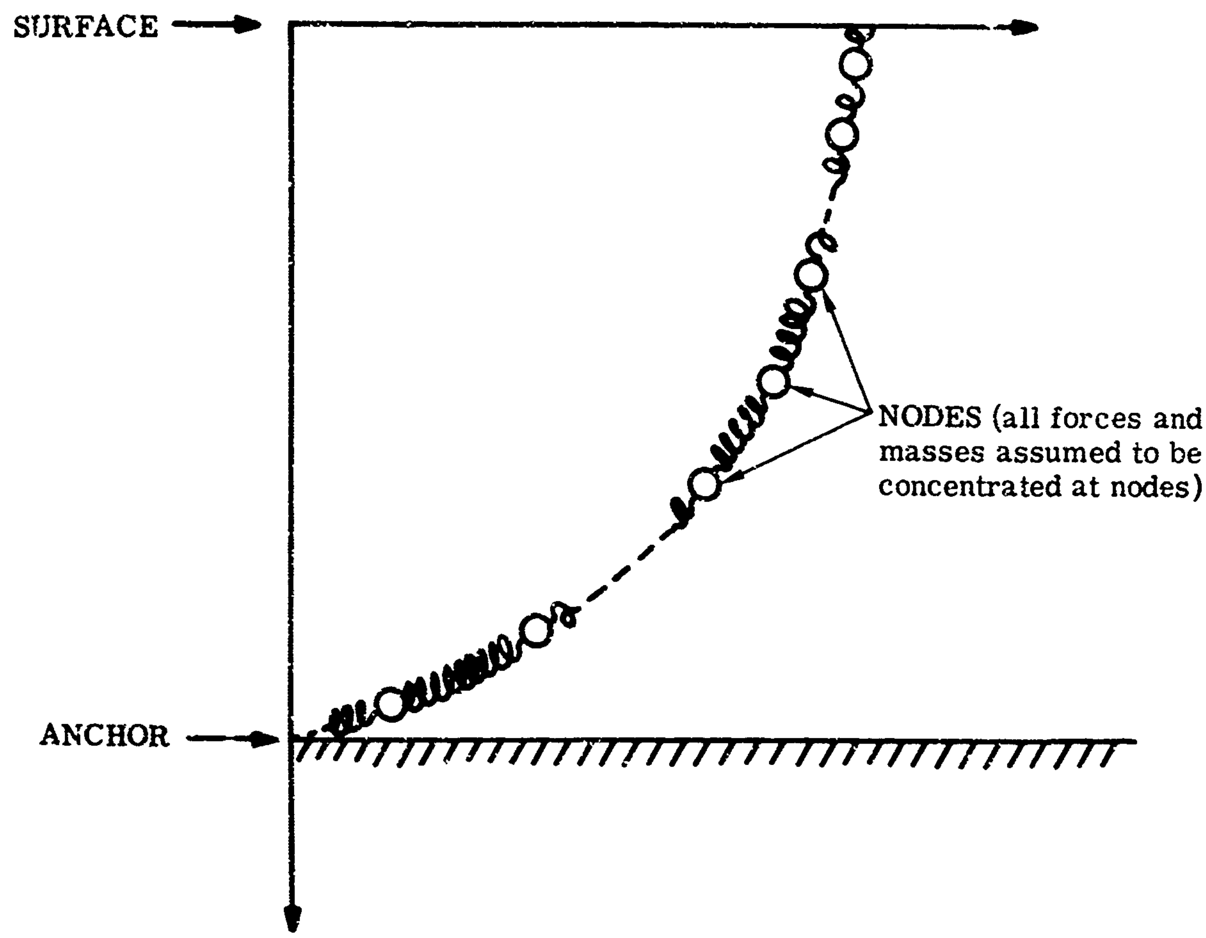

Figure 1 Lumped-Parameter Simulation of Mooring Line

In the static simulation, the nodes were all constrained to move at constant depth, and the rope was permitted to lengthen between nodes, as necessary. Elasticity did not enter into this case. Reduction in rope diameter by stretching was assumed to be negligible. Water drag was taken as proportional to the square of the component of velocity perpendicular to the rope.

DRAG COEFFICIENT

The drag coefficient was taken to be 1.8 (instead of the 1.4 used by Wilson in Reference 1) to allow for the effects of rope flutter caused by vortex shedding. This choice requires explanation.

All of the work upon which the frequently quoted values of drag coefficient are based was done by towing lengths of rope so short as to be incapable of flutter. The flutter which occurs in long ropes absorbs energy and increases the drag. The meager quantitative information available on the subject follows.

Johnson and Lampietti[(8)] report the calculations of Daniel Savitsky, who calculated theoretically for 11,500 feet of 3/16-inch (diameter) wire rope at 0.3 knot a drag coefficient of 1.9. Rather, et al.,[(9)] report an experiment in which 0.465-inch well-logging cable was towed at 4.0 knots, and the cable shape corresponded to a drag coefficient of 1.9. As Rather, et al., suggest, some decrease in drag coefficient may occur at lower velocities, but since Savitsky's estimate at low velocity is also 1.9, it seems safer to retain a high value throughout the velocity range, compromising on a value of 1.8.

The tangential drag coefficient for the rope was taken to be 0.02 of the normal drag coefficient.

WATER AND WIND VELOCITIES

Two basic water-velocity profiles were used, one slightly modified from Wilson's Design Current B (in Ref. 2), the other a weak current of 0.5 knot lumped, for convenience, in the upper 500 feet (Fig. 2). Wilson's represents a strong current, such as the Gulf Stream; the other approximates a weak current, such as the

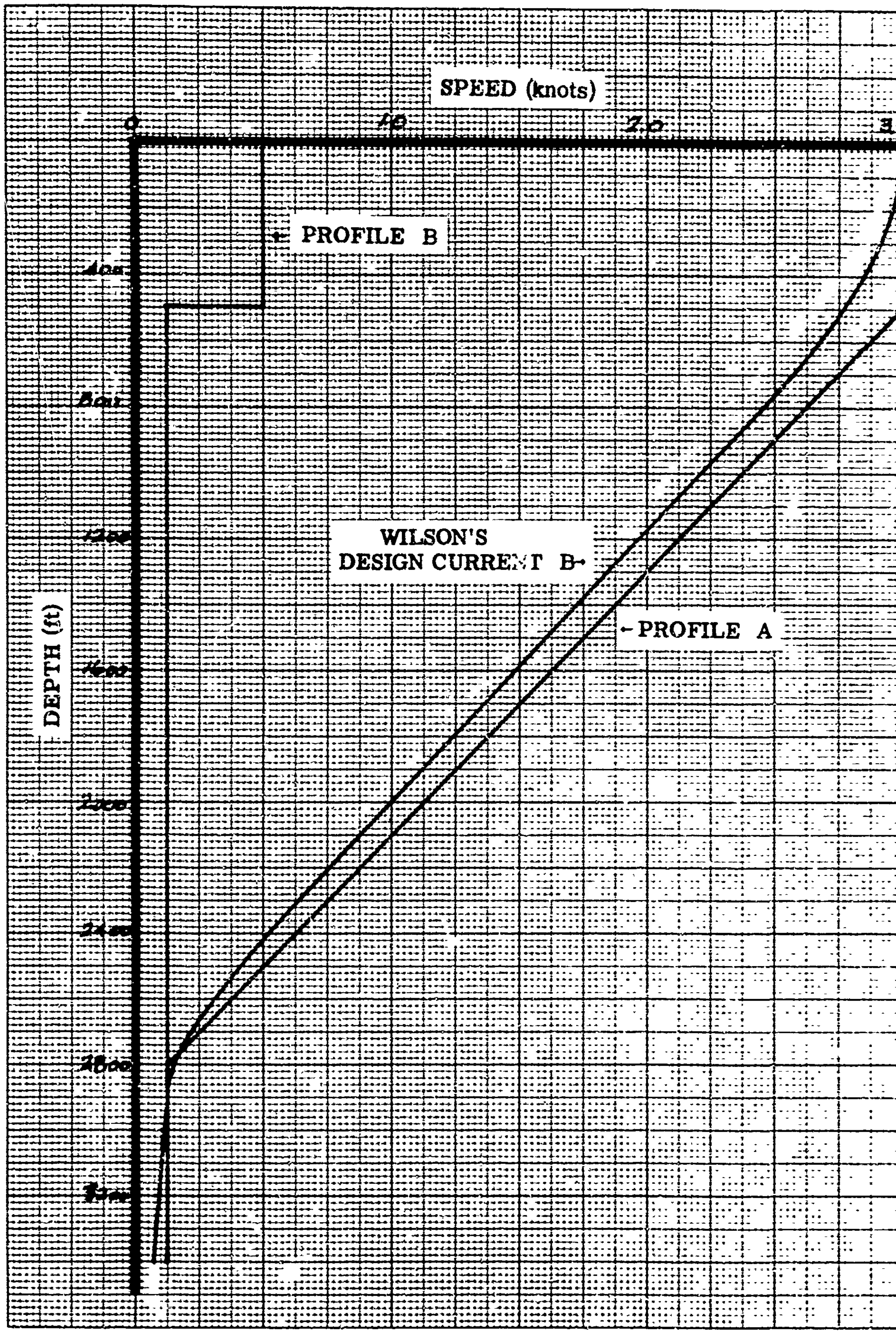

Figure 2 Basic Current Profiles

California Current in mild weather conditions. Variations were assumed to be the result of brief storms that would increase the speed of water near the surface. One would ordinarily assume the increase in water velocity to be about 2 percent of the wind velocity, depending upon which of several formulas in the literature was used. The penetration of storm-driven current downward into the mixed layer could not be estimated so simply, however. Thus, rather than enter the complexities of modifying the water velocity profile below the surface, a considerably higher value of water velocity was used, so that effects of storm-driven current on the rope might be lumped as buoy drag. The velocities chosen are admittedly somewhat subjective.

Five such current-wind conditions were assigned originally, though only four were used. Called Current Profile 2 through 5, they are characterized in the table below.

Table 1
DEFINITION OF CURRENT PROFILES

Current Profile	2	3	4	5
Wind (knots)	20	20	50	100
Basic Current Profile	B	A	A	A
Surface Skin Current (knots)	0.5	3.0	6.0	10.0

BUOY DRAG

The increasing multiplicity of variables did not permit a specification of several independent buoy drags. Instead, buoy drag was assumed to be proportional to rope strength at each current-wind condition. To estimate the proportionality constants, drag was calculated for several buoys* described in the literature: NOMAD,[10, 11] the Woods Hole toroid,[12] the Isaacs-Schick catamaran,[13] and the Vinogradov spar.[14] Since all the required data was not available from the descriptions, it was sometimes necessary to scale photographs or make estimates.

* The Convair discus was not included because a suitable mooring line had not yet been chosen.

The water drag on bodies which penetrate the water surface is not easily estimated, because the submerged portion is not often a simple geometrical shape. Part of the drag is form drag, proportional to the cross section of the immersed volume; part is skin drag, proportional to the wetted surface area; and part is due to energy lost in making waves (this was neglected). Vinogradov's spar was readily treated as a cylindrical body, mostly form drag, with a drag coefficient of 0.35. The Isaacs-Schick catamaran was assumed to have frontal area for form drag of about 2 ft^2 (increasing at high rope loads) and a wetted area of 74 ft^2. For form drag, the usual drag equation was used with a drag coefficient of 1.0.

For skin drag the formula quoted by Wilson in Reference 1 on page 47 was used.

$$(T_s)_x = 0.00421\ A_w\ V + 0.00657\ A_w\ V^2$$

where $(T_s)_x$ is the drag, A_w is the wetted area in ft^2, and V is the water velocity in knots. (This formula is intended to describe the total drag of ships, which have mostly skin drag. In lieu of a better formula it was used here to calculate skin drag.) The other buoys were treated similarly.

Devereux, et al.,[15] and Uyeda[16] report the results of towing buoy models, extrapolating the drag to full scale by techniques used for ship models. By extrapolation of Devereux's curves, drag has been estimated for two of the buoy types mentioned. In each case the extrapolated drag was several times larger than that calculated by formula. The results calculated by formula were preferred, partly to avoid inconsistency and partly to avoid the questionable results of extrapolation.

Tables 2 and 3, which summarize the computation of the final drag estimates, show that the drag/rope-strength ratio is surprisingly constant for each current-wind condition. This is, perhaps, not so surprising after all, considering that these buoys have remained in place at sea. The resulting mean ratio was used to calculate a buoy drag for each current-wind condition and each mooring line.

Table 2

CONSTANTS OF SEVERAL MOORED BUOYS

Buoy	Body Dimensions L, W, and H (ft)	Mass x 10^{-3} (lb)	Mooring Line			Windage Area (ft^2)
			Material	Diam., (in.)	Strength x 10^{-3} (lb)	
NOMAD	20 x 10 x 5.4	24	Polypropylene	1.0	14	40.5
Woods Hole	8 x 8 x 2.5	0.8	Nylon	0.562	8.3	24
Isaacs-Schick	12 x 8 x 1.1	0.8	Nylon	0.375	4.2	7.7 ?
Vinogradov	5.3 x 5.3 x 12.8	2.8	Steel	0.315	9.2	13.5

Table 3

CALCULATED DRAGS OF BUOYS

Buoy	Current Profile	Assumed Angle of Tilt (deg)	Vert. Immersed Section (ft^2)	Drag Coefficient	Wetted Area (ft^2)	Windage Area (ft^2)	Drag (lb)						Drag / Rope Strength	Accepted Ratio ***
							Form	Skin	Total Water	Total Water (Devereux)	Windage	Total Accepted		
NOMAD	2	*	37	0.1	200	40.5	3	1	4	**	160	164	0.0117	0.009
	3	*	37				95	14	109	(545)	160	269	0.0192	0.02
	4	*	37				381	50	431	(2700)	1000	1431	0.102	0.11
	5	*	37				1057	140	1197	(14,000)	4000	5197	0.371	0.43
Woods Hole	2	0	5	0.1	42	24	0.4	0.2	1	**	96	97	0.0108	
	3	11	6				1.5	3	18	**	96	114	0.0127	
	4	24	29				300	11	311	(1000)	600	911	0.101	
	5	30	43				1260	29	1289	**	2400	3689	0.41	
Isaacs-Schick Cata-maran	2	0	2	1.0	74	7.7	1	0	1		32	33	0.0079	
	3	0	2				50	5	55		32	87	0.0207	
	4	0	3				310	19	329		200	529	0.129	
	5	20	4				1140	52	1192		800	1992	0.475	
Vino-gradov	2	*	27	0.35	89	13.5	11	†	11		56	67	0.0073	
	3	*	27				245		245		56	301	0.0329	
	4	*	27				979		979		350	1329	0.145	
	5	*	27				2695		2695		1400	4095	0.447	

* Not considered
** Extrapolation unjustified
*** For all buoys
† Included in form drag

SIMULATION OF CURRENT METERS

The mass, virtual mass, and drag of a current meter comparable to the Geodyne Corporation Woods Hole Current Meter were included at each node, except the anchor and buoy. The constants chosen for the meter were as follows:

Length, effective (in.)	50
Diameter (in.)	7
Mass (lb)	105
Weight in water (lb)	30
Virtual mass lateral (lb)	75
Virtual mass longitudinal (lb)	6
Drag coefficient, lateral	0.8
Drag coefficient, longitudinal	1.0

The drag coefficients and virtual masses were taken from Saunders.(17)

To reduce complications for the static case, the current meter drag was computed as though the meter body has a constant tilt of 30 degrees in the plane of flow. This causes very little error. It was not necessary, however, to use this simplification for the dynamic study.

The advisability of simulating current meters in this problem may seem doubtful. Since the properties of the current meter were lumped with those of the rope half-segments on either side, the meter appears only as increased rope weight and drag. The effect is slight in dense and long ropes, more significant in short and less dense ropes. Furthermore, the simulation does not develop all of the behaviors of a concentrated mass on a vibrating rope unless a much more detailed simulation of the rope in the vicinity of a current meter is set up.

We feel that the added complexity of simulating current meters was justified. Otherwise, the nylon ropes probably would have exhibited motions less violent than in reality. Detailed simulation in the vicinity of the meter was obviously too expensive, but most likely the effects of this deficiency are slight when the ropes are relatively taut. In the less taut nylon ropes and possibly even in the short steel ropes, our simulation probably gives lateral current meter excursions that are too small.

WATER DEPTHS

Depths of 18,000, 6,000, and 1,800 feet were chosen as a reasonable bracketing of practical conditions. We actually expected the dynamic conditions in 1,800 feet of water to demonstrate what an impractical depth this is for many purposes.

ROPE DIAMETERS, MATERIALS, AND TENSIONS

We had originally intended to study three synthetic fibers, plus fiberglass and steel, in a number of rope diameters. But again the multiplicity of factors forced a retrenchment. Only nylon, fiberglass, and steel were chosen, all with a diameter of 1/2 inch except for five cases of 2-inch nylon in 18,000 feet of water. (The 67 static cases studied are summarized in Table 4.) When the dynamic problem was set up, it became necessary to eliminate both the fiberglass and the 2-inch nylon, so that finally the dynamic cases were limited to 1/2-inch rope of either nylon or steel.

The manner of choosing tensions may be explained as follows: In the static cases, once all the constants for current profile, rope and current meters, drag, depth, etc., had been entered, the independent variable was the tension at Node 1 just below the buoy.* The dependent variables calculated by the computer were the y increments for each rope segment, the x and y components of tension at each node, and the length of each segment. Thus, the choice of tension at Node 1 determined all the other variables.

The two extremes of tension are the breaking strength of the rope and the tension (if one exists) at which the anchored end of the rope sags enough to become tangent to the sea bottom. In practice it was not possible to reach the condition of tangency on the computer, because it meant that the entire bottom segment of rope would have to lie horizontally. Its length necessarily would be simulated as infinite, and the corresponding amplifier would limit. Generally it was practicable to approach the horizontal within 10 degrees; beyond this point tension settings were very critical. (There are cases with high water velocities and low-density

* The tension at Node 1 was very nearly the same as at Node 0; for much of this report the difference between them is ignored.

Table 4

SUMMARY OF STATIC MOORING LINE CALCULATIONS

Depth (ft)	Rope Mat'l	Rope Diam (in.)	Current Profile	Tension Node 1 (lb)	Tension Anchor (lb)	Rope Length (ft)	Offset of Buoy (ft)	Angle Buoy (deg)	Angle Anchor (deg)	Page
18,000	Steel	0.5	2	10,000	2,573	18,030	830	1.4	8.1	3
			2	7,834	274	18,510	2,271	1.5	87.5	4
			3	20,000	12,530	18,340	3,142	2.1	13.2	5
			3	10,000	2,786	23,320	12,730	4.0	87.0	6
18,000	Glass	0.5	3	16,150	14,670	18,370	3,241	2.4	11.1	7
			3	8,075	6,628	19,280	6,946	4.7	24.3	8
			3	4,843	3,401	23,050	14,150	8.2	48.1	9
			3	3,910	2,508	29,620	22,850	10.2	72.0	10
			4	16,150	14,680	18,710	5,368	9.0	17.9	11
			4	8,075	6,637	21,910	12,530	17.7	39.6	12
			4	6,460	5,052	25,240	17,590	22.1	52.6	13
			4	3,444	4,081	31,440	25,520	26.0	68.5	14
			5	16,150	14,750	23,950	15,690	32.8	43.7	15
			5	12,920	11,580	28,940	23,920	42.2	57.8	16
			5	11,652	10,360	38,570	31,830	47.9	67.2	17
18,000	Nylon	0.5	2	3,600	3,205	17,980	489	1.1	2.5	18
			2	2,160	1,770	18,080	1,019	1.8	4.5	19
			2	720	342	18,400	3,319	5.2	23.5	20
			2	480	135	22,310	10,980	8.9	83.1	21
			3	7,200	6,782	18,080	6,537	3.6	21.5	22
			3	3,600	3,315	23,430	14,600	7.2	43.1	23
			3	2,160	1,840	38,430	33,700	11.3	70.3	24
			4	7,200	6,785	18,830	6,382	3.8	26.7	25
			4	3,600	3,248	26,890	19,630	17.1	51.7	26
			5	7,200	6,857	24,320	16,320	24.6	44.1	27
18,000	Nylon	2.0	3	53,000	50,810	18,470	4,042	3.7	13.5	28
			3	31,850	29,380	19,280	6,972	6.1	22.9	29
			3	20,000	17,800	21,350	11,620	9.4	36.2	30
			3	20,000	17,590	21,560	12,000	9.8	37.4	31 (a)
			3	15,800	13,440	24,370	16,270	12.2	46.0	32
6,000	Steel	0.5	2	10,000	7,328	6,003	156	1.1	1.8	33
			2	6,000	3,352	6,025	288	1.7	4.0	34
			2	3,000	373	6,150	1,070	3.5	38.5	35
			2	2,838	240	6,581	1,629	3.7	79.5	36
			3	20,050	17,210	6,077	844	1.5	9.6	37
			3	10,000	7,365	6,282	1,986	2.9	22.5	38
			3	6,000	3,402	7,034	4,065	4.9	51.2	39
			3	5,184	2,594	9,483	6,759	5.7	81.9	40
			4	20,000	17,350	6,173	1,442	5.6	15.9	41
			4	10,000	7,288	6,886	3,359	13.3	38.9	42
			4	8,000	5,502	7,750	4,818	16.7	51.4	43
			4	6,894	4,047	8,848	8,573	20.3	81.8	44
6,000	Glass	0.5	3	10,000	9,344	6,211	1,629	3.0	17.6	45
			3	5,000	4,372	7,024	3,620	5.9	38.5	46
			3	3,000	3,425	10,650	7,859	9.8	64.5	47
			3	2,584	2,048	13,970	12,240	11.3	90.7	48
			4	10,000	9,350	6,639	2,859	13.3	28.1	49
			4	5,000	4,438	9,450	7,236	27.1	57.0	50
			4	3,774	3,282	18,380	15,070	30.7	80.3	51
6,000	Nylon	0.5	2	3,600	3,204	6,033	144	1.1	2.0	52
			2	2,160	1,770	6,016	307	1.8	3.9	53
			2	720	342	6,125	1,056	5.1	19.8	54
			3	3,600	3,333	7,588	4,482	4.1	42.3	55
			3	2,160	1,952	11,270	9,288	7.5	65.5	56
			3	1,880	1,717	13,910	12,307	7.8	72.3	57
			4	3,600	3,340	8,575	6,043	14.4	50.6	58
			4	2,880	2,685	10,400	8,388	18.0	60.7	59
			4	2,860	2,657	13,380	8,368	18.0	60.8	60 (b)
			4	2,120	1,974	16,230	14,930	24.2	75.4	61
1,800	Steel	0.5	3	10,000	7,388	1,688	426	2.5	21.8	65
			3	6,000	3,431	2,046	888	4.0	47.4	66
			3	4,858	2,224	2,505	1,386	5.0	80.2	[illegible]
1,800	Nylon	0.5	3	3,600	3,383	2,051	882	2.3	40.6	62
			3	2,160	1,984	2,632	1,781	3.8	61.7	63
			3	1,440	1,281	4,312	3,730	5.6	79.2	64
12,000	Steel	0.5	A (c)	11,142	7,344	31,181	16,882	58.5	74.7	[illegible]
			A (c)	7,075	3,330	15,788	8,889	12.9	27.1	[illegible]

(a) A repetition with improved computer scaling.
(b) A duplicate run to check the computer after lapse of one day.
(c) From Wilson (2), used for checking purposes.

ropes in which tangency at the bottom cannot occur at any rope length. There also are cases in which tangency theoretically could have been attained but only at rope lengths exceeding the dynamic range of the amplifiers.)

The upper limit of tension was usually half the breaking strength of the rope in question.* In some cases, however, the full breaking strength was introduced at Node 1. The problem is so nonlinear that it was not feasible to pre-select intermediate points. Instead, they were chosen by trial, so that the rope shapes interpolated reasonably well between the two extremes.

ROPE PROPERTIES

Table 5 summarizes the constants descriptive of the various ropes. For the elasticity of steel rope the data in United States Steel Wire Rope Handbook,[18] Section 20, were used. All cases are for ropes with steel cores.** The Handbook apparently calculates the metallic area of the rope normal to the strand. This is the area used in calculating the elasticity. The area given in the table is the effective area normal to the rope, obtained by dividing linear rope density by the bulk density of steel.

The properties of fiberglass rope were obtained by measuring a sample of laid fiberglass rope made by the Materials Section of the Sea Operations Department† in mid-1964. (Newer constructions are stronger.) The sample was 0.312 inches in diameter; properties for the 1/2-inch diameter were calculated on the assumption that strength and elasticity vary as the square of the diameter.

Properties of the synthetic-fiber ropes, except for elasticity, were taken from standard tables and from the tables issued by Plymouth Cordage Co. for their "Standard" rope constructions.

---

* Breaking strengths for 1/2-inch ropes taken as: steel, 20,000 lb; nylon, 7,200 lb; glass (GM DRL design), 32,300 lb.

** Wilson[1] apparently calculated for fiber-cored rope.

† GM Defense Research Laboratories, General Motors Corporation.

Table 5

PROPERTIES OF ROPES, ONE-HALF INCH IN DIAMETER

Material	Specific Gravity	Unit Weight Air (lb/ft)	Unit Weight Water (lb/ft)	Mass Including Virtual Mass (lb/ft)	Solid Section (ft^2)	Breaking Strength (lb)	Elasticity (lb/unit extension)
Nylon	1.14	0.0695	0.00695	0.157	0.000976	7,200	10,000 – 200,000
Polypropylene	0.91	0.0475	-0.00606	0.135	0.000837	4,200	
Glass	2.01	0.1353	0.0664	0.222	0.00108	32,300	1,042,000
Steel	7.81	0.46	0.40	0.55	0.000944	20,000	1,530,000

ELASTICITY OF SYNTHETIC FIBERS

Elasticity in a synthetic fiber is a complex property which depends upon the unit strain, the rate of stretching, the cyclic amplitude, the temperature, and perhaps the pressure. Hysteresis is marked. Creep under moderate loads is considerable, usually approaching a limit in several tens of minutes. Under high loadings the rope may creep to destruction. Such behavior has been noted with polypropylene at stresses above about half the breaking stress.

Since dynamic elasticities were not available, some studies were made with the Tinius Olsen testing machine at GM DRL. Standard nylon rope, 1/2-inch in diameter, was pulled to a series of mean tensions and finally to destruction. In two cases, the rope was cycled ± 180 lb and ± 400 lb about each mean tension pulling at 1.2 inches/minute. In a third test the mean tension was maintained at 2,000 lb, and the rope was cycled ± 140, ± 280, ± 560, and ± 1,120 lb at pulling rates increasing with amplitude. In some other tests, run with 9/16-inch plaited nylon rope, the results were in essential agreement.

Figure 3 is a reproduction of the test record in which the cyclic loading was ± 180 lb. At each cycling point there is at first a fairly rapid creep which at last becomes slow enough that the shape of the loop may be considered reasonably well stabilized. The dynamic spring constant was determined by measuring the slope between the extreme points of a stabilized hysteresis loop. The resulting spring constants are shown in Figure 4. They are evidently much greater (stiffer spring) than those for slow unidirectional pulling.

Figure 5 is a tracing of the record made at various cyclic amplitudes, and Figure 6 shows the resulting spring constant as a function of cyclic amplitude.

It was then assumed that the semi-log plot of Figure 6 could be moved parallel to itself to produce similar plots for different mean tensions. These curves were located by the already-determined relation between spring constant and mean tension. The resulting diagram, augmented by lines of equal strain variation, is shown in Figure 7.

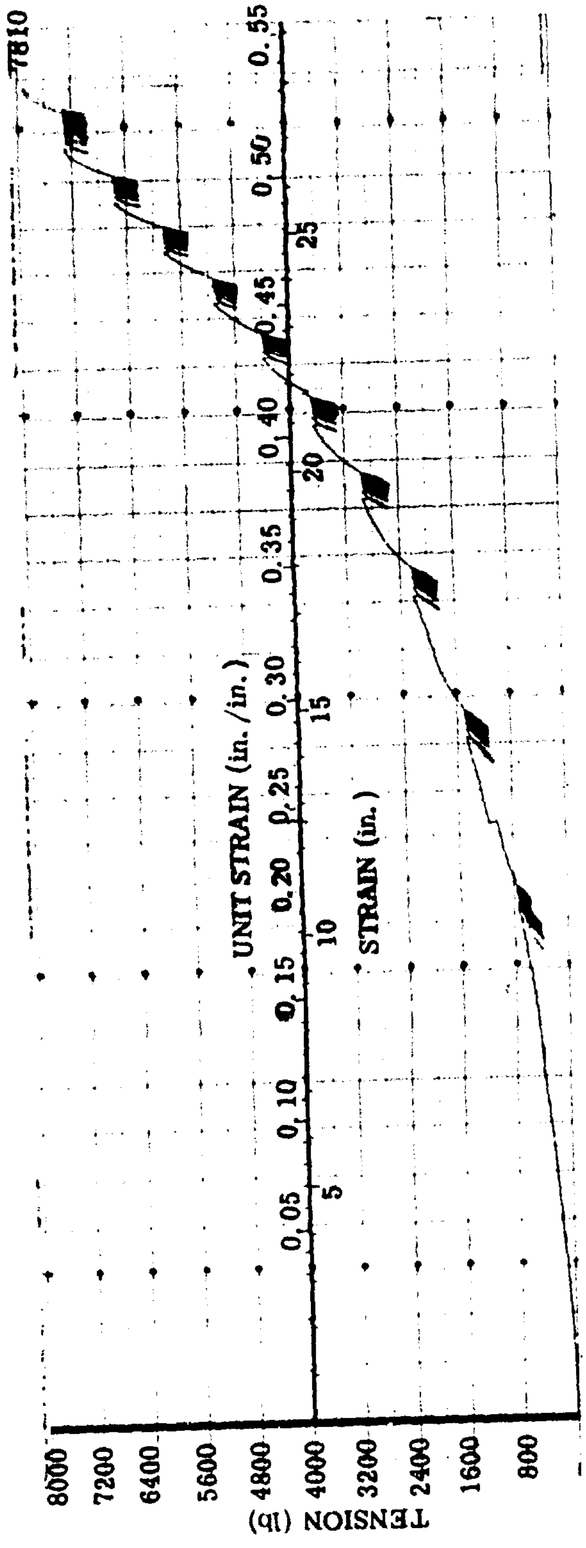

Figure 3 Test Records of Dynamic Stress-Strain Relation in Half-Inch Nylon Rope

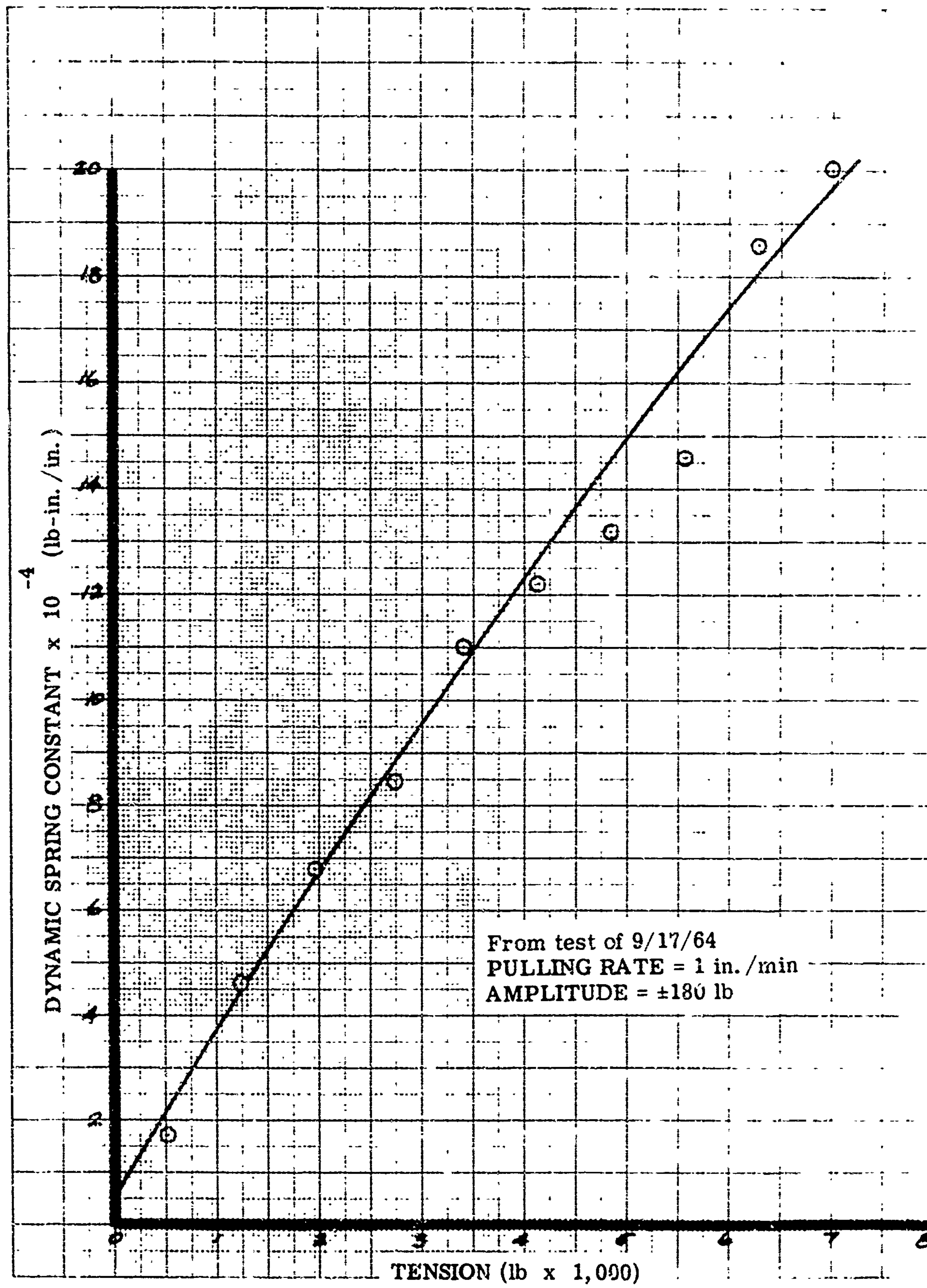

Figure 4 Dyanmic Spring Constant of Half-Inch Nylon Rope

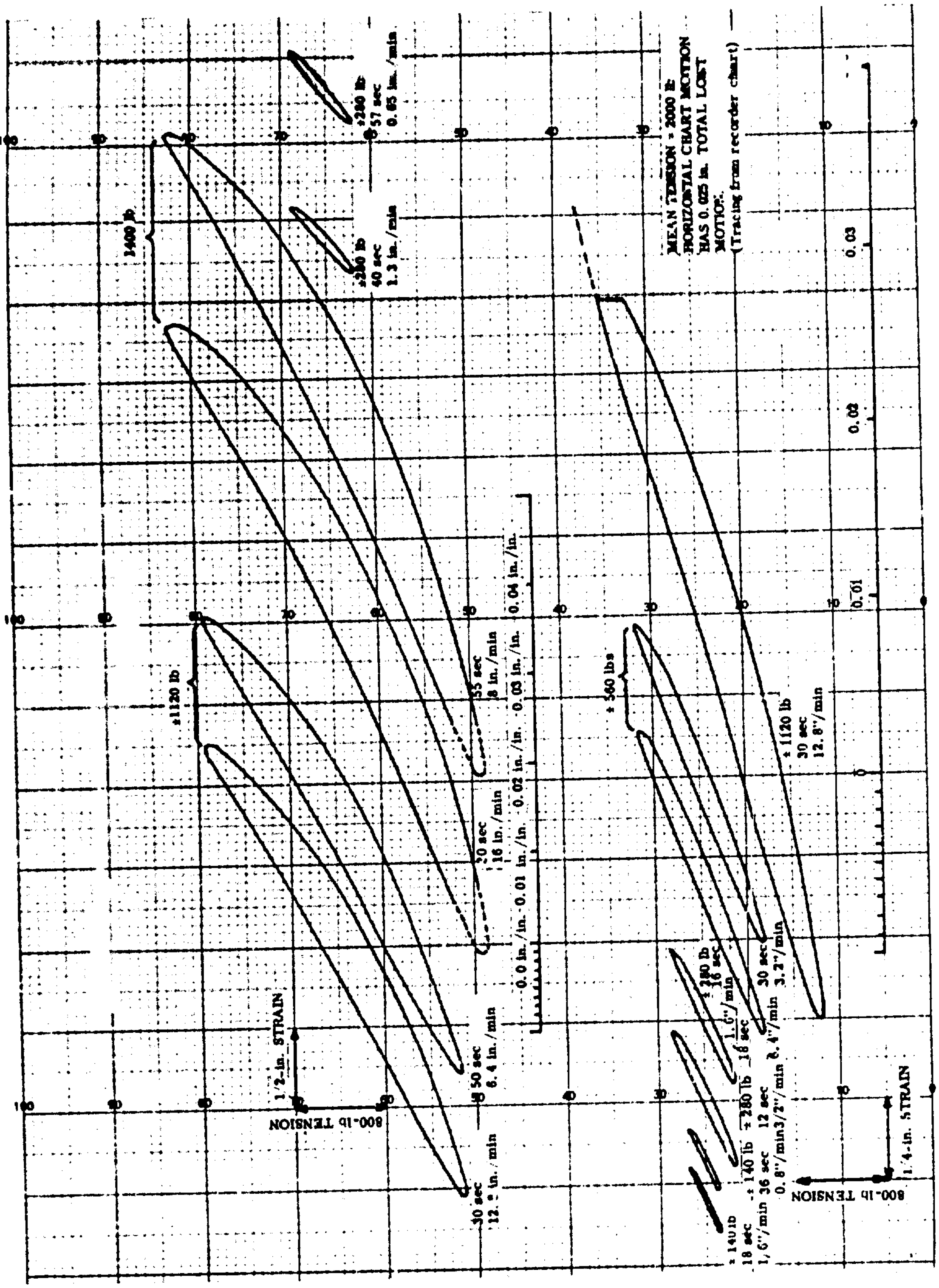

Figure 5 Tracing of Test Record Hysteresis and Dynamic Spring Constant of Half-Inch Nylon Rope as Function of Cyclic Amplitude

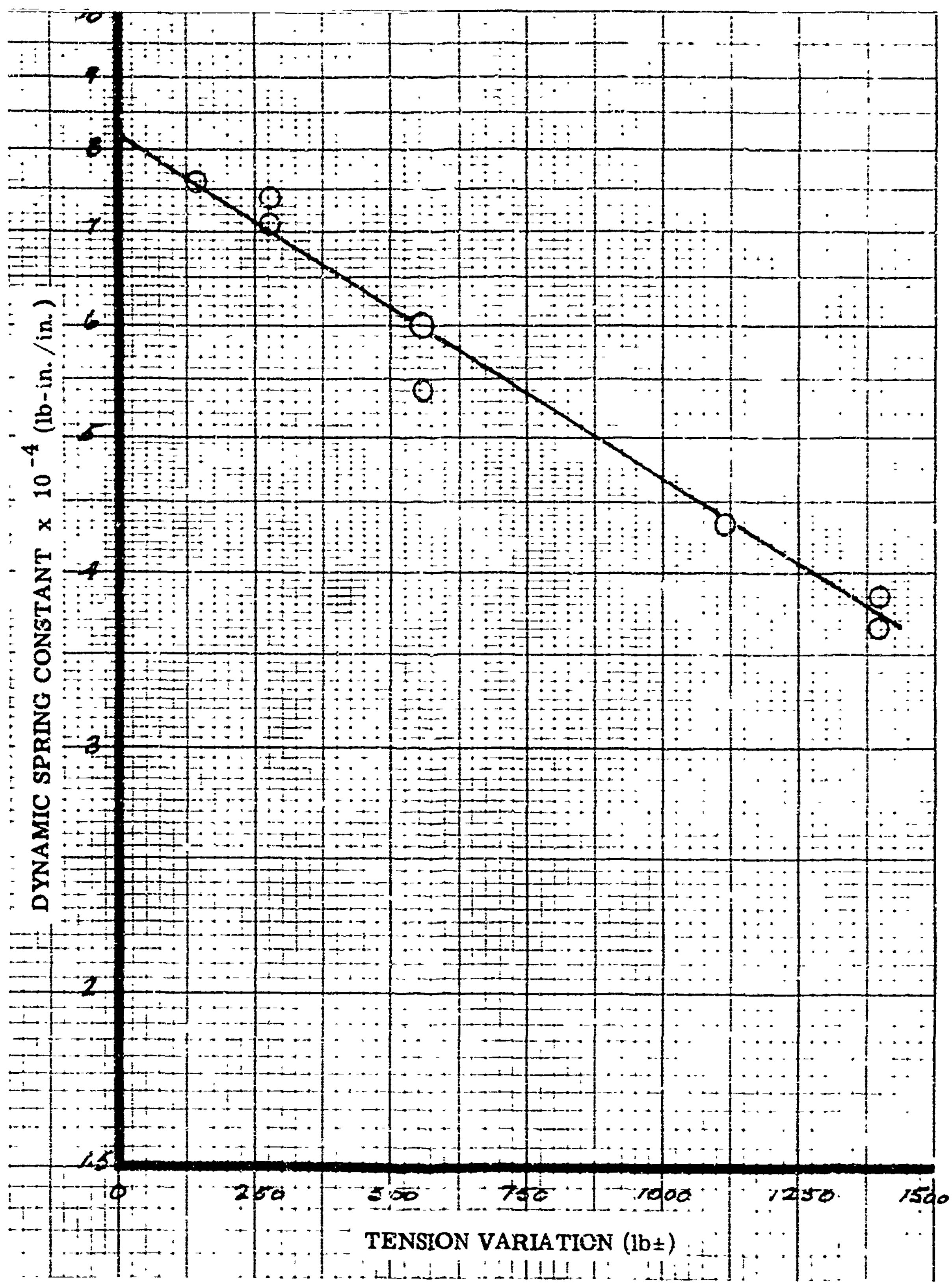

Figure 6 Dynamic Spring Constant of Half-Inch Nylon Rope as a Function of Cyclic Amplitude (mean tension = 2,000 lb)

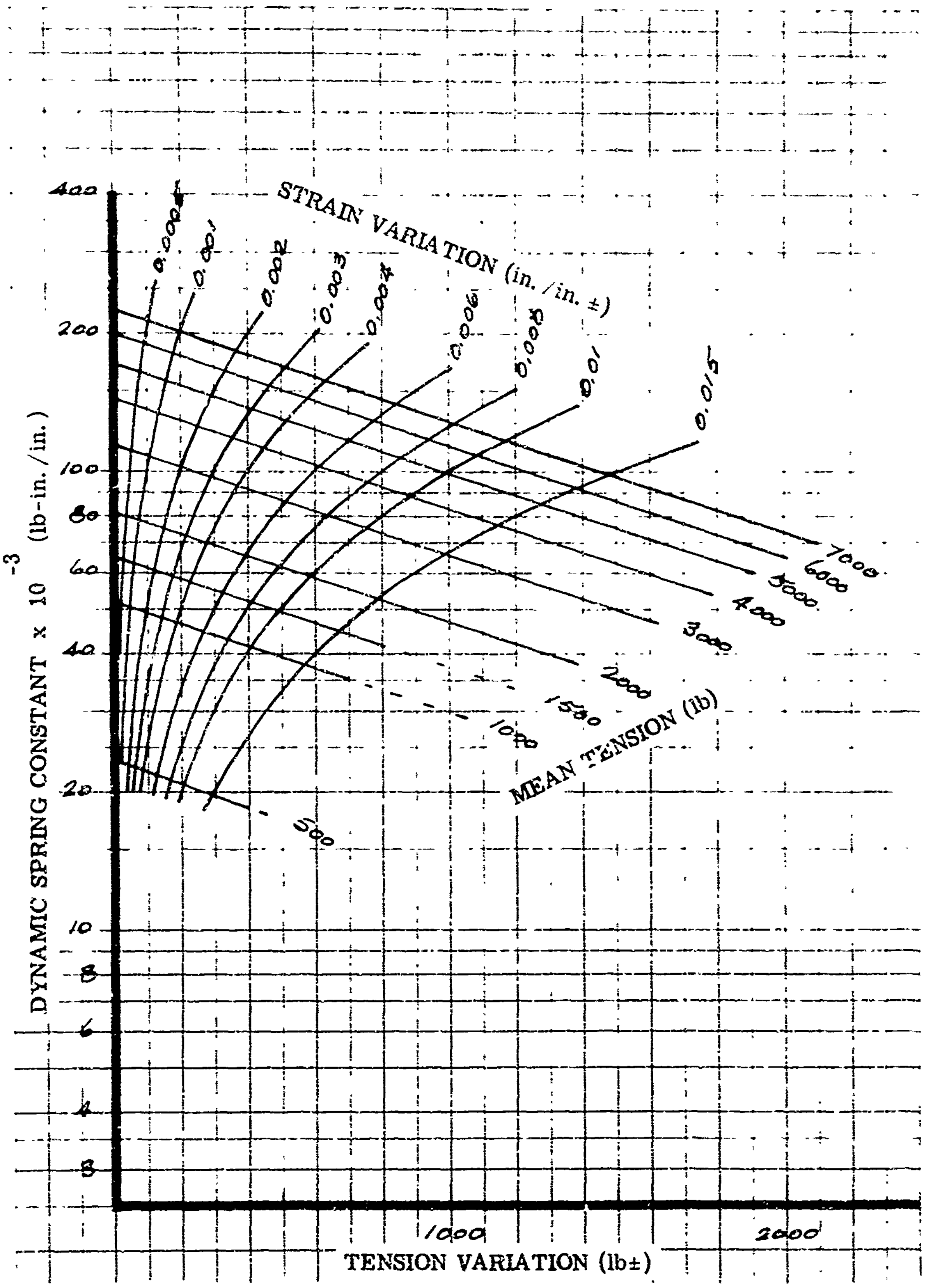

Figure 7 Dynamic Spring Constant of Half-Inch Nylon Rope as Function of Mean Tension and Amplitude

To determine the spring constant for a particular set of conditions, the cyclic strain variation throughout the rope was assumed to be both uniform and equal to 7-1/2 feet divided by the length of the rope. Using the mean tension at the top of the rope, a spring constant was picked from the graph and used for all the wave amplitudes of that run. The errors due to this procedure are relatively small.

The hysteresis of nylon rope also was measured, and one set of values is presented in Table 6. At the higher values of cyclic tension, the hysteresis certainly is significant. It was not feasible to introduce hysteresis into the problem directly, but part of its effect was included by using the experimentally measured dynamic spring constant; thus we would expect to get approximately correct values for the maximum cyclic tensions. However, phase shifts and energy losses in the rope might result in damping some of the resonances observed in our results. Insofar as resonances modified the tensions, it may be expected that a failure to introduce hysteresis would cause some error, positive or negative.

WAVE EXCITATION

First to be discussed will be choices of wave periods and heights, then the manner in which excitation was applied to the system.

The range of wave periods taken was from 2 to 32 seconds,* increasing by factors of two. Three wave heights were used, 5 feet, 15 feet, and 50 feet, peak to trough. These encompass the conditions of interest. Since 2-second and 4-second periods are unlikely to be associated with 50-foot waves and a 5-foot wave with a 32-second period would be so mild as to be uninteresting, the following combinations were selected:

Period (sec)	2**	4	8	16	32
	(5)	5	5	5	
Height (ft)	15	15	15	15	
			50	50	50

* It was recognized, of course, that there is very little energy in the 2-second and 32-second periods; these were selected merely to give outer reference points for interpolation.

** The 5-foot amplitude at 2 seconds was infrequently measured, and when the 2-second period could not be reached because of amplifier limiting, 3 seconds was substituted.

Table 6

HYSTERESIS IN HALF-INCH NYLON ROPE
(MEAN TENSION 2000 lb)

Tension Variation (lb)	Hysteresis per cycle $\frac{(\text{ft - lb})}{\text{ft length}}$
± 140	0.12
± 280	0.52
± 560	2.3
± 1120	15.2
± 1400	29.7

This study was restricted to buoys with a large buoyancy coefficient, since they could be expected to sink only slightly with the increases in rope tension. Thus it was possible to ignore inertial effects in the buoy, assuming that in the vertical it rose and fell with the waves.

The horizontal component of motion was not so easily established. In one extreme the buoy might move vertically up and down; in the other it might respond completely to wave particle motion and move in a circle. Neither is correct. Although we could have simulated the true motion on the computer, we were already at the practical limits of complexity and felt it best to make a simplifying assumption. Consequently, the excitation was introduced as an elliptical displacement with the vertical axis four times as great as the horizontal.

We now believe that the horizontal component of motion had very little effect on the system, since its effects could not be detected with any certainty, even at the first node below the buoy.

DIFFERENCES BETWEEN TEN-SEGMENT AND FOUR-SEGMENT ROPE SHAPES

There is a difference in rope shape which results from the 4-segment simulation. To obtain the rope shape for the 4-segment cases, corresponding 10-segment rope shapes were plotted on a large scale and divided into four equal lengths. Secants were then drawn between the five resultant nodal positions. A body equivalent to 2-1/2 current meters was simulated at each of the three nodes in the rope span to retain similarity with the 10-segment simulations. The length of the secant was taken to be equal to one-fourth of the total rope length. This approximation is believed to be reasonably good in all cases in which the rope has moderate curvature, a condition existing in all cases except D and L . In Case D the secant nearest the bottom departed widely from the 10-segment curve. In Case L the departure was only about half as great as in Case D, but it was at the top.

The situation for Case D, illustrated in Figure 8, is of particular interest because dynamic tensions were determined for both the 4-segment and the 10-segment simulations. The dynamic tensions for the 4-segment case are much higher than for the 10-segment case, because in the latter with its highly curved lower section the motion of the buoy was mostly expended in lifting the bottom one or two segments of rope, without much necessity for stretching the rope. In the 4-segment case, the easily lifted arc of rope is absent, so that the concentrated lateral drag at Node 3 forces the rope to stretch, thereby developing high tensions. The discrepancy in tension, a factor of 3 at the 50-ft wave height and 32-seconds period, decreases with period and amplitude until there is scarcely any difference with 5-foot wave heights.

Case L also would be expected to give dynamic tensions that are higher than they would have been with the 10-segment rope shape. But the discrepancy should be less by a factor of about 3, since the secant is only half as far from the 10-segment shape and the rope is nylon in which a larger fraction of the mechanism already is one of stretching the rope.

CHECKING

The static simulation was checked by duplicating two of Wilson's cases, using his current structure and rope constants. * The total rope lengths and maximum horizontal coordinates checked within 0.5 percent and the tensions at the bottom within 1.3 percent, which was regarded as satisfactory.

To check the dynamic simulation, one of Whicker's cases[3] was computed, using two arbitrary values of longitudinal drag. (Whicker himself used no drag.) Our results compared well with Whicker's in nonresonant conditions; but where Whicker had forces approaching infinity due to resonance, our forces were finite and the resonant frequency decreased slightly with increasing damping, as would be expected.

---

* pp. 166 and 170 of Reference 2, Vol. 2.

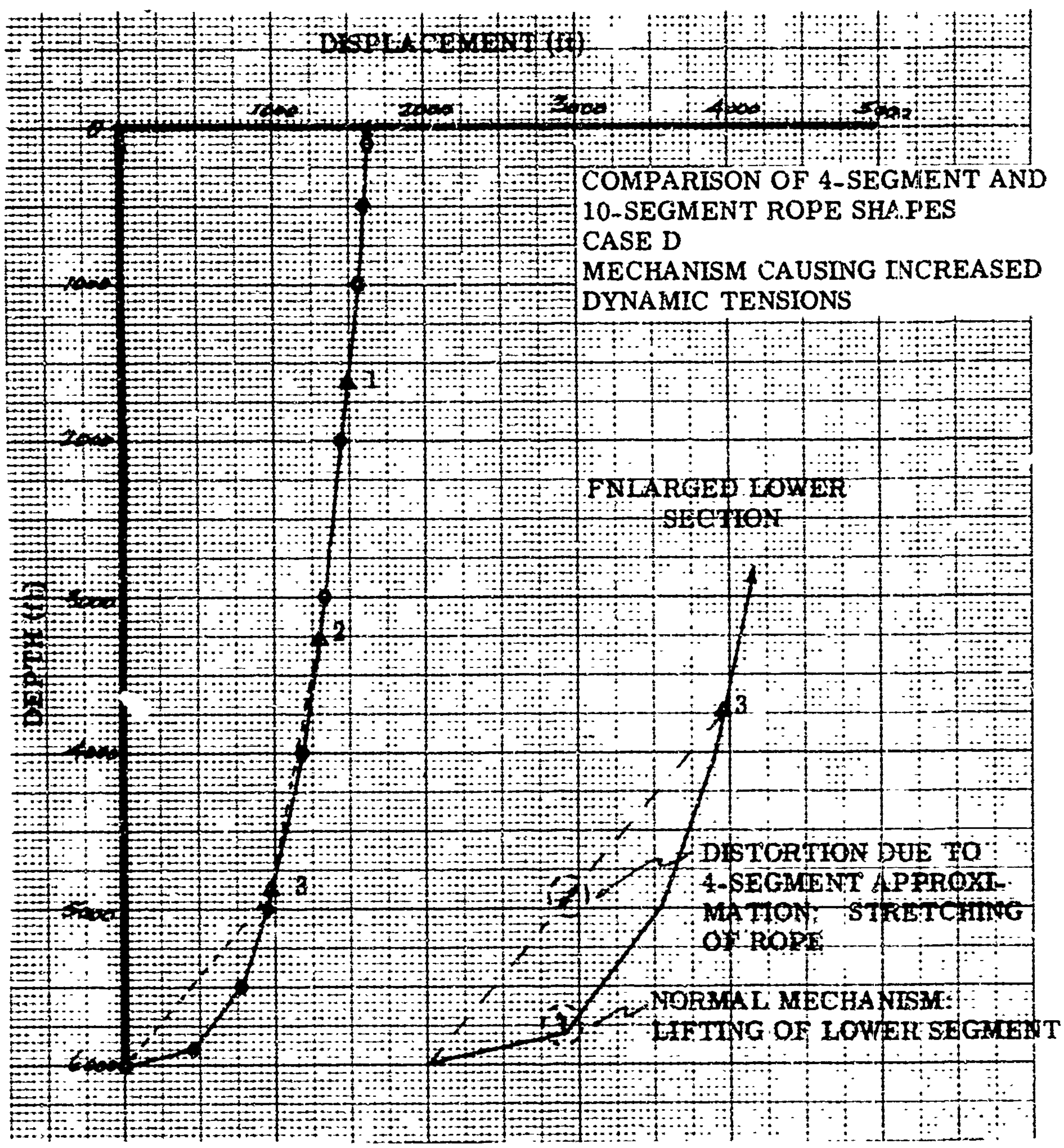
DISPLACEMENT (ft)
DEPTH (ft)
COMPARISON OF 4-SEGMENT AND
10-SEGMENT ROPE SHAPES
CASE D
MECHANISM CAUSING INCREASED
DYNAMIC TENSIONS
ENLARGED LOWER
SECTION
DISTORTION DUE TO
4-SEGMENT APPROXI-
MATION; STRETCHING
OF ROPE
NORMAL MECHANISM:
LIFTING OF LOWER SEGMENT
1
2
3
2
3
3

Figure 8

III. RESULTS

STATIC SOLUTIONS

Analog Computer Output

Computer outputs in the static rope-shape simulation were read out automatically on an electric typewriter. The first of two sample pages, shown as Tables 7 and 8, is the simulation of one of Wilson's cases referred to in Section II. Column headings, printed in capitals because of machine limitations, have the following meanings: N is the number of the node, counting downward from zero at the buoy; YSUB(N-1)-YSUB(N) is the length of the projection on the y-axis of the rope segment between Nodes n-1 and n; XSUB(N) is the vertical coordinate of Node n and S SUB(N) is the length of the rope segment between Nodes n-1 and n; T SIN THETA and T COS THETA are the horizontal and vertical components of the rope tension just above the respective nodes. The numbers in these columns are expressed as a four-digit decimal followed by a scaling factor consisting of a multiplier and exponent of 10. Thus 0.2765/2E3 indicates that 0.2765 must be multiplied by 2×10^3. The numbers 1f67, 1a.86, etc., which are the numbers of the amplifiers being read, may be ignored for the purposes of this report. The page number entered in the lower right corner is for identification and reference.

Reduction of Analog Computer Results

All of the results from the original print-out were converted in the IBM 7040 digital computer to obtain the x and y coordinates of nodes, the accumulated rope length measured from the anchor, the tension just above each node, and $\bar{\theta}_n$, the angle from the vertical just above the node. These quantities are labelled as barred or mean quantities in anticipation of their use later on as the rest states for the dynamic studies. Sixty-five cases (Reference Page Numbers 3–67)* are presented in Section VI.

---

* The first two are check cases, not shown.

Table 7

SAMPLE ANALOG COMPUTER PRINT-OUT FOR ROPE SHAPE AND TENSION (Ref. p. 2)

CABLE CONFIGURATION AND TENSIONS

CABLE MATERIAL STEEL
WEIGHT PER FOOT RUN IN WATER .312 LBS
BREAKING STRENGTH 17,500 LBS
T SUB(1) 7,075 LBS

CURRENT PROFILE A
OCEAN DEPTH 12,000 FEET
CABLE DIAMETER .500 INCHES

N	XSUB(N) FEET	YSUB(N-1)-YSUB(N) FEET			T SIN THETA			T COS THETA			S SUB(N) FEET		
0	0	-			1f67	0.0844	/2E4	1a70	0.3462	/2E4	-		
1	200	1a62	0.0491	/1E3	1f67	0.0844	/2E4	1a77	0.3431	/2E4	1a64	0.2055	/1E3
2	1,000	1a56	0.1351	/2E3	1a16	0.0551-	/4E4	1m07	0.3249	/2E4	1a03	0.4218-	/2E3
3	2,000	1a21	0.2386	/2E3	1p20	0.0721-	/4E4	1m17	0.2970	/2E4	1a23	0.5536-	/2E3
4	4,000	1a76	0.1130	/1E4	1q30	0.0151	/2E5	1a45	0.2639-	/2E4	1a33	0.2283-	/1E4
5	6,000	1a41	0.1331	/1E4	1q23	0.0152-	/2E5	1m37	0.2277	/2E4	1a43	0.2396-	/1E4
6	8,000	1f63	0.1565	/1E4	1p44	0.0151	/2E5	1a81	0.1889-	/2E4	1a38	0.2537-	/1E4
7	10,000	1a26	0.2021	/1E4	1q26	0.0151-	/2E5	1m77	0.1469	/2E4	1a28	0.2827-	/1E4
8	11,000	1a59	0.1330	/1E4	1q15	0.0152	/2E5	1a15	0.1127-	/2E4	1m56	0.1599-	/1E4
9	11,800	1a51	0.1299	/1E4	1q16	0.0076-	/4E5	1a71	0.0875-	/2E4	1a33	0.1527	/1E4
10	12,000	1a68	0.4268	/1E3	1a91	0.0152	/2E5	1a82	0.0718-	/2E4	1a84	0.4709	/1E3
	ANCHOR	-			1a92	0.1114-	/2E4	1a90	0.0682-	/2E4	-		

T_{10} = 0.16605/2E4 = 3321 lb
Wilson : 3346 lb

S_{TOTAL} = 15,796 ft.
Wilson : 15,872 ft.

2

Table 8

SAMPLE ANALOG COMPUTER PRINT-OUT FOR ROPE SHAPE AND TENSION (Ref. p. 22)

CABLE CONFIGURATION AND TENSIONS

CABLE MATERIAL NYLON
WEIGHT PER FOOT RUN IN WATER .00695 LBS
BREAKING STRENGTH 7,200 LBS
T SUB(1) 7,200 LBS

CURRENT PROFILE 3
OCEAN DEPTH 18,000 FEET
CABLE DIAMETER .500 INCHES

N	XSUB(N) FEET	YSUB(N-1)-YSUB(N) FEET			T SIN THETA			T COS THETA			S SUB(N) FEET		
0	0	-			1f67	0.0229	/2E4	1a70	0.3608	/2E4	-		
1	300	1a62	0.0187	/1E3	1f67	0.0229	/2E4	1a77	0.3598	/2E4	1a64	0.3009	/1E3
2	1,500	1a56	0.1460	/2E3	1a16	0.0415-	/4E4	1m07	0.3461	/2E4	1a03	0.6174-	/2E3
3	3,000	1a21	0.2714	/2E3	1a11	0.0604	/4E4	1m17	0.3335	/2E4	1a23	0.3976-	/4E3
4	6,000	1a76	0.1110	/1E4	1q30	0.0123	/2E5	1a45	0.3308-	/2E4	1a33	0.3187-	/1E4
5	9,000	1a41	0.1127	/1E4	1q23	0.0124-	/2E5	1m37	0.3282	/2E4	1a43	0.3193-	/1E4
6	12,000	1f63	0.1142	/1E4	1p44	0.0124	/2E5	1a81	0.3253-	/2E4	1a38	0.3198-	/1E4
7	15,000	1a26	0.1154	/1E4	1q26	0.0124	/2E5	1m77	0.3223	/2E4	1a28	0.3207-	/1E4
8	16,500	1a59	0.0580	/1E4	1q15	0.0124	/2E5	1a15	0.3196-	/2E4	1m56	0.1581-	/1E4
9	17,700	1a51	0.0453	/1E4	1q16	0.0123	/2E5	1a71	0.3180	/2E4	1a53	0.1279	/1E4
10	18,000	1a88	0.0589	/2E3	1a91	0.0124	/2E5	1a82	0.3162-	/2E4	1a84	0.1612	/2E3
	ANCHOR	-			1a92	0.1242-	/2E4	1a90	0.3161	/2E4	-		

22

DYNAMIC SOLUTIONS

Cases Studied

The twelve cases studied are summarized in Table 9. Lettered A through L, these are identified also by the reference page number of the static solution used for the rest state of the system. Steel and nylon ropes of 1/2-in. diameter were studied in two tension conditions (one-half breaking strength and a relatively slack condition) and three water depths. The tauter rope conditions were all taken from cases in Current Profile 3, as were Cases F and L; all but these two of the less taut conditions were taken from cases in Current Profile 2. Six of the twelve cases were done with the 10-segment simulation and six with the 4-segment simulation. The 4-segment simulation was necessary for steel rope in the 6,000- and 1,800-foot depths, and for nylon in the 1,800-foot depth.

Analog Computer Outputs

The analog computer outputs were in two forms: a strip-chart and an x-y plot. Tensions T_1', T_7', T_{10}', and some of the $x_n - x_{n-1}$ and $y_{n-1} - y_n$ quantities were read out on two eight-channel oscillographs, each channel ± 20 millimeters in width, full-scale. The portions of two separate records shown in Figure 9 include one of the noisiest, purposely chosen to give a feeling for the worst conditions encountered. Only a small proportion of the records were as noisy as this, though it will be noted that even here the true signal may be extracted from the noise by reading the middle of the densest portion of the trace.

The records of $x_n - x_{n-1}$ and $y_{n-1} - y_n$ served a diagnostic purpose, making it easier to find the source of trouble in case of anomalous behavior of the computer.

Tensions were read visually from the strip charts. They are presented in Section VI. where they also are plotted as a function of wave height on a log-log scale.

The cyclic motions of all nine active nodes, including the buoy, were plotted successively by an 11 by 17-inch x-y plotter for each period/wave-height combination of each case (Figs. 10–15 are examples). The plots were read

Table 9

SUMMARY OF DYNAMIC CASES STUDIED

Case	Page	Material	Depth (ft)	Segments	Tension (lb)	Profile
A	6	Steel	18,000	10	10,000	3
B	4	Steel	18,000	10	7,634	2
C	38	Steel	6,000	4	10,000	3
D	36	Steel	6,000	4	2,838	2
E	65	Steel	1,800	4	10,000	3
F	67	Steel	1,800	4	4,858	3
G	23	Nylon	18,000	10	3,600	3
H	21	Nylon	18,000	10	460	2
I	55	Nylon	6,000	10	3,600	3
J	54	Nylon	6,000	10	720	2
K	62	Nylon	1,800	4	3,600	3
L	64	Nylon	1,800	4	1,440	3

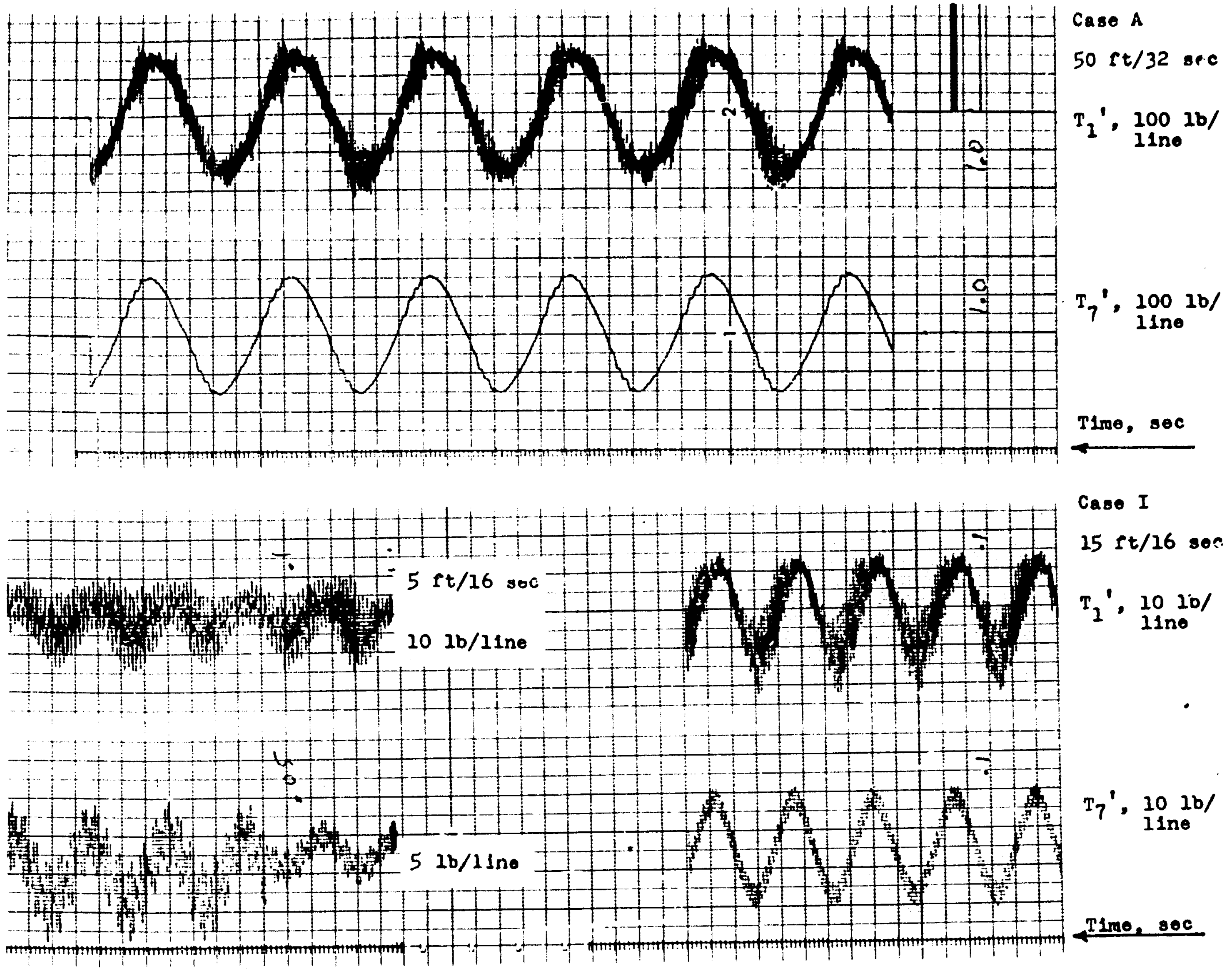

Figure 9 Portions of Two Strip Chart Records Showing Tensions

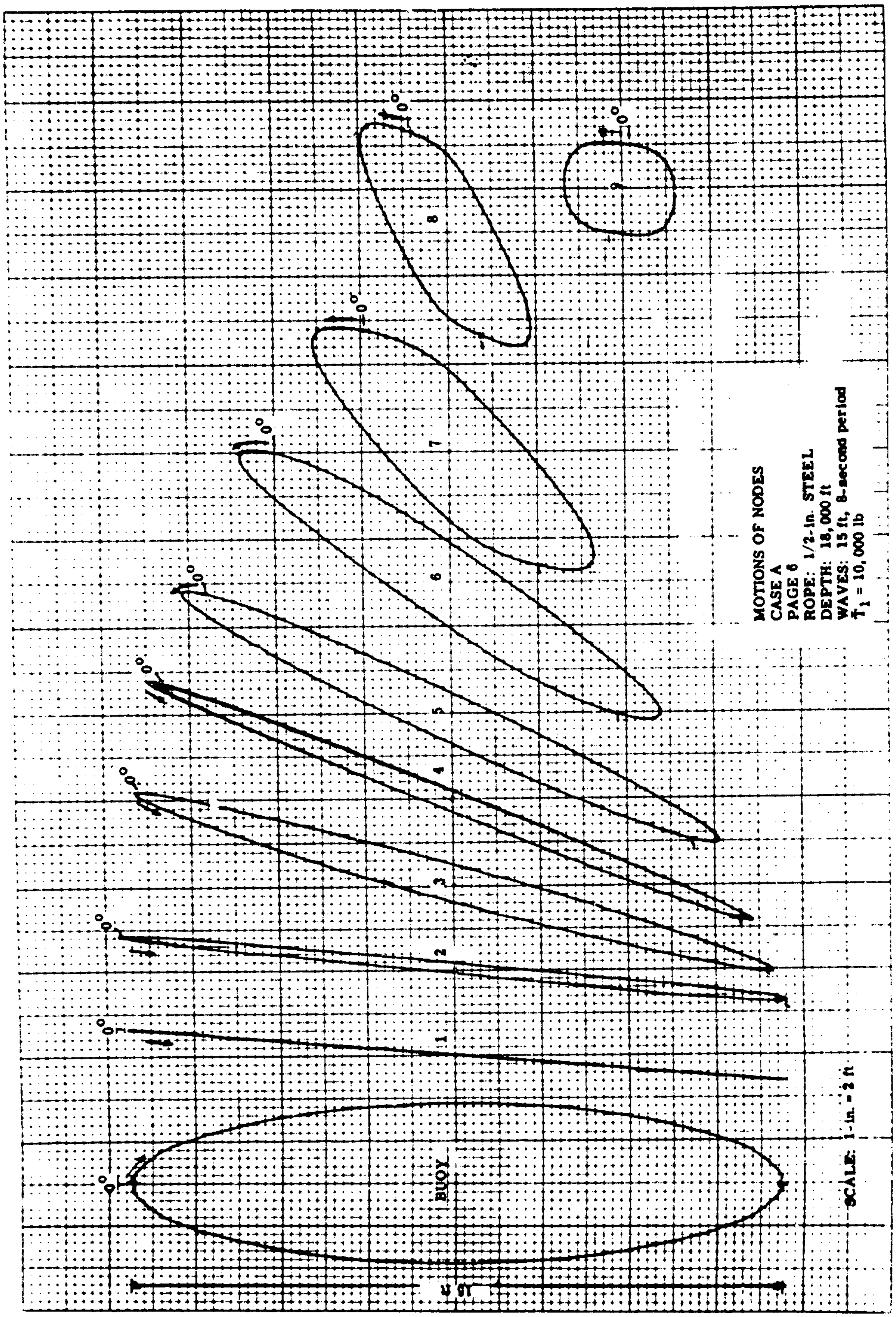
MOTIONS OF NODES
CASE A
PAGE 6
ROPE: 1/2-in. STEEL
DEPTH: 18,000 ft
WAVES: 15 ft, 8-second period
T_1 = 10,000 lb
SCALE: 1-in. = 2 ft
BUOY
16 ft
1
2
3
4
5
6
7
8
9
0°

Figure 10

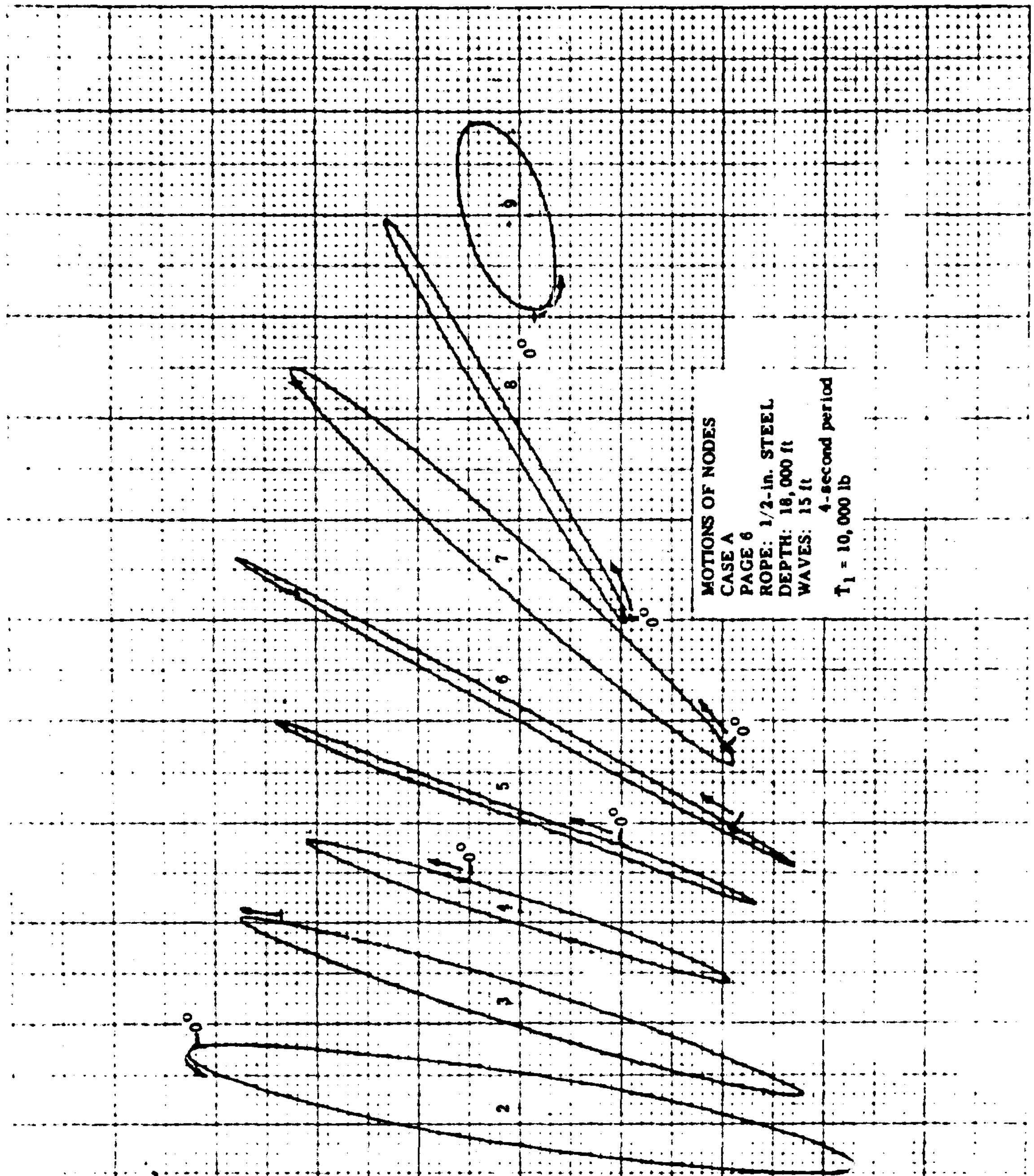
MOTIONS OF NODES
CASE A
PAGE 6
ROPE: 1/2-in. STEEL
DEPTH: 18,000 ft
WAVES: 15 ft
4-second period
T_1 = 10,000 lb
BUOY
SCALE: 1 in. = 2 ft
15 ft
1
2
3
4
5
6
7
8
9
0°

Figure 11

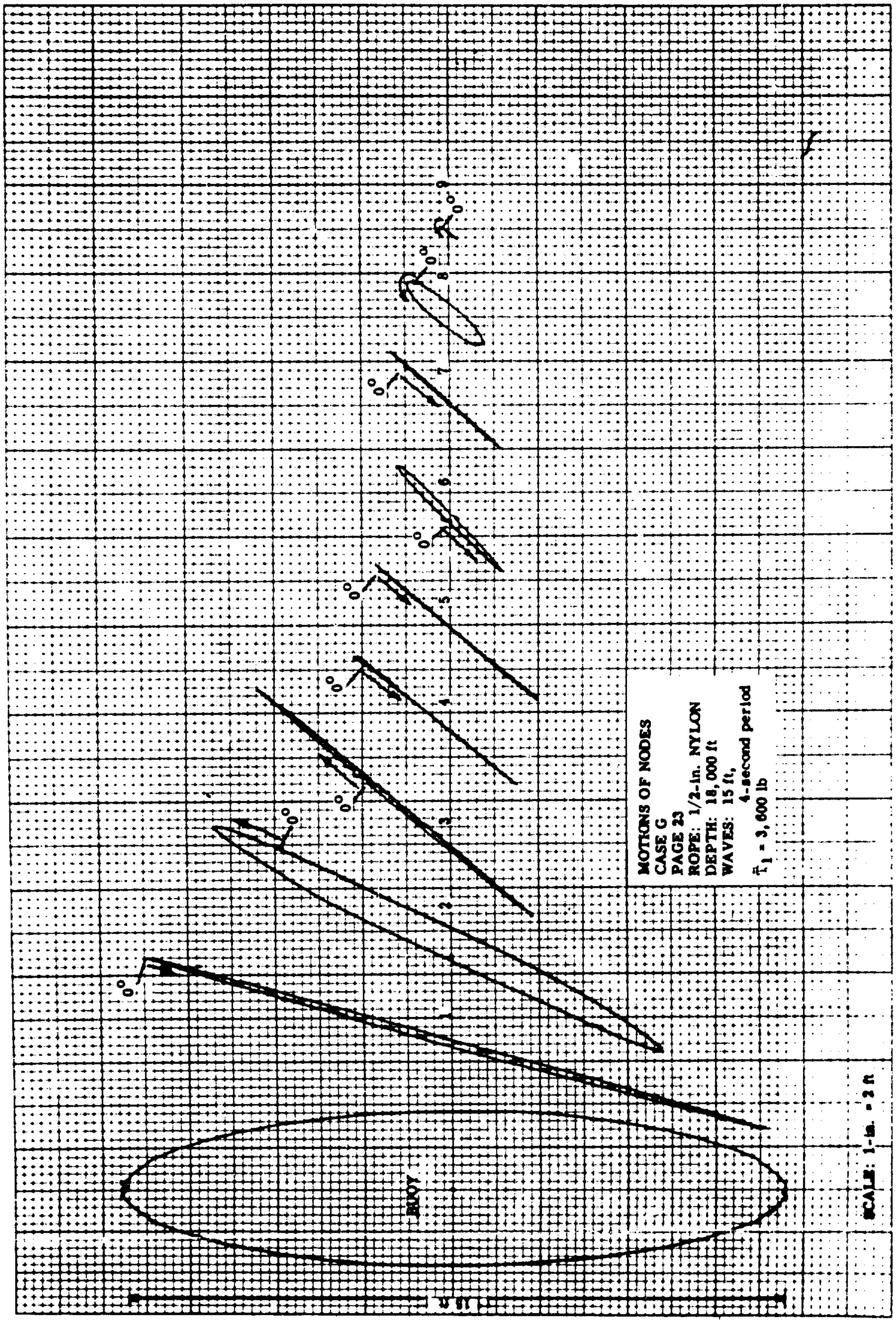
MOTIONS OF NODES
CASE G
PAGE 23
ROPE: 1/2-in. NYLON
DEPTH: 18,000 ft
WAVES: 15 ft, 4-second period
$\bar{T}_1$ = 3,600 lb
SCALE: 1-in. = 2 ft
BUOY
18 ft

Figure 12

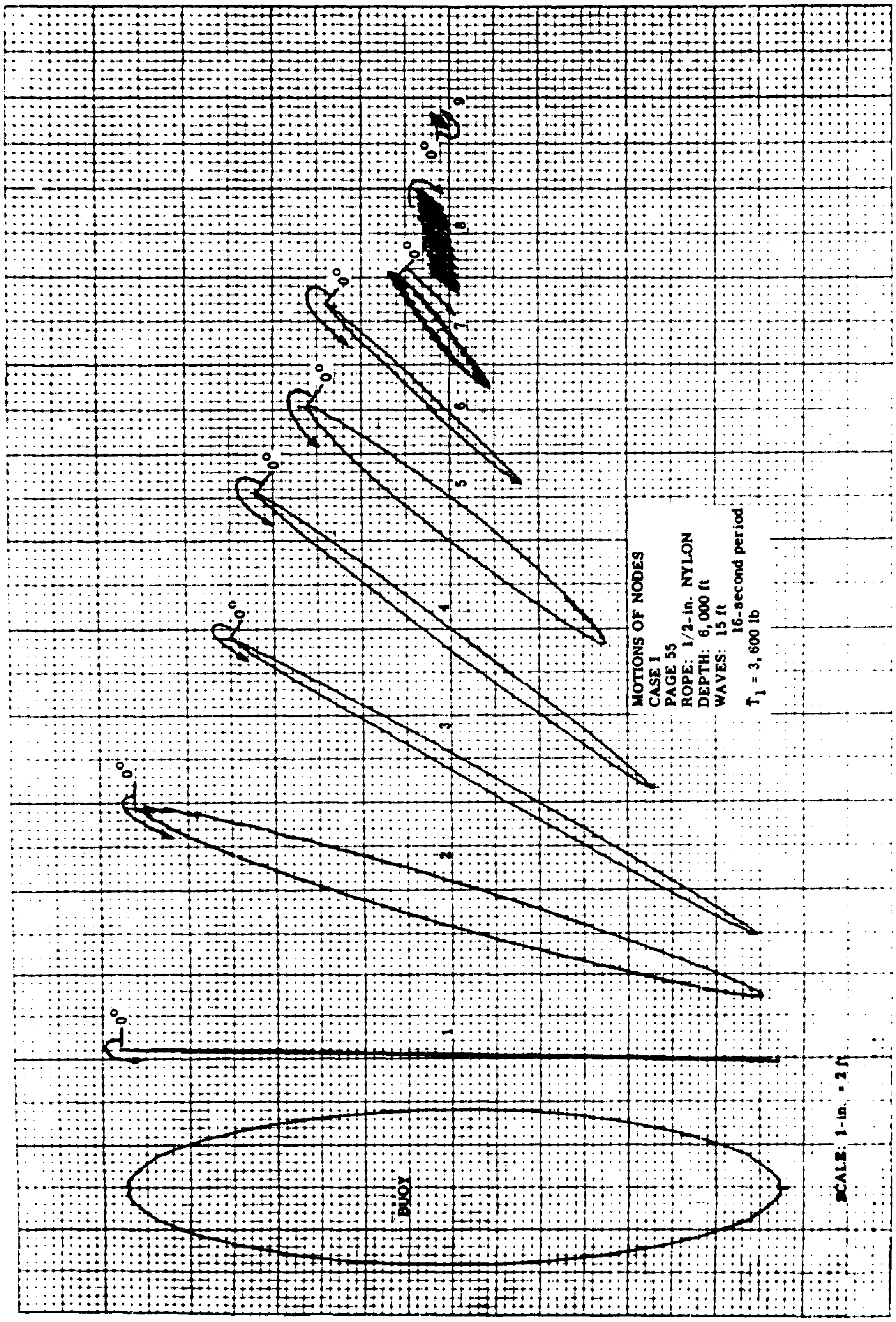
MOTIONS OF NODES
CASE I
PAGE 55
ROPE: 1/2-in. NYLON
DEPTH: 6,000 ft
WAVES: 15 ft
16-second period
T_1 = 3,600 lb
BUOY
SCALE: 1-in. = 2 ft
0°
1
2
3
4
5
6
7
8
9

Figure 13

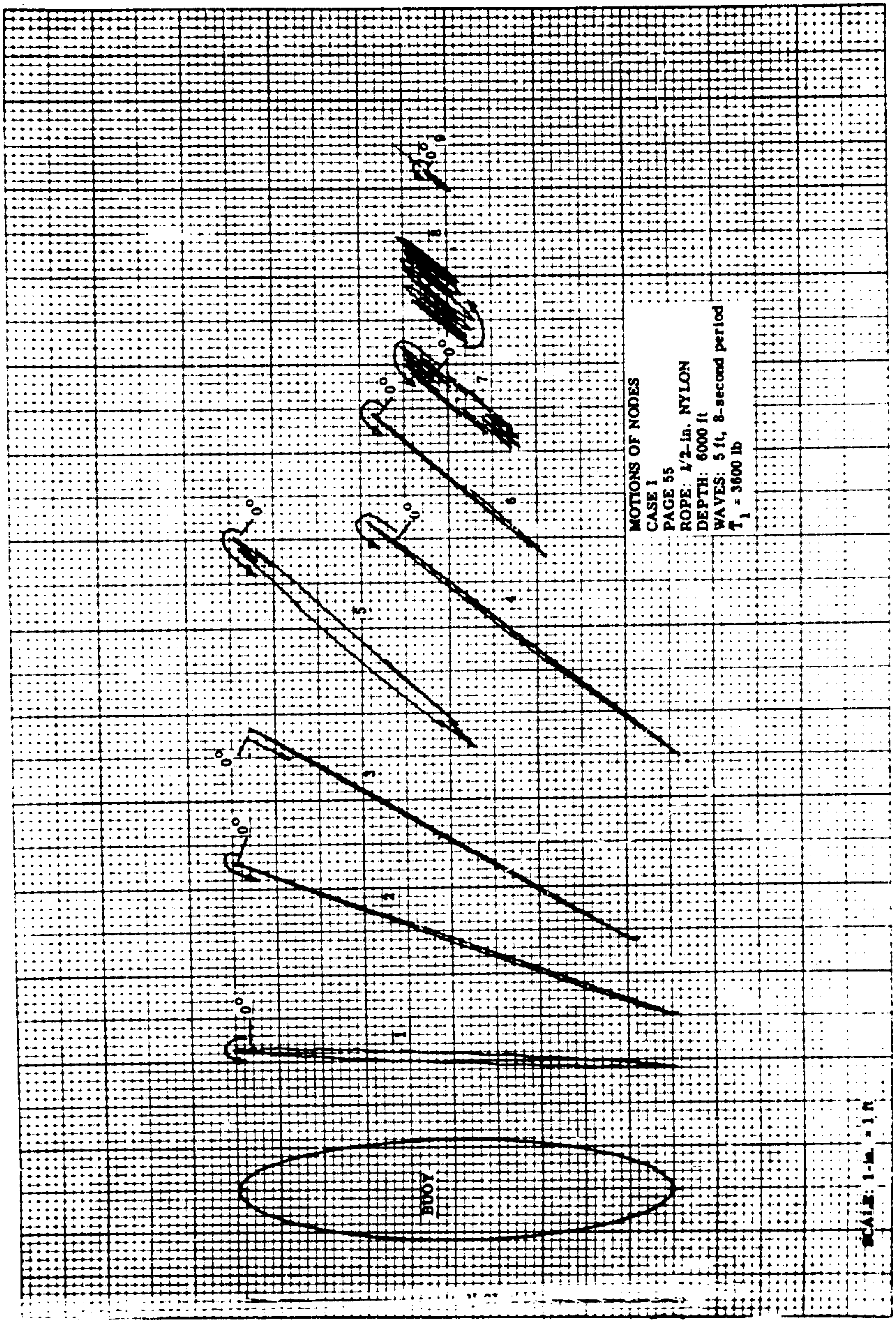
MOTIONS OF NODES
CASE I
PAGE 55
ROPE: 1/2-in. NYLON
DEPTH: 6000 ft
WAVES: 5 ft, 8-second period
T_1 = 3600 lb
BUOY
SCALE: 1-in. = 1 ft

Figure 14

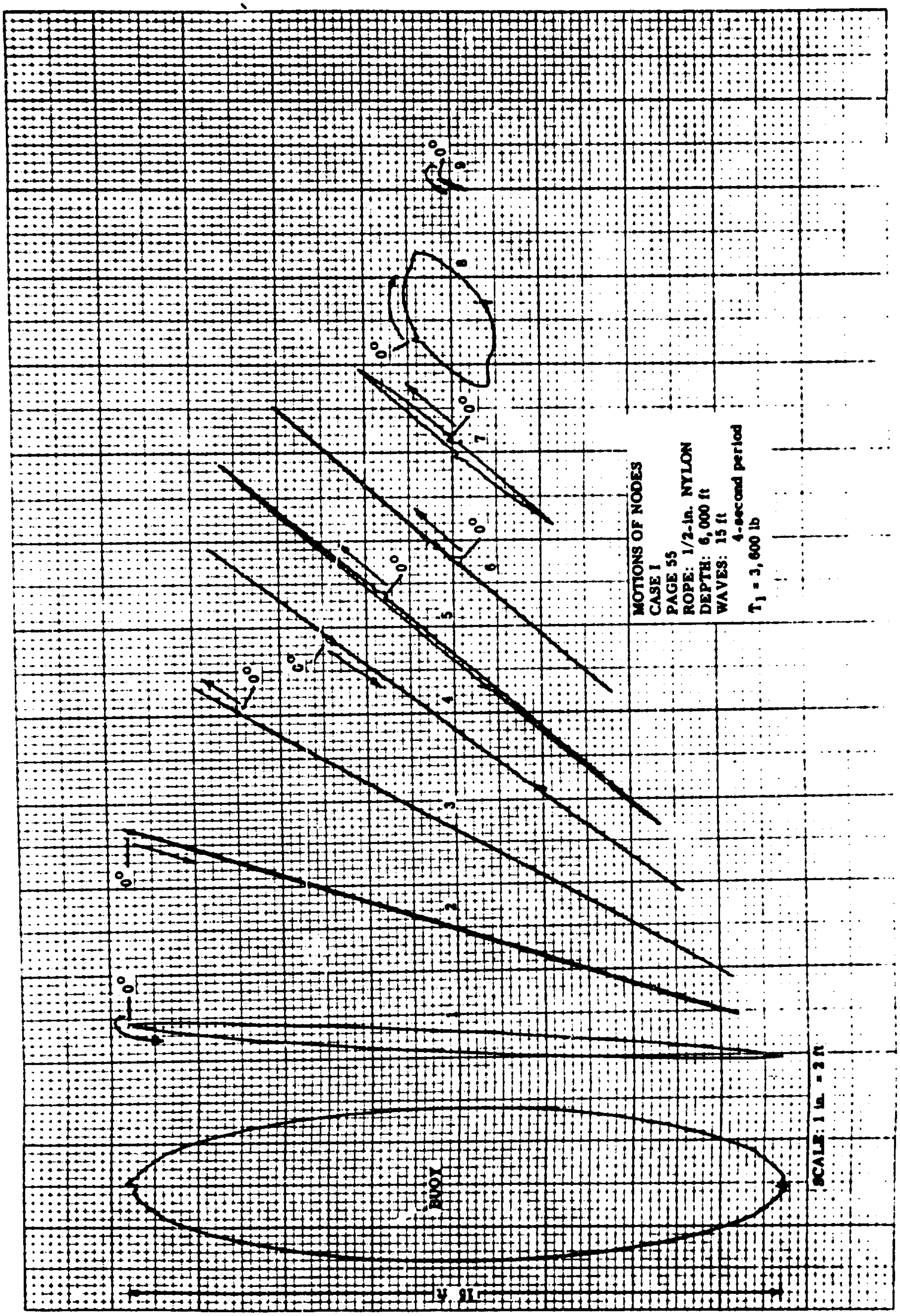
MOTIONS OF NODES
CASE I
PAGE 55
ROPE: 1/2-in. NYLON
DEPTH: 6,000 ft
WAVES: 15 ft
4-second period
T_1 = 3,600 lb
BUOY
SCALE: 1 in. = 2 ft
16 ft

Figure 15

visually, and the results are tabulated in Section VI, Motions of Nodes. These tables give the lengths of the major and minor axes of the quasi-elliptical motions in feet. In addition, at each node they give the mean rope angle ι_n and the angle of the major axis of the loop, both measured from the vertical. Toward the bottom of the mooring line where the loops sometimes were more nearly circular, the choice of major axis direction was subjective.

Each loop of the x-y plot has two phase marks, sometimes difficult to discern, consisting of small perturbations deliberately introduced into the record when the input ellipse was at its maximum at the top or its minimum at the bottom. These marks, identified when necessary and marked as 0^o and 180^o by referring to the scale on the resolver generating the input, served as reference marks to measure the phase of the major axis of the loop. Positive phase angle was indicated when the major axis occurred later in time than the zero-degree phase mark. We discovered later that the phases had been read incorrectly, and since they are of minor importance, they were omitted.

There are no data on motions of nodes for the 10-segment simulation of Case D, the case which prompted the decision to convert to a 4-segment simulation. The dynamic tensions were recorded and tabulated, however, for both 10-segment and 4-segment simulations.

Noise and Offsets

Noise in the system most likely arose from the wiper contacts of the resolvers. These small noise sources probably were exciting the individual vibrating systems formed by current meter masses and the connecting rope segments. Although this noise was regarded as a nuisance in the idealized solution of the problem, it possibly has some real significance. Noise sources equivalent to the wiper noise must exist in a real mooring and must excite similar real behaviors.

An interesting behavior in some of the dynamic records, both strip-charts and x-y plots, was the development of an offset from the original mean value. This was quite troublesome when the offset was too great to be overcome by the offset controls on the recorders, making it necessary to record x-y plots in an unnatural order or to reduce the gain on the strip-chart recorder with a consequent loss of accuracy. This, too, is a phenomenon with probably some real basis, since the mooring is a nonlinear system and some rectification of cyclic displacements and tensions would be expected.

IV. DISCUSSION OF RESULTS

STATIC ROPE SHAPES AND TENSIONS

Accuracy

Neglecting, for the moment, the reduction of rope diameter with stretch, we believe that the error in rope shape and tension is in the region of 2 percent, with the possibility of larger errors near the bottom where rope curvature is occasionally quite sharp. This conclusion is prompted by the favorable comparisons with Wilson's results.[2] Bear in mind that, except for the two check cases, our ropes have current meters at the nodes and a simulated horizontal buoy drag – hence, they cannot be compared directly to ropes not containing these.

Like Wilson, we have neglected the reduction in rope diameter with tension. (Otherwise, each change of tension would have required a time-consuming recomputation and change of potentiometer settings.) This amounts to only one or two percent in steel or glass rope but to much more in nylon. In nylon the elongation at half the breaking strength is about 42 percent, resulting in a reduction of rope diameter from 10 to 20 percent. (This is a behavior for which we have no experimental data.) Hence, at high tensions the water drag would be correspondingly reduced so that the rope would be straighter than calculated. However, with a slightly larger rope that has been reduced to the nominal size by stretching, the results would be directly applicable.

Adequacy of Method

Wilson's digital-computer solution[2] is relatively easy to carry out and probably less expensive than the method used here. However, much of the thinking that went into setting up the analog computer for the static case was introductory to the dynamic case and thus doubly useful. In any further studies we would probably use digital methods to establish static rope shapes and tensions.

Comparison of Rope Shapes

To give some feeling for the peculiarities of different ropes, several rope shapes in Current Profile 3 are presented in Figures 16 and 17 where ropes of different materials and diameters are compared when the tension at the buoy is half the breaking strength.

In 18,000 feet of water the less dense ropes, nylon and glass, form relatively straight lines and the 1/2-inch nylon is carried out to a horizontal displacement that is 3.7 times as great as the 2-inch nylon. This results from the fact that the drag/strength ratio in vertical ropes is inversely proportional to the rope diameters. The relation between rope diameter and horizontal displacement is complex and it may be only a coincidence that the observed 3.7 is so close to 4.0. The obvious conclusion is that large buoys with mooring lines of large diameter may be held closer to the anchor than small buoys.

The 1/2-inch steel rope, with its high density, shows a pronounced catenary and a correspondingly substantial horizontal displacement comparable to that of the 1/2-inch nylon. If steel were to be compared with nylon at the same strength, we would expect relative drag to increase in the steel rope as diameter is reduced, with consequent larger displacements.

Glass rope yields the least displacement of all because of its high strength and low density. However, as will be apparent below, such short tethers with ropes that have high spring constants will produce high transient tensions when the buoy is lifted by waves.

In 6,000 feet of water the 1/2-inch steel rope shows much less displacement than the 1/2-inch nylon, because now it no longer contains the highly curved lower catenary. Drawn as tautly as in Figure 17, the steel, like the glass, will show high transient tensions in waves.

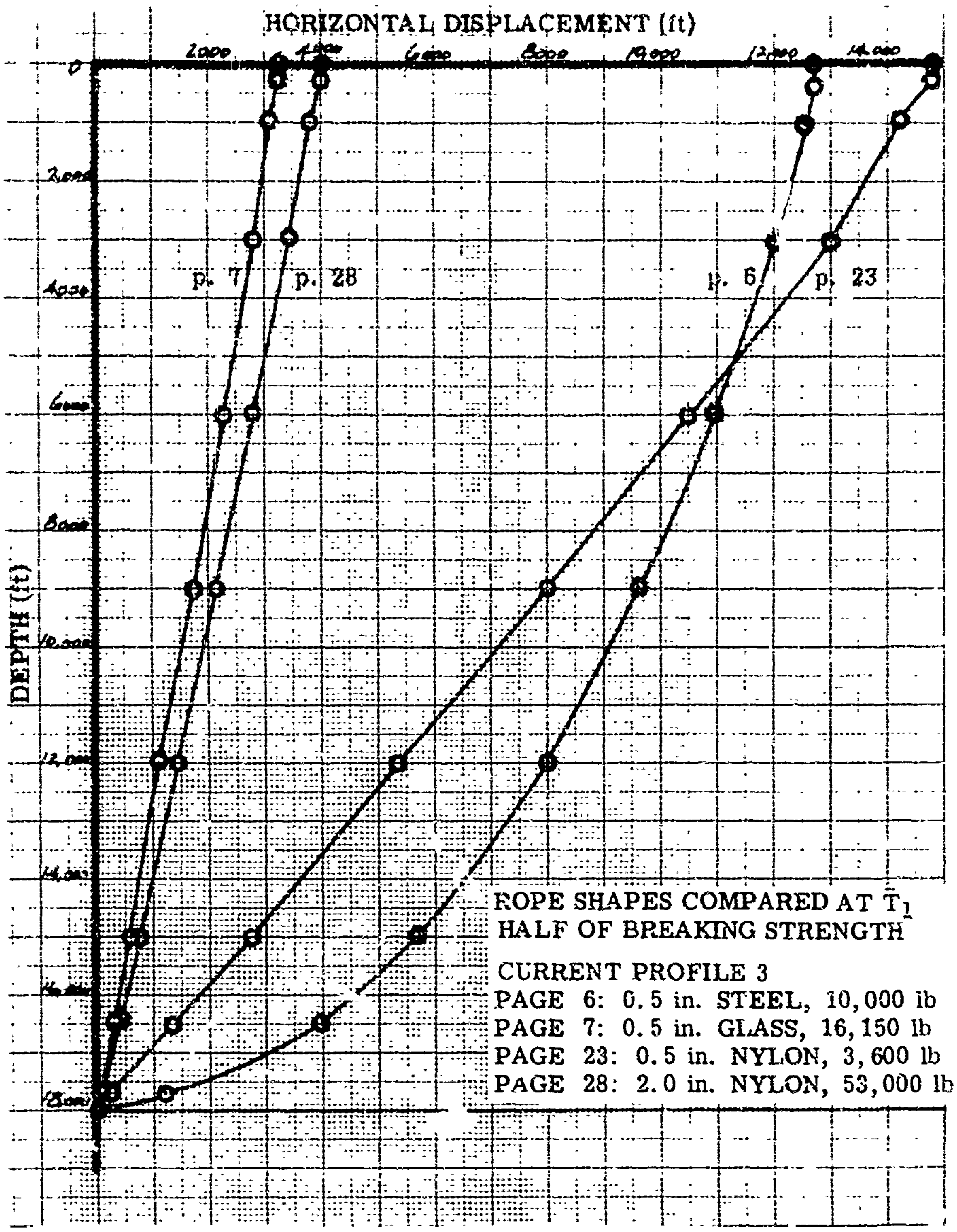
HORIZONTAL DISPLACEMENT (ft)
2000
4000
6000
8000
10,000
12,000
14,000
0
2,000
4,000
6,000
8,000
10,000
12,000
14,000
16,000
DEPTH (ft)
p. 7
p. 28
p. 6
p. 23
ROPE SHAPES COMPARED AT $\bar{T}_1$
HALF OF BREAKING STRENGTH
CURRENT PROFILE 3
PAGE 6: 0.5 in. STEEL, 10,000 lb
PAGE 7: 0.5 in. GLASS, 16,150 lb
PAGE 23: 0.5 in. NYLON, 3,600 lb
PAGE 28: 2.0 in. NYLON, 53,000 lb

Figure 16

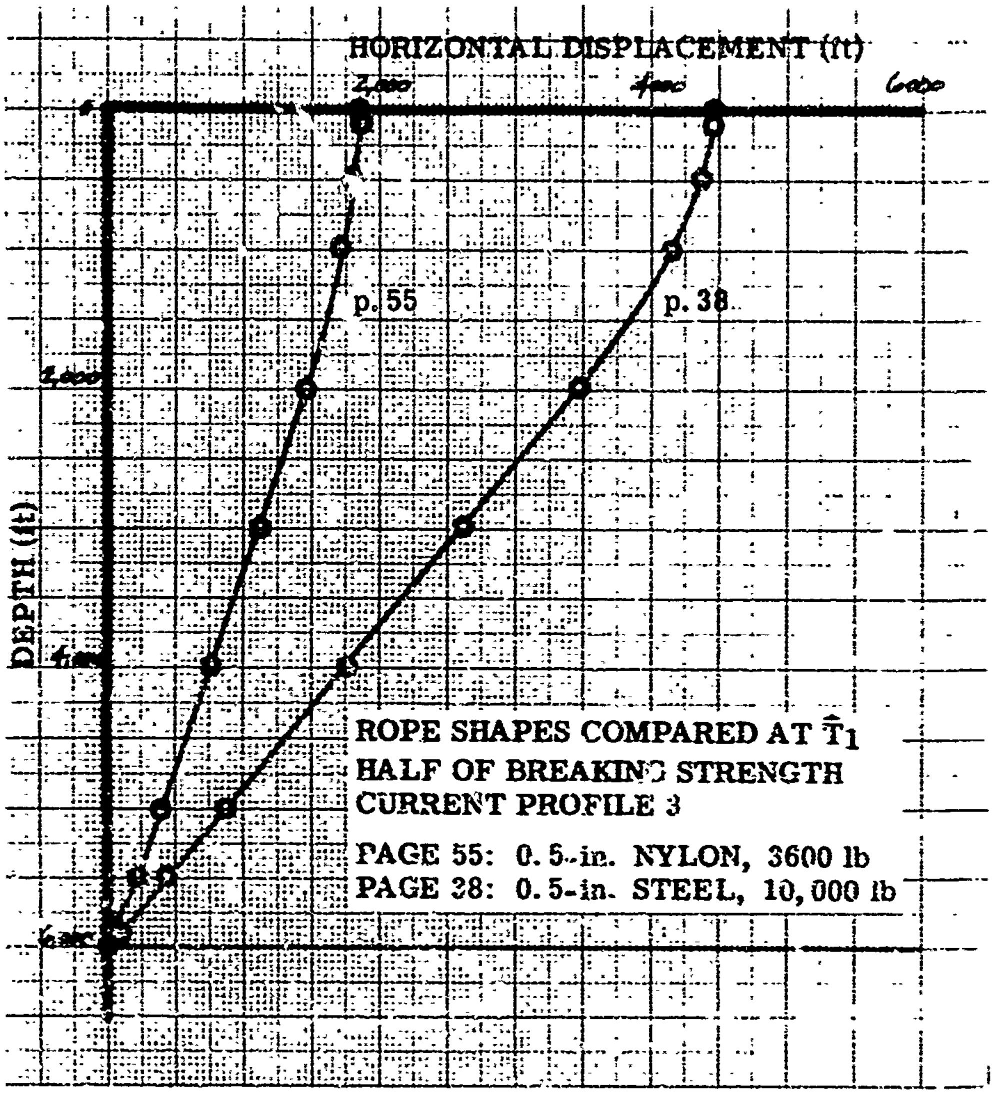
HORIZONTAL DISPLACEMENT (ft)
2,000
4,000
6,000
DEPTH (ft)
2,000
4,000
6,000
p. 55
p. 38
ROPE SHAPES COMPARED AT $\hat{T}_1$
HALF OF BREAKING STRENGTH
CURRENT PROFILE 3
PAGE 55: 0.5-in. NYLON, 3600 lb
PAGE 38: 0.5-in. STEEL, 10,000 lb

Figure 17

DYNAMIC DISPLACEMENTS AND TENSIONS

Accuracy

The results contain three types of errors: those inherent in the simulation, those due to an incorrect choice of constants, and those caused by human error in reading data from the charts.

The principal errors in the dynamic simulation itself arise from:

- deficiencies of the 4-segment simulation, or the less serious deficiencies of the 10-segment simulation
- approximations made in solving the equations of motion
- inability to provide for all the effects of hysteresis in nylon rope
- the necessity of choosing a fixed value of elasticity for nylon rope

Inadequacies of the 10-segment simulation are negligible compared to the other errors.

We lack a good estimate of the error due to converting to the 4-segment simulation; and the only comparison we have between the 4- and the 10-segment simulations is for Case D, which unfortunately is the one in which there should be by far the greatest error. In spite of the likelihood of conclusions that are too pessimistic, we compare tensions in the two simulations, plotted as a function of wave period (Figs. 18 and 19). The two compare well in some regions and poorly in others. The general tendency for this particular 4-segment simulation to show higher tensions than the 10-segment simulation was accounted for in Section II. The two simulations should become more nearly the same at shorter wave periods, because the resulting higher drag and inertia in the mooring would induce stretching rather than lifting. The curves do agree, to some extent, at short periods; but the tensions at Node 1 in the 4-segment case deviate sharply downward near the 3-seconds period. Since a bit of the same phenomenon shows in the 10-segment data, we suspect a mechanism that exaggerates the response at this period in the simpler simulation.

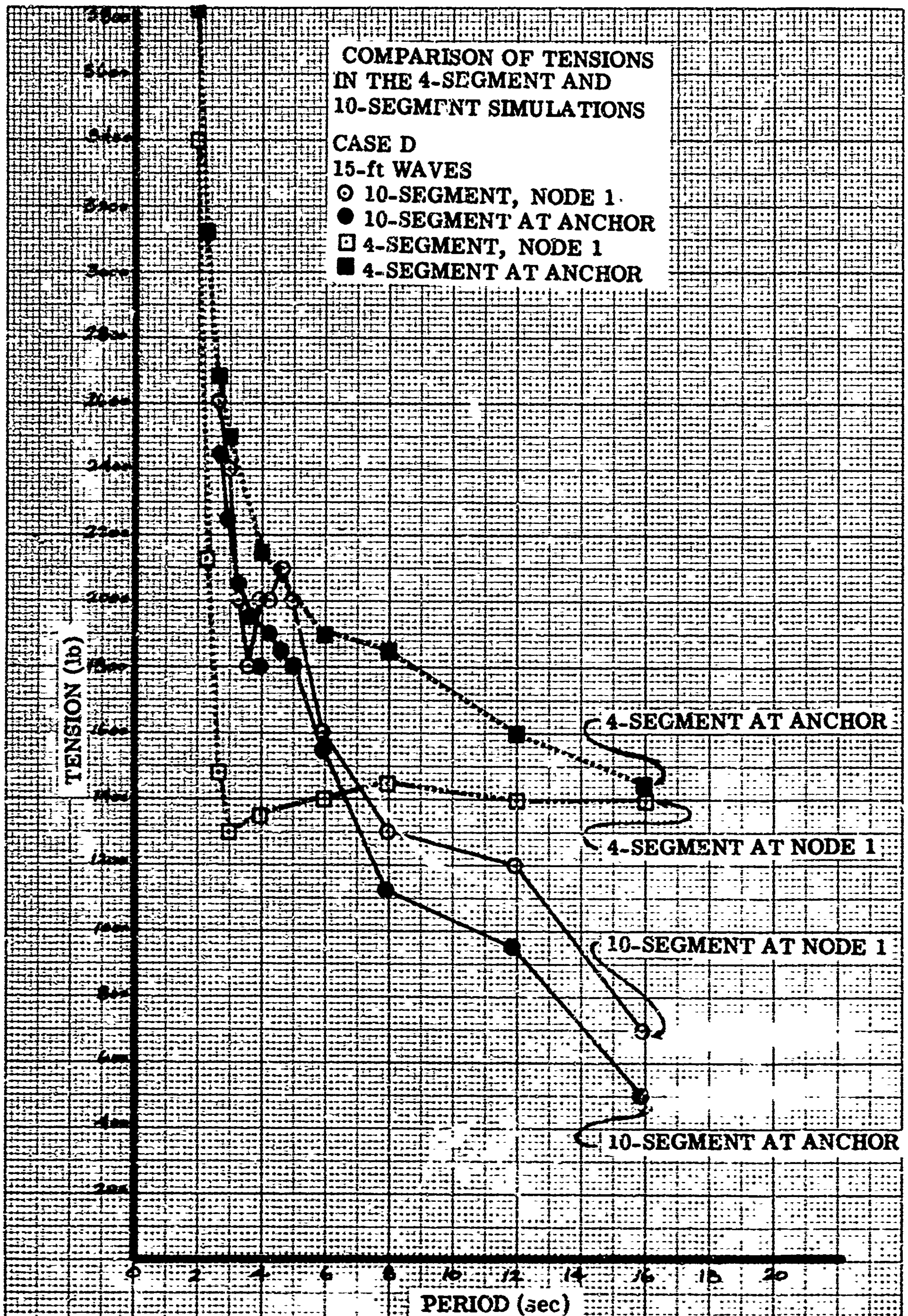
COMPARISON OF TENSIONS IN THE 4-SEGMENT AND 10-SEGMENT SIMULATIONS
CASE D
15-ft WAVES
10-SEGMENT, NODE 1
10-SEGMENT AT ANCHOR
4-SEGMENT, NODE 1
4-SEGMENT AT ANCHOR
4-SEGMENT AT ANCHOR
4-SEGMENT AT NODE 1
10-SEGMENT AT NODE 1
10-SEGMENT AT ANCHOR
TENSION (lb)
PERIOD (sec)
0
2
4
6
8
10
12
14
16
18
20

Figure 16

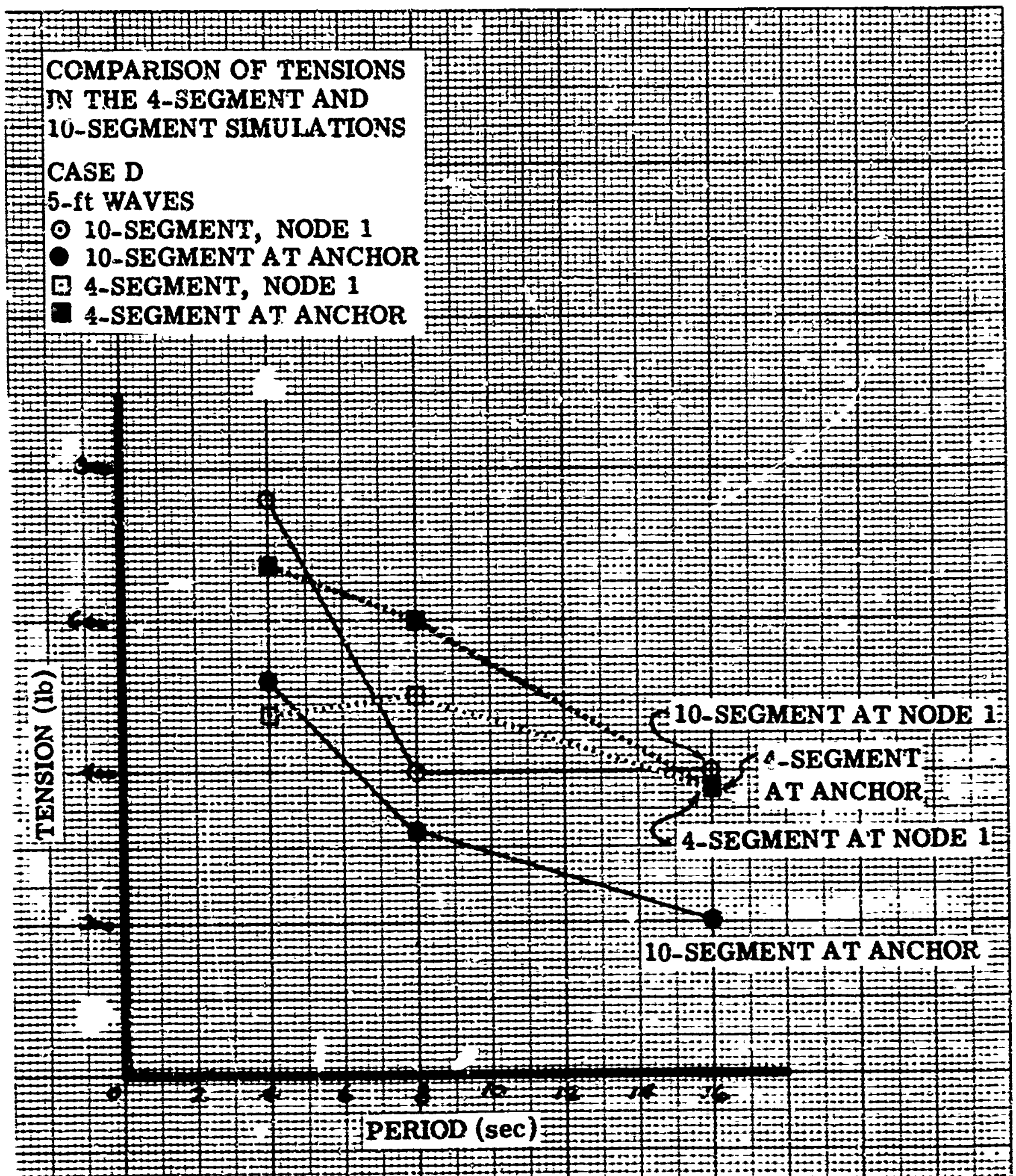
COMPARISON OF TENSIONS
IN THE 4-SEGMENT AND
10-SEGMENT SIMULATIONS
CASE D
5-ft WAVES
⊙ 10-SEGMENT, NODE 1
● 10-SEGMENT AT ANCHOR
□ 4-SEGMENT, NODE 1
■ 4-SEGMENT AT ANCHOR
TENSION (lb)
PERIOD (sec)
10-SEGMENT AT NODE 1
4-SEGMENT
AT ANCHOR
4-SEGMENT AT NODE 1
10-SEGMENT AT ANCHOR
0
2
4
6
8
10
12
14
16

Figure 19

The explanation is as follows: Pronounced near-resonance phenomena of which this must be an example, should occur only in ropes that are long enough or at periods that are short enough to make the rope length nearly an integral number of quarter-wavelengths for the travel of a longitudinal elastic wave through the rope. In 1/2-inch steel rope, the velocity of an undamped longitudinal wave is 10,350 ft/sec. When the rope length is 6,580 feet, as in Case D, the buoy would first become a standing-wave node, with a consequent maximum decrease in tension, at a period of (4)(6580)/10,350 = 2.54 sec. Because of damping, the period is actually longer. The conclusion must be that the four-segment rope with its lesser curvature is stretching more at short periods, as well as at long periods – hence the exaggeration of phenomena associated with stretching. At the anchor, where the phase difference is only about a quarter-wavelength, the agreement at short periods is good.

We admit that as a measure of accuracy it would be more satisfying to bring forward two cases which should act the same. But without any other duplications, we must be satisfied with the argument given above. Although there is little basis for a quantitative estimate of error, we suggest that the error due to using a four-segment simulation is less than a factor of 1.3, or 1/1.3, in all instances except Cases D and L.

As mentioned in the Appendix, the approximations made in simplifying the perturbation equations produced significant error in two cases,* both steel rope in 1,800 feet of water, at 50- and 25-foot wave heights. In these, the errors in the matrix quantity K_n were a negative 34 and 24 percent. In all other cases the errors in K_n were less than 20 percent. Tension error will not be so large, since tension is not directly proportional to K_n ; consequently, we may expect the recorded tensions to be a little low in the more extreme cases (steel rope, short length, large waves).

---

* Cases E and F.

The effects of neglecting hysteresis in nylon are difficult to estimate. As pointed out, a dynamic spring constant that is different from the slope of the slowly developed stress-strain curve is one of the effects of hysteresis. By using a dynamic spring constant, we have partially provided for hysteresis. But the necessity of using a mean value of the constant has resulted in a spring that is too resilient at the higher wave heights, so that the observed tensions in nylon are too low at the 50-foot wave heights; and, conversely, they are too high at the 5-foot wave heights.

The energy loss due to the hysteresis loop is a significant factor, one far greater than longitudinal drag near the bottom of the rope (where dynamic drag effects are small). We would expect, therefore, that in nature there will be more attenuation of the longitudinal elastic wave, lower tensions at the anchor, and shifted and reduced resonance effects.

The use of the nominal rope diameter instead of the stretched diameter fortunately produced little error. It was estimated earlier that at 3,600 lb mean tension the diameter of the rope will decrease 10–20 percent. The assumption of a fixed nominal diameter causes the rope to show, incorrectly, a larger lateral drag which reduces the tendency of the rope to straighten out when pulled and forces more motion into the stretching mode. However, since a substantial proportion of the wave motion already is acting in the stretching mode (because lateral drag is fairly high in nylon in comparison to the elastic forces) little error need be expected. *

Human errors are confined mainly to reading charts. The probable errors from misreading the strip charts are limited to ± 15 percent. Dimensions of the nodal ellipses generally could be read to within one-fourth of a small division, or 0.025 foot for 5-foot waves, 0.05 foot for 15-foot waves and 0.25 foot for 50-foot waves.

* It must be pointed out that since the static rope shapes are somewhat in error for the same reason, the dynamic simulation was applied to rope shapes that do not correspond exactly to the assumed current-wind conditions.

Displacements of Nodes

The displacements of nodes are generally in quasi-elliptical loops, decreasing in size from top to bottom. In taut ropes that are relatively straight, the motion tends to be nearly longitudinal, along the rope, with very little lateral motion, especially at the shorter periods. (As has been explained, more motion goes into the longitudinal stretching mode at short periods.) In the sharply curved catenaries, the loops open up into almost rectangular shapes near the bottom of the rope because of the large proportion of lifting and the change of curvature taking place in this region. Because they are more curved than nylon ropes, steel ropes give more open loops.

The Effect of Displacements on Current Meters

It is difficult to make a simple general statement about current meter errors from these complex results. Let us exclude from consideration the steel ropes, which have large curvatures and excessive nodal movement, and examine the nylon moorings, which show the smallest motions.

As an average condition, consider ropes oscillating at a 16-second period in 15-foot waves. In Cases G, H, I, and J, the length of the minor axis is relatively constant at all depths, averaging slightly greater than 0.3 ft. (Cases K and L, which show much more displacement, are left to be mentioned later.) We shall ignore momentarily the effect of axial motion on the meter; and to come a little closer to reality we shall change the period to one more probable in the sea and assume that these same displacements would occur at a 12-second period. Then, in still water a current meter which cannot distinguish positive water motion from negative would be exposed to cumulative apparent water motion of (0.3) (2)/12 or 0.05 ft/sec. In moving water at speeds greater than 0.05 ft/sec, the mean error would disappear if the speed sensor were ideal. However, it is well known that rotors tend to over-register in fluctuating flow, so some effect always would remain.

The effect on current meter sensors of motion normal to the sensitive axis of the speed sensor* is not well known. Gaul[19] showed that Savonius rotors ran

* We call this "axial motion" for want of a more rigorous term.

significantly slower when oscillated axially only one or two feet. Gaul ran no tests in still water where it is likely that spurious rotor turns would have been produced by the turbulence around the meter. Had he tested bucket wheels and propellers, he would have found marked increases in apparent velocity (see Paquette, Ref. 20).

Probably more important than pure axial motion is axial motion combined with a slight dynamic tilting of the current meter, a not improbable behavior of a long massive body on a disturbed rope. This kind of behavior would cause additional errors in apparent speed that would be largest near the surface.

Cases K and L have been ignored until now because our results indicate that simple moorings in such shallow water in the open sea are undesirable from the point of view of both nodal motion and dynamic tensions. It is sufficient to note that the lateral motion is nearly seven times greater than in moorings in deeper water.

We believe that near wave frequency an erroneous apparent speed vector of 0.05 ft/sec (1.5 cm/sec) is smaller than that observed in practice. We must, therefore, conclude that axial motion combined with dynamic tilting of the meter is responsible for as much or more error than that caused by lateral motion.

We wish to avoid leaving the uninitiated with an impression that we have now expressed the principal sources of current meter error. We have studied only those errors which can be ascribed directly to the action of waves on a buoy at the surface. The sources of what has been called "mooring noise" are numerous and serious. The simple fact that rope is flexible and that it may yield locally or in toto to turbulent forces of all time scales and from any direction leads to a spectrum of velocity errors that are beyond the scope of this report.

V. CONCLUSIONS

For a system consisting of a buoy excited by ocean waves and anchored to the bottom by a simple mooring, we make the following conclusions:

1. All points in the mooring rope undergo quasi-elliptical motion, with the loops usually elongated approximately along the rope direction.
2. The motion is probably large enough to account for the errors observed at wave frequency in moored current meters if motion along the rope direction can be assumed to contribute some error.
3. Fairly taut, resilient ropes of low density, like nylon, produce the least lateral motion and probably the smallest current meter errors if depths significantly less than 6,000 feet are avoided.
4. Dynamic tensions are moderate in long ropes and those buffered by resilience or [illegible] a well developed catenary. In taut, only slightly curved ropes [illegible]eel, dynamic tensions can rise to dangerous values in storms; this can happen even in moderate weather if the ropes are as short as about 1,800 feet. Resilient, synthetic fiber ropes develop much lower dynamic tensions, even when the ratio of dynamic tension to breaking strength is considered.
5. Resonances develop in the ropes, but tensions due to them are small compared to those generated by the more direct mechanisms. (Exceptions occur in moderately short ropes, but only at the short resonant periods where there is little wave energy.)

VI. DATA

CABLE CONFIGURATIONS AND TENSIONS

CABLE MATERIAL STEEL
CURRENT PROFILE 2
T SUB(1) 10000 LBS

CABLE DIAMETER 0.5 IN
OCEAN DEPTH 18000 FEET
PAGE 3

N	X SUB(N) BAR FEET	Y SUB(N) BAR FEET	CABLE LENGTH FEET	MEAN TENSION LBS	THETA SUB(N) BAR DEGREES
0	0	829	18033	10052	1.2
1	300	823	17734	9992	1.2
2	1500	794	16533	9664	1.4
3	3000	756	15038	9092	1.4
4	6000	679	12032	8163	1.7
5	9000	568	9023	6926	2.0
6	12000	450	6015	5693	2.6
7	15000	269	2995	4465	3.3
8	16500	173	1511	3539	4.2
9	17700	41	302	2961	5.0
10	18000	-0	-0	2634	6.1
ANCHOR				2572	6.1

CABLE MATERIAL STEEL
CURRENT PROFILE 2
T SUB(1) 7634 LBS

CABLE DIAMETER 0.5 IN
OCEAN DEPTH 18000 FEET
PAGE 4

N	X SUB(N) BAR FEET	Y SUB(N) BAR FEET	CABLE LENGTH FEET	MEAN TENSION LBS	THETA SUB(N) BAR DEGREES
0	0	2270	18505	7688	1.5
1	300	2263	18205	7628	1.5
2	1500	2223	17004	7297	1.9
3	3000	2171	15511	6729	1.9
4	6000	2064	12502	5800	2.2
5	9000	1893	9485	4566	3.0
6	12000	1688	6466	3330	4.5
7	15000	1299	3417	2094	7.1
8	16500	1036	1919	1175	12.8
9	17700	552	629	613	27.1
10	18000	-0	-0	310	64.4
ANCHOR				274	89.2

CABLE CONFIGURATIONS AND TENSIONS

CABLE MATERIAL STEEL
CURRENT PROFILE 3
T SUB(1) 20000 LBS

CABLE DIAMETER 0.5 IN
OCEAN DEPTH 18000 FEET
PAGE 5

N	X SUB(N) BAR FEET	Y SUB(N) BAR FEET	CABLE LENGTH FEET	MEAN TENSION LBS	THETA SUB(N) BAR DEGREES
0	0	3142	18339	20059	2.1
1	300	3131	18039	19984	2.0
2	1500	3010	16831	19630	5.8
3	3000	2788	15320	19063	8.4
4	6000	2323	12262	18134	9.1
5	9000	1808	9197	16891	9.6
6	12000	1258	6128	15649	10.5
7	15000	654	3049	14410	11.4
8	16500	344	1537	13484	12.2
9	17700	71	308	12916	12.9
10	18000	-0	-0	12589	13.1
ANCHOR				12527	13.2

CABLE MATERIAL STEEL
CURRENT PROFILE 3
T SUB(1) 10000 LBS

CABLE DIAMETER 0.5 IN
OCEAN DEPTH 18000 FEET
PAGE 6

N	X SUB(N) BAR FEET	Y SUB(N) BAR FEET	CABLE LENGTH FEET	MEAN TENSION LBS	THETA SUB(N) BAR DEGREES
0	0	12732	23315	10210	4.0
1	300	12711	23013	10129	4.0
2	1500	12468	21789	9754	11.5
3	3000	12003	20215	9193	17.1
4	6000	10950	17052	8268	19.5
5	9000	9674	13797	7047	23.2
6	12000	8040	10387	5824	28.5
7	15000	5769	6624	4580	37.4
8	16500	4053	4364	3671	49.2
9	17700	1725	1745	3127	63.5
10	18000	-0	-0	2823	79.9
ANCHOR				2785	87.0

CABLE CONFIGURATIONS AND TENSIONS

CABLE MATERIAL GLASS
CURRENT PROFILE 3
T SUB(1) 16150 LBS

CABLE DIAMETER 0.5 IN
OCEAN DEPTH 18000 FEET
PAGE 7

N	X SUB(N) BAR FEET	Y SUB(N) BAR FEET	CABLE LENGTH FEET	MEAN TENSION LBS	THETA SUB(N) BAR DEGREES
0	0	3240	18366	16174	2.4
1	300	3228	18066	16151	2.5
2	1500	3078	16856	16043	7.0
3	3000	2815	15335	15927	9.9
4	6000	2282	12263	15750	10.4
5	9000	1733	9190	15518	10.4
6	12000	1172	6118	15286	10.6
7	15000	599	3042	15054	10.7
8	16500	303	1527	14879	10.9
9	17700	60	305	14763	11.2
10	18000	-0	-0	14677	11.2
ANCHOR				14666	11.1

CABLE MATERIAL GLASS
CURRENT PROFILE 3
T SUB(1) 8075 LBS

CABLE DIAMETER 0.5 IN
OCEAN DEPTH 18000 FEET
PAGE 8

N	X SUB(N) BAR FEET	Y SUB(N) BAR FEET	CABLE LENGTH FEET	MEAN TENSION LBS	THETA SUB(N) BAR DEGREES
0	0	6945	19288	8135	4.8
1	300	6919	18986	8104	5.0
2	1500	6620	17749	7972	13.9
3	3000	6077	16150	7861	19.8
4	6000	4967	12961	7691	20.7
5	9000	3802	9750	7467	21.4
6	12000	2587	6519	7247	22.2
7	15000	1326	3266	7009	22.8
8	16500	663	1636	6835	23.6
9	17700	136	329	6711	23.9
10	18000	-0	-0	6645	24.4
ANCHOR				6627	24.3

CABLE CONFIGURATIONS AND TENSIONS

CABLE MATERIAL GLASS
CURRENT PROFILE 3
T SUB(1) 4845 LBS

CABLE DIAMETER 0.5 IN
OCEAN DEPTH 18000 FEET
PAGE 9

N	X SUB(N) BAR FEET	Y SUB(N) BAR FEET	CABLE LENGTH FEET	MEAN TENSION LBS	THETA SUB(N) BAR DEGREES
0	0	14147	23050	4897	8.2
1	300	14103	22747	4845	3.3
2	1500	13600	21447	4694	22.9
3	3000	12644	19676	4601	32.6
4	6000	10578	16054	4437	34.6
5	9000	8323	12302	4212	36.7
6	12000	5830	8381	3998	39.4
7	15000	3100	4313	3774	42.3
8	16500	1596	2189	3623	45.0
9	17700	332	448	3487	46.7
10	18000	-0	-0	3433	48.2
ANCHOR				3400	48.1

CABLE MATERIAL GLASS
CURRENT PROFILE 3
T SUB(1) 3910 LBS

CABLE DIAMETER 0.5 IN
OCEAN DEPTH 18000 FEET
PAGE 10

N	X SUB(N) BAR FEET	Y SUB(N) BAR FEET	CABLE LENGTH FEET	MEAN TENSION LBS	THETA SUB(N) BAR DEGREES
0	0	22846	29616	3970	10.2
1	300	22793	29312	3906	10.1
2	1500	22162	27957	3743	28.0
3	3000	20909	26025	3657	39.9
4	6000	18149	21938	3495	42.9
5	9000	14976	17584	3259	46.4
6	12000	11315	12839	3057	51.1
7	15000	6710	7352	2822	56.7
8	16500	3761	4042	2690	63.1
9	17700	854	904	2589	68.0
10	18000	-0	-0	2532	71.4
ANCHOR				2506	72.0

CABLE CONFIGURATIONS AND TENSIONS

CABLE MATERIAL GLASS
CURRENT PROFILE 4
T SUB(1) 16150 LBS

CABLE DIAMETER 0.5 IN
OCEAN DEPTH 18000 FEET
PAGE 11

N	X SUB(N) BAR FEET	Y SUB(N) BAR FEET	CABLE LENGTH FEET	MEAN TENSION LBS	THETA SUB(N) BAR DEGREES
0	0	5365	18706	16206	8.9
1	300	5318	18403	16150	8.9
2	1500	5036	17170	16047	13.4
3	3000	4599	15606	15926	16.2
4	6000	3713	12484	15760	16.7
5	9000	2810	9361	15520	16.9
6	12000	1896	6239	15291	17.2
7	15000	965	3112	15071	17.4
8	16500	485	1573	14886	17.7
9	17700	97	315	14784	18.0
10	18000	-0	-0	14698	18.0
ANCHOR				14679	17.9

CABLE MATERIAL GLASS
CURRENT PROFILE 4
T SUB(1) 8075 LBS

CABLE DIAMETER 0.5 IN
OCEAN DEPTH 18000 FEET
PAGE 12

N	X SUB(N) BAR FEET	Y SUB(N) BAR FEET	CABLE LENGTH FEET	MEAN TENSION LBS	THETA SUB(N) BAR DEGREES
0	0	12532	21907	8161	17.7
1	300	12435	21592	8070	17.9
2	1500	11837	20256	7947	26.5
3	3000	10896	18493	7846	32.2
4	6000	8921	14935	7679	33.3
5	9000	6842	11308	7469	34.6
6	12000	4663	7611	7242	35.8
7	15000	2389	3845	7009	37.2
8	16500	1204	1923	6863	38.4
9	17700	248	391	6729	39.1
10	18000	-0	-0	6656	39.6
ANCHOR				6636	39.6

CABLE CONFIGURATIONS AND TENSIONS

CABLE MATERIAL GLASS
CURRENT PROFILE 4
T SUB(1) 6460 LBS

CABLE DIAMETER 0.5 IN
OCEAN DEPTH 18000 FEET
PAGE 13

N	X SUB(N) BAR FEET	Y SUB(N) BAR FEET	CABLE LENGTH FEET	MEAN TENSION LBS	THETA SUB(N) BAR DEGREES
0	0	17587	25242	6561	22.1
1	300	17462	24918	6456	22.5
2	1500	16690	23492	6332	32.7
3	3000	15454	21550	6230	39.6
4	6000	12854	17555	6077	41.4
5	9000	10034	13437	5846	43.2
6	12000	6963	9150	5623	45.3
7	15000	3639	4679	5393	47.9
8	16500	1870	2399	5266	50.2
9	17700	380	484	5134	51.5
10	18000	-0	-0	5066	52.5
ANCHOR				5052	52.6

CABLE MATERIAL GLASS
CURRENT PROFILE 4
T SUB(1) 5444 LBS

CABLE DIAMETER 0.5 IN
OCEAN DEPTH 18000 FEET
PAGE 14

N	X SUB(N) BAR FEET	Y SUB(N) BAR FEET	CABLE LENGTH FEET	MEAN TENSION LBS	THETA SUB(N) BAR DEGREES
0	0	25520	31439	5565	26.0
1	300	25368	31104	5447	26.7
2	1500	24428	29580	5324	38.2
3	3000	22873	27430	5224	46.0
4	6000	19518	22945	5079	48.4
5	9000	15738	18120	4840	51.3
6	12000	11474	12899	4637	55.0
7	15000	6470	7079	4403	59.1
8	16500	3434	3742	4277	63.3
9	17700	737	795	4173	66.2
10	18000	-0	-0	4113	68.2
ANCHOR				4080	68.5

CABLE CONFIGURATIONS AND TENSIONS

CABLE MATERIAL GLASS
CURRENT PROFILE 5
T SUB(1) 16150 LBS

CABLE DIAMETER 0.5 IN
OCEAN DEPTH 18000 FEET
PAGE 15

N	X SUB(N) BAR FEET	Y SUB(N) BAR FEET	CABLE LENGTH FEET	MEAN TENSION LBS	THETA SUB(N) BAR DEGREES
0	0	15686	23950	16282	32.9
1	300	15490	23591	16155	33.1
2	1500	14588	22091	16064	36.9
3	3000	13348	20146	15957	39.6
4	6000	10819	16196	15700	39.8
5	9000	8216	12291	15555	40.9
6	12000	5548	8170	15328	41.6
7	15000	2814	4109	15228	42.9
8	16500	1424	2069	15059	43.5
9	17700	283	413	14778	43.2
10	18000	-0	-0	14776	43.8
ANCHOR				14750	43.8

CABLE MATERIAL GLASS
CURRENT PROFILE 5
T SUB(1) 12920 LBS

CABLE DIAMETER 0.5 IN
OCEAN DEPTH 18000 FEET
PAGE 16

N	X SUB(N) BAR FEET	Y SUB(N) BAR FEET	CABLE LENGTH FEET	MEAN TENSION LBS	THETA SUB(N) BAR DEGREES
0	0	23921	29939	13051	42.3
1	300	23643	29529	12941	42.7
2	1500	22358	27771	12842	46.9
3	3000	20581	25443	12744	50.0
4	6000	16889	20683	12517	50.8
5	9000	13004	15776	12466	52.5
6	12000	8925	10709	12155	53.7
7	15000	4606	5456	11959	55.2
8	16500	2346	2782	11700	56.2
9	17700	473	560	11611	57.0
10	18000	-0	-0	11596	57.7
ANCHOR				11579	57.7

CABLE CONFIGURATIONS AND TENSIONS

CABLE MATERIAL GLASS
CURRENT PROFILE 5
T SUB(1) 11652 LBS

CABLE DIAMETER 0.5 IN
OCEAN DEPTH 18000 FEET
PAGE 17

N	X SUB(N) BAR FEET	Y SUB(N) BAR FEET	CABLE LENGTH FEET	MEAN TENSION LBS	THETA SUB(N) BAR DEGREES
0	0	31828	36569	11779	48.0
1	300	31487	36115	11674	48.5
2	1500	29902	34128	11583	52.8
3	3000	27683	31472	11486	56.0
4	6000	23032	25942	11362	57.5
5	9000	18014	20105	11149	59.2
6	12000	12611	13911	10919	61.1
7	15000	6667	7295	10669	63.2
8	16500	3431	3739	10558	65.1
9	17700	702	763	10475	66.4
10	18000	-0	-0	10377	67.1
ANCHOR				10356	67.2

CABLE MATERIAL NYLON
CURRENT PROFILE 2
T SUB(1) 3600 LBS

CABLE DIAMETER 0.5 IN
OCEAN DEPTH 18000 FEET
PAGE 18

N	X SUB(N) BAR FEET	Y SUB(N) BAR FEET	CABLE LENGTH FEET	MEAN TENSION LBS	THETA SUB(N) BAR DEGREES
0	0	488	17992	3596	1.1
1	300	482	17692	3594	1.2
2	1500	456	16492	3563	1.4
3	3000	423	14998	3525	1.6
4	6000	353	11991	3477	1.6
5	9000	274	8984	3430	2.0
6	12000	188	5980	3382	2.0
7	15000	98	2971	3328	2.1
8	16500	50	1501	3280	2.4
9	17700	10	300	3243	2.5
10	18000	-0	-0	3209	2.5
ANCHOR				3204	2.5

CABLE CONFIGURATIONS AND TENSIONS

CABLE MATERIAL NYLON
CURRENT PROFILE 2
T SUB(1) 2160 LBS

CABLE DIAMETER 0.5 IN
OCEAN DEPTH 18000 FEET
PAGE 19

N	X SUB(N) BAR FEET	Y SUB(N) BAR FEET	CABLE LENGTH FEET	MEAN TENSION LBS	THETA SUB(N) BAR DEGREES
0	0	1018	18057	2161	1.8
1	300	1009	17757	2159	1.8
2	1500	956	16555	2125	2.5
3	3000	887	15058	2086	2.5
4	6000	734	12043	2040	2.8
5	9000	569	9027	1994	2.9
6	12000	390	6011	1943	3.5
7	15000	202	2991	1891	3.6
8	16500	102	1506	1835	4.4
9	17700	20	301	1809	4.4
10	18000	-0	-0	1773	4.5
ANCHOR				1769	4.5

CABLE MATERIAL NYLON
CURRENT PROFILE 2
T SUB(1) 720 LBS

CABLE DIAMETER 0.5 IN
OCEAN DEPTH 18000 FEET
PAGE 20

N	X SUB(N) BAR FEET	Y SUB(N) BAR FEET	CABLE LENGTH FEET	MEAN TENSION LBS	THETA SUB(N) BAR DEGREES
0	0	3319	18401	723	5.2
1	300	3292	18099	721	5.4
2	1500	3168	16892	687	7.0
3	3000	2918	15377	650	8.1
4	6000	2491	12325	606	9.5
5	9000	2019	9266	560	10.3
6	12000	1489	6200	512	13.5
7	15000	918	3125	456	15.3
8	16500	498	1578	421	19.4
9	17700	93	314	377	18.5
10	18000	-0	-0	349	23.6
ANCHOR				348	23.3

CABLE CONFIGURATIONS AND TENSIONS

CABLE MATERIAL NYLON
CURRENT PROFILE 2
T SUB(1) 460 LBS

CABLE DIAMETER 0.5 IN
OCEAN DEPTH 18000 FEET
PAGE 21

N	X SUB(N) BAR FEET	Y SUB(N) BAR FEET	CABLE LENGTH FEET	MEAN TENSION LBS	THETA SUB(N) BAR DEGREES
0	0	10956	22305	461	8.7
1	300	10910	22002	459	8.8
2	1500	10617	20767	425	11.9
3	3000	10287	19232	389	13.7
4	6000	9715	16165	346	16.8
5	9000	8265	12834	299	19.5
6	12000	6711	9458	252	28.4
7	15000	5017	6020	211	34.6
8	16500	3460	3863	185	48.9
9	17700	1736	1761	157	62.8
10	18000	-0	-0	142	79.5
ANCHOR				132	83.1

CABLE MATERIAL NYLON
CURRENT PROFILE 3
T SUB(1) 7200 LBS

CABLE DIAMETER 0.5 IN
OCEAN DEPTH 18000 FEET
PAGE 22

N	X SUB(N) BAR FEET	Y SUB(N) BAR FEET	CABLE LENGTH FEET	MEAN TENSION LBS	THETA SUB(N) BAR DEGREES
0	0	6537	19093	7230	3.6
1	300	6518	18792	7210	3.6
2	1500	6226	17557	7118	13.5
3	3000	5683	15967	7094	19.9
4	6000	4573	12780	7058	20.4
5	9000	3446	9587	7016	20.7
6	12000	2304	6389	6962	20.9
7	15000	1150	3182	6906	21.0
8	16500	570	1601	6856	21.2
9	17700	117	322	6819	21.1
10	18000	-0	-0	6792	21.4
ANCHOR				6792	21.5

CABLE CONFIGURATIONS AND TENSIONS

CABLE MATERIAL NYLON
CURRENT PROFILE 3
T SUB(1) 3600 LBS

CABLE DIAMETER 0.5 IN
OCEAN DEPTH 18000 FEET
PAGE 23

N	X SUB(N) BAR FEET	Y SUB(N) BAR FEET	CABLE LENGTH FEET	MEAN TENSION LBS	THETA SUB(N) BAR DEGREES
0	0	14802	23432	3640	7.2
1	300	14764	23130	3602	7.2
2	1500	14191	21807	3500	27.0
3	3000	13003	19904	3466	38.4
4	6000	10540	15999	3437	38.9
5	9000	7965	12043	3396	40.4
6	12000	5361	8052	3353	40.5
7	15000	2701	4025	3315	41.1
8	16500	1349	2013	3258	42.0
9	17700	279	409	3230	42.4
10	18000	-0	-0	3216	43.2
ANCHOR				3214	43.1

CABLE MATERIAL NYLON
CURRENT PROFILE 3
T SUB(1) 2160 LBS

CABLE DIAMETER 0.5 IN
OCEAN DEPTH 18000 FEET
PAGE 24

N	X SUB(N) BAR FEET	Y SUB(N) BAR FEET	CABLE LENGTH FEET	MEAN TENSION LBS	THETA SUB(N) BAR DEGREES
0	0	33697	38433	2219	11.6
1	300	33634	38127	2158	11.9
2	1500	32617	36557	2016	40.3
3	3000	30300	33830	2027	57.2
4	6000	25277	27988	2000	59.3
5	9000	19916	21840	1965	61.0
6	12000	13909	15130	1930	63.0
7	15000	7467	8023	1893	65.3
8	16500	3750	4030	1847	66.9
9	17700	810	863	1864	68.9
10	18000	-0	-0	1829	70.1
ANCHOR				1840	70.2

CABLE CONFIGURATIONS AND TENSIONS

CABLE MATERIAL NYLON
CURRENT PROFILE 4
T SUB(1) 7200 LBS

CABLE DIAMETER 0.5 IN
OCEAN DEPTH 18000 FEET
PAGE 25

N	X SUB(N) BAR FEET	Y SUB(N) BAR FEET	CABLE LENGTH FEET	MEAN TENSION LBS	THETA SUB(N) BAR DEGREES
0	0	8382	19828	7242	8.8
1	300	8336	19525	7199	8.8
2	1500	7931	18265	7115	18.8
3	3000	7234	16613	7081	24.8
4	6000	5827	13300	7047	25.4
5	9000	4403	9981	7007	25.7
6	12000	2965	6655	6948	25.8
7	15000	1513	3322	6903	26.1
8	16500	752	1677	6847	26.2
9	17700	153	338	6815	26.3
10	18000	-0	-0	6794	26.6
ANCHOR				6794	26.7

CABLE MATERIAL NYLON
CURRENT PROFILE 4
T SUB(1) 3600 LBS

CABLE DIAMETER 0.5 IN
OCEAN DEPTH 18000 FEET
PAGE 26

N	X SUB(N) BAR FEET	Y SUB(N) BAR FEET	CABLE LENGTH FEET	MEAN TENSION LBS	THETA SUB(N) BAR DEGREES
0	0	19630	26692	3678	17.1
1	300	19536	26378	3594	17.5
2	1500	18697	24916	3490	35.2
3	3000	17147	22766	3486	46.1
4	6000	13923	18376	3457	47.3
5	9000	10603	13909	3415	48.0
6	12000	7181	9350	3373	48.8
7	15000	3666	4730	3334	49.6
8	16500	1825	2365	3323	50.4
9	17700	384	488	3267	51.0
10	18000	-0	-0	3259	51.8
ANCHOR				3248	51.7

CABLE CONFIGURATIONS AND TENSIONS

CABLE MATERIAL NYLON
CURRENT PROFILE 5
T SUB(1) 7200 LBS

CABLE DIAMETER 0.5 IN
OCEAN DEPTH 18000 FEET
PAGE 27

N	X SUB(N) BAR FEET	Y SUB(N) BAR FEET	CABLE LENGTH FEET	MEAN TENSION LBS	THETA SUB(N) BAR DEGREES
0	0	16317	24315	7309	27.3
1	300	16159	23977	7208	27.7
2	1500	15282	22493	7143	36.2
3	3000	13957	20490	7112	41.6
4	6000	11249	16435	7086	42.2
5	9000	8502	12360	7052	42.7
6	12000	5719	8265	6992	42.9
7	15000	2900	4149	6958	43.2
8	16500	1445	2084	6920	43.5
9	17700	296	422	6880	43.8
10	18000	-0	-0	6865	44.1
ANCHOR				6856	44.1

CABLE MATERIAL NYLON
CURRENT PROFILE 3
T SUB(1) 53000 LBS

CABLE DIAMETER 2.0 IN
OCEAN DEPTH 18000 FEET
PAGE 28

N	X SUB(N) BAR FEET	Y SUB(N) BAR FEET	CABLE LENGTH FEET	MEAN TENSION LBS	THETA SUB(N) BAR DEGREES
0	0	4041	18469	53191	3.7
1	300	4022	18168	53087	3.7
2	1500	3833	16955	52865	9.1
3	3000	3498	15420	52694	12.6
4	6000	2827	12332	52400	12.8
5	9000	2145	9243	52049	12.9
6	12000	1456	6154	51685	13.2
7	15000	762	3063	51237	13.3
8	16500	387	1547	51003	13.4
9	17700	75	309	50724	13.2
10	18000	-0	-0	50653	13.5
ANCHOR				50614	13.5

CABLE CONFIGURATIONS AND TENSIONS

CABLE MATERIAL NYLON
CURRENT PROFILE 3
T SUB(1) 31600 LBS

CABLE DIAMETER 2.0 IN
OCEAN DEPTH 18000 FEET
PAGE 29

N	X SUB(N) BAR FEET	Y SUB(N) BAR FEET	CABLE LENGTH FEET	MEAN TENSION LBS	THETA SUB(N) BAR DEGREES
0	0	6971	19277	31983	6.1
1	300	6939	18975	31848	6.2
2	1500	6623	17735	31553	15.0
3	3000	6057	16129	31413	20.7
4	6000	4898	12923	31124	21.1
5	9000	3708	9704	30733	21.4
6	12000	2494	6474	30398	22.0
7	15000	1252	3231	30046	22.3
8	16500	635	1626	29658	22.6
9	17700	124	324	29529	22.7
10	18000	-0	-0	29400	22.8
ANCHOR				29378	22.9

CABLE MATERIAL NYLON
CURRENT PROFILE 3
T SUB(1) 20000 LBS

CABLE DIAMETER 2.0 IN
OCEAN DEPTH 18000 FEET
PAGE 30

N	X SUB(N) BAR FEET	Y SUB(N) BAR FEET	CABLE LENGTH FEET	MEAN TENSION LBS	THETA SUB(N) BAR DEGREES
0	0	11624	21346	20192	9.4
1	300	11574	21042	19987	9.5
2	1500	11066	19741	19593	22.9
3	3000	10141	17985	19498	31.7
4	6000	8229	14456	19279	32.9
5	9000	6255	10901	18830	33.2
6	12000	4226	7310	18526	34.1
7	15000	2136	3676	18137	34.8
8	16500	1078	1849	17879	35.5
9	17700	219	372	17780	36.3
10	18000	-0	-0	17624	36.3
ANCHOR				17598	36.3

CABLE CONFIGURATIONS AND TENSIONS

CABLE MATERIAL NYLON
CURRENT PROFILE 3
T SUB(1) 20000 LBS

CABLE DIAMETER 2.0 IN
OCEAN DEPTH 18000 FEET
PAGE 31

N	X SUB(N) BAR FEET	Y SUB(N) BAR FEET	CABLE LENGTH FEET	MEAN TENSION LBS	THETA SUB(N) BAR DEGREES
0	0	11999	21583	20214	9.8
1	300	11947	21279	19993	9.9
2	1500	11440	19978	19635	23.4
3	3000	10508	18219	19554	32.1
4	6000	8505	14646	19343	33.2
5	9000	6453	11040	18959	34.0
6	12000	4352	7398	18580	34.8
7	15000	2205	3724	18139	35.8
8	16500	1140	1886	17961	36.2
9	17700	216	371	17704	36.8
10	18000	-0	-0	17697	37.6
ANCHOR				17592	37.4

CABLE MATERIAL NYLON
CURRENT PROFILE 3
T SUB(1) 15900 LBS

CABLE DIAMETER 2.0 IN
OCEAN DEPTH 18000 FEET
PAGE 32

N	X SUB(N) BAR FEET	Y SUB(N) BAR FEET	CABLE LENGTH FEET	MEAN TENSION LBS	THETA SUB(N) BAR DEGREES
0	0	16270	24374	16146	12.2
1	300	16204	24067	15892	12.4
2	1500	15540	22696	15449	28.9
3	3000	14311	20760	15375	39.4
4	6000	11740	16782	15063	40.6
5	9000	9038	12732	14687	41.9
6	12000	6198	8606	14456	43.8
7	15000	3243	4414	14128	45.1
8	16500	1674	2248	13862	46.2
9	17700	326	444	13601	47.3
10	18000	-0	-0	13460	47.9
ANCHOR				13438	48.0

CABLE CONFIGURATIONS AND TENSIONS

CABLE MATERIAL STEEL
CURRENT PROFILE 2
T SUB(1) 10000 LBS

CABLE DIAMETER 2.0 IN
OCEAN DEPTH 6000 FEET
PAGE 33

N	X SUB(N) BAR FEET	Y SUB(N) BAR FEET	CABLE LENGTH FEET	MEAN TENSION LBS	THETA SUB(N) BAR DEGREES
0	0	156	6003	10009	1.1
1	100	154	5903	9991	1.1
2	500	146	5503	9861	1.0
3	1000	134	5004	9652	1.3
4	2000	110	4002	9318	1.4
5	3000	86	3000	8892	1.4
6	4000	60	1998	8460	1.5
7	5000	34	996	8035	1.6
8	5500	17	500	7705	1.6
9	5900	3	100	7491	1.8
10	6000	-0	-0	7361	1.9
ANCHOR				7337	1.8

CABLE MATERIAL STEEL
CURRENT PROFILE 2
T SUB(1) 6000 LBS

CABLE DIAMETER 0.5 IN
OCEAN DEPTH 6000 FEET
PAGE 34

N	X SUB(N) BAR FEET	Y SUB(N) BAR FEET	CABLE LENGTH FEET	MEAN TENSION LBS	THETA SUB(N) BAR DEGREES
0	0	288	6014	6016	1.7
1	100	285	5914	5998	1.7
2	500	271	5514	5853	2.1
3	1000	252	5015	5659	2.1
4	2000	210	4012	5332	2.4
5	3000	159	3007	4900	2.6
6	4000	107	2002	4471	2.8
7	5000	54	997	4037	3.1
8	5500	27	501	3727	3.7
9	5900	5	100	3502	3.9
10	6000	-0	-0	3370	4.1
ANCHOR				3352	4.0

CABLE CONFIGURATIONS AND TENSIONS

CABLE MATERIAL STEEL
CURRENT PROFILE 2
T SUB(1) 3000 LBS

CABLE DIAMETER 0.5 IN
OCEAN DEPTH 6000 FEET
PAGE 35

N	X SUB(N) BAR FEET	Y SUB(N) BAR FEET	CABLE LENGTH FEET	MEAN TENSION LBS	THETA SUB(N) BAR DEGREES
0	0	1019	6150	3023	3.5
1	100	1013	6049	3003	3.6
2	500	984	5648	2873	4.1
3	1000	945	5148	2666	4.6
4	2000	836	4135	2336	5.4
5	3000	726	3121	1912	6.6
6	4000	600	2107	1476	8.6
7	5000	399	1080	1049	13.2
8	5500	253	566	722	17.7
9	5900	94	137	513	25.4
10	6000	-0	-0	400	36.9
ANCHOR				372	38.5

CABLE MATERIAL STEEL
CURRENT PROFILE 2
T SUB(1) 2838 LBS

CABLE DIAMETER 0.5 IN
OCEAN DEPTH 6000 FEET
PAGE 36

N	X SUB(N) BAR FEET	Y SUB(N) BAR FEET	CABLE LENGTH FEET	MEAN TENSION LBS	THETA SUB(N) BAR DEGREES
0	0	1629	6580	2861	3.7
1	100	1622	6480	2841	3.7
2	500	1592	6079	2713	4.1
3	1000	1551	5578	2504	4.8
4	2000	1442	4565	2175	5.8
5	3000	1332	3552	1745	7.2
6	4000	1178	2533	1323	10.4
7	5000	949	1502	893	14.3
8	5500	776	979	564	22.9
9	5900	457	466	367	40.8
10	6000	-0	-0	246	77.3
ANCHOR				240	79.4

CABLE CONFIGURATIONS AND TENSIONS

CABLE MATERIAL STEEL
CURRENT PROFILE 3
T SUB(1) 20000 LBS

CABLE DIAMETER 0.5 IN
OCEAN DEPTH 6000 FEET
PAGE 37

N	X SUB(N) BAR FEET	Y SUB(N) BAR FEET	CABLE LENGTH FEET	MEAN TENSION LBS	THETA SUB(N) BAR DEGREES
0	0	843	6077	19998	1.5
1	100	841	5977	19976	1.5
2	500	820	5576	19843	3.0
3	1000	773	5075	19630	5.3
4	2000	638	4059	19291	7.7
5	3000	486	3040	18864	8.7
6	4000	330	2021	18432	9.0
7	5000	168	1000	17993	9.1
8	5500	86	507	17628	9.3
9	5900	17	101	17451	9.4
10	6000	-0	-0	17328	9.6
ANCHOR				17305	9.6

CABLE MATERIAL STEEL
CURRENT PROFILE 3
T SUB(1) 10000 LBS

CABLE DIAMETER 0.5 IN
OCEAN DEPTH 6000 FEET
PAGE 38

N	X SUB(N) BAR FEET	Y SUB(N) BAR FEET	CABLE LENGTH FEET	MEAN TENSION LBS	THETA SUB(N) BAR DEGREES
0	0	1889	6282	10030	2.9
1	100	1884	6181	10007	2.9
2	500	1841	5779	9868	6.0
3	1000	1746	5270	9659	10.8
4	2000	1466	4233	9317	15.6
5	3000	1130	3185	8905	18.3
6	4000	774	2129	8474	19.4
7	5000	404	1067	8050	20.5
8	5500	207	540	7718	21.1
9	5900	41	108	7520	22.2
10	6000	-0	-0	7383	22.5
ANCHOR				7364	22.5

CABLE CONFIGURATIONS AND TENSIONS

CABLE MATERIAL STEEL
CURRENT PROFILE 3
T SUB(1) 6000 LBS

CABLE DIAMETER 0.5 IN
OCEAN DEPTH 6000 FEET
PAGE 39

N	X SUB(N) BAR FEET	Y SUB(N) BAR FEET	CABLE LENGTH FEET	MEAN TENSION LBS	THETA SUB(N) BAR DEGREES
0	0	4065	7364	6045	4.9
1	100	4056	7263	6020	4.9
2	500	3984	6857	5978	10.1
3	1000	3819	6330	5665	15.1
4	2000	3307	5207	5329	25.8
5	3000	2658	4030	4915	32.5
6	4000	1946	2796	4480	36.1
7	5000	1074	1465	4069	4[illegible].8
8	5500	571	759	3753	45.1
9	5900	122	158	3534	4[illegible].3
10	6000	-0	-0	3432	50.8
ANCHOR				3402	51.2

CABLE MATERIAL STEEL
CURRENT PROFILE 3
T SUB(1) 5164 LBS

CABLE DIAMETER 0.5 IN
OCEAN DEPTH 6000 FEET
PAGE 40

N	X SUB(N) BAR FEET	Y SUB(N) BAR FEET	CABLE LENGTH FEET	MEAN TENSION LBS	THETA SUB(N) BAR DEGREES
0	0	6754	9483	5205	5.7
1	100	6744	9382	5175	5.7
2	500	6660	8974	5019	11.8
3	1000	6464	8437	4820	21.3
4	2000	5853	7271	4479	31.5
5	3000	5035	5974	4052	38.8
6	4000	4052	4578	3637	44.7
7	5000	2726	2918	3214	52.8
8	5500	1786	1852	2903	61.8
9	5900	566	575	2703	71.2
10	6000	-0	-0	2622	79.6
ANCHOR				2594	82.2

CABLE CONFIGURATIONS AND TENSIONS

CABLE MATERIAL STEEL
CURRENT PROFILE 4
T SUB(1) 20000 LBS

CABLE DIAMETER 0.5 IN
OCEAN DEPTH 6000 FEET
PAGE 41

N	X SUB(N) BAR FEET	Y SUB(N) BAR FEET	CABLE LENGTH FEET	MEAN TENSION LBS	THETA SUB(N) BAR DEGREES
0	0	1441	6172	20037	6.6
1	100	1430	6071	20007	6.6
2	500	1371	5668	19879	8.3
3	1000	1277	5159	19665	10.6
4	2000	1050	4130	19333	13.0
5	3000	797	3096	18901	14.0
6	4000	539	2063	18461	14.5
7	5000	275	1027	18029	14.7
8	5500	140	518	17684	14.9
9	5900	28	103	17490	15.2
10	6000	-0	-0	17373	15.4
ANCHOR				17352	15.4

CABLE MATERIAL STEEL
CURRENT PROFILE 4
T SUB(1) 10000 LBS

CABLE DIAMETER 0.5 IN
OCEAN DEPTH 6000 FEET
PAGE 42

N	X SUB(N) BAR FEET	Y SUB(N) BAR FEET	CABLE LENGTH FEET	MEAN TENSION LBS	THETA SUB(N) BAR DEGREES
0	0	3358	6885	10027	13.3
1	100	3335	6782	9986	13.4
2	500	3216	6366	9849	16.5
3	1000	3022	5829	9641	21.3
4	2000	2535	4718	9288	26.1
5	3000	1970	3573	8887	29.4
6	4000	1366	2411	8470	31.1
7	5000	716	1229	8033	32.9
8	5500	369	622	7683	34.2
9	5900	74	124	7501	35.5
10	6000	-0	-0	7389	36.3
ANCHOR				7368	36.5

CABLE CONFIGURATIONS AND TENSIONS

CABLE MATERIAL STEEL
CURRENT PROFILE 4
T SUB(1) 8000 LBS

CABLE DIAMETER 0.5 IN
OCEAN DEPTH 6000 FEET
PAGE 43

N	X SUB(N) BAR FEET	Y SUB(N) BAR FEET	CABLE LENGTH FEET	MEAN TENSION LBS	THETA SUB(N) BAR DEGREES
0	0	4818	7750	8037	16.7
1	100	4788	7646	7994	16.8
2	500	4638	7219	7856	20.7
3	1000	4387	6661	7649	26.7
4	2000	3730	5476	7317	33.1
5	3000	2962	4214	6908	37.6
6	4000	2101	2887	6476	40.6
7	5000	1117	1489	6050	44.2
8	5500	581	767	5768	47.9
9	5900	123	158	5549	49.8
10	6000	-0	-0	5416	51.2
ANCHOR				5402	51.4

CABLE MATERIAL STEEL
CURRENT PROFILE 4
T SUB(1) 6604 LBS

CABLE DIAMETER 0.5 IN
OCEAN DEPTH 6000 FEET
PAGE 44

N	X SUB(N) BAR FEET	Y SUB(N) BAR FEET	CABLE LENGTH FEET	MEAN TENSION LBS	THETA SUB(N) BAR DEGREES
0	0	857[illegible]	10799	6646	20.3
1	100	8535	10693	6596	20.5
2	500	8345	10252	6485	25.6
3	1000	8024	9664	6233	32.1
4	2000	7183	8350	5924	40.4
5	3000	6119	6893	5490	46.5
6	4000	4832	5260	5079	52.0
7	5000	3151	3307	4670	59.4
8	5500	1994	2053	4354	66.7
9	5900	581	588	4176	74.3
10	6000	-0	-0	4059	80.2
ANCHOR				4047	81.8

CABLE CONFIGURATIONS AND TENSIONS

CABLE MATERIAL GLASS
CURRENT PROFILE 3
T SUB(1) 10000 LBS

CABLE DIAMETER 0.5 IN
OCEAN DEPTH 6000 FEET
PAGE 45

N	X SUB(N) BAR FEET	Y SUB(N) BAR FEET	CABLE LENGTH FEET	MEAN TENSION LBS	THETA SUB(N) BAR DEGREES
0	0	1628	6210	10015	3.0
1	100	1624	6110	10007	3.0
2	500	1582	5707	9954	6.0
3	1000	1488	5199	9891	10.5
4	2000	1227	4164	9804	14.8
5	3000	928	3125	9721	16.7
6	4000	623	2084	9625	17.0
7	5000	312	1041	9550	17.4
8	5500	156	522	9458	17.5
9	5900	31	104	9397	17.6
10	6000	-0	-0	9347	17.6
ANCHOR				9344	17.6

CABLE MATERIAL GLASS
CURRENT PROFILE 3
T SUB(1) 5000 LBS

CABLE DIAMETER 0.5 IN
OCEAN DEPTH 6000 FEET
PAGE 46

N	X SUB(N) BAR FEET	Y SUB(N) BAR FEET	CABLE LENGTH FEET	MEAN TENSION LBS	THETA SUB(N) BAR DEGREES
0	0	3620	7023	5024	5.9
1	100	3609	6923	5010	5.9
2	500	3524	6514	4948	11.9
3	1000	3332	5978	4887	20.9
4	2000	2777	4837	4814	29.4
5	3000	2119	3652	4726	33.1
6	4000	1439	2451	4639	34.1
7	5000	739	1236	4536	34.7
8	5500	378	626	4483	35.8
9	5900	74	124	4428	36.3
10	6000	-0	-0	4376	36.5
ANCHOR				4371	36.5

CABLE CONFIGURATIONS AND TENSIONS

CABLE MATERIAL GLASS
CURRENT PROFILE 3
T SUB(1) 3000 LBS

CABLE DIAMETER 0.5 IN
OCEAN DEPTH 6000 FEET
PAGE 47

N	X SUB(N) BAR FEET	Y SUB(N) BAR FEET	CABLE LENGTH FEET	MEAN TENSION LBS	THETA SUB(N) BAR DEGREES
0	0	7858	10045	3020	9.8
1	100	7841	9944	3000	9.9
2	500	7697	9520	2932	19.8
3	1000	7359	8919	2879	34.0
4	2000	6295	7463	2805	46.6
5	3000	4972	5806	2715	52.7
6	4000	3495	4020	2645	55.5
7	5000	1879	2126	2562	58.3
8	5500	985	1104	2482	60.5
9	5900	204	227	2451	62.8
10	6000	-0	-0	2422	64.2
ANCHOR				2425	64.4

CABLE MATERIAL GLASS
CURRENT PROFILE 3
T SUB(1) 2584 LBS

CABLE DIAMETER 0.5 IN
OCEAN DEPTH 6000 FEET
PAGE 48

N	X SUB(N) BAR FEET	Y SUB(N) BAR FEET	CABLE LENGTH FEET	MEAN TENSION LBS	THETA SUB(N) BAR DEGREES
0	0	12244	13968	2604	11.3
1	100	12224	13866	2583	11.4
2	500	12057	13433	2510	22.7
3	1000	11658	12795	2464	38.9
4	2000	10347	11146	2388	52.7
5	3000	8612	9142	2311	59.9
6	4000	6554	6850	2246	64.1
7	5000	4004	4112	2168	68.6
8	5500	2313	2361	2089	73.2
9	5900	582	589	2070	77.3
10	6000	-0	-0	2050	80.1
ANCHOR				2048	80.7

CABLE CONFIGURATIONS AND TENSIONS

CABLE MATERIAL GLASS
CURRENT PROFILE 4
T SUB(1) 10000 LBS

CABLE DIAMETER 0.5 IN
OCEAN DEPTH 6000 FEET
PAGE 49

N	X SUB(N) BAR FEET	Y SUB(N) BAR FEET	CABLE LENGTH FEET	MEAN TENSION LBS	THETA SUB(N) BAR DEGREES
0	0	2858	6638	10010	13.3
1	100	2834	6536	9984	13.4
2	500	2717	6119	9933	16.3
3	1000	2527	5584	9872	20.8
4	2000	2063	4482	9777	24.8
5	3000	1561	3364	9706	26.8
6	4000	1051	2242	9615	27.2
7	5000	535	1117	9525	27.6
8	5500	267	566	9423	27.6
9	5900	54	113	9405	28.2
10	6000	-0	-0	9342	28.1
ANCHOR				9339	28.1

CABLE MATERIAL GLASS
CURRENT PROFILE 4
T SUB(1) 5000 LBS

CABLE DIAMETER 0.5 IN
OCEAN DEPTH 6000 FEET
PAGE 50

N	X SUB(N) BAR FEET	Y SUB(N) BAR FEET	CABLE LENGTH FEET	MEAN TENSION LBS	THETA SUB(N) BAR DEGREES
0	0	7236	9449	5044	27.1
1	100	7184	9337	5002	27.2
2	500	6927	8862	4953	32.8
3	1000	6500	8204	4899	40.5
4	2000	5410	6730	4837	47.7
5	3000	4152	5124	4758	51.4
6	4000	2838	3469	4674	52.7
7	5000	1465	1773	4575	54.0
8	5500	742	894	4537	55.5
9	5900	153	183	4457	56.1
10	6000	-0	-0	4441	56.9
ANCHOR				4437	57.0

CABLE CONFIGURATIONS AND TENSIONS

CABLE MATERIAL GLASS
CURRENT PROFILE 4
T SUB(1) 3774 LBS

CABLE DIAMETER .5 IN
OCEAN DEPTH 6000 FEET
PAGE 51

N	X SUB(N) BAR FEET	Y SUB(N) BAR FEET	CABLE LENGTH FEET	MEAN TENSION LBS	THETA SUB(N) BAR DEGREES
0	0	15065	16381	3817	36.7
1	100	14989	16256	3774	37.1
2	500	14607	15703	3721	43.6
3	1000	13937	14982	3680	52.7
4	2000	12164	12829	3622	60.7
5	3000	9969	10418	3540	65.4
6	4000	7443	7697	3489	68.[illegible]
7	5000	4373	4472	3424	72.1
8	5500	2409	2458	3364	75.[illegible]
9	5900	577	594	3290	78.1
10	6000	-0	-0	3263	[illegible]
ANCHOR				3262	[illegible]

CABLE MATERIAL NYLON
CURRENT PROFILE 2
T SUB(1) 3600 LBS

CABLE DIAMETER 0.5 IN
OCEAN DEPTH 6000 FEET
PAGE 52

N	X SUB(N) BAR FEET	Y SUB(N) BAR FEET	CABLE LENGTH FEET	MEAN TENSION LBS	THETA SUB(N) BAR DEGREES
0	0	143	6002	3596	1.1
1	100	142	5902	3596	1.0
2	500	134	5502	3562	1.2
3	1000	124	5004	3525	1.6
4	2000	102	4002	3477	1.6
5	3000	78	3000	3425	1.7
6	4000	52	1998	3375	1.7
7	5000	27	995	3331	1.7
8	5500	13	499	3286	2.1
9	5900	2	99	3241	1.8
10	6000	-0	-0	3206	2.1
ANCHOR				3204	2.0

CABLE CONFIGURATIONS AND TENSIONS

CABLE MATERIAL NYLON
CURRENT PROFILE 2
T SUB(1) 2160 LBS

CABLE DIAMETER 0.5 IN
OCEAN DEPTH 6000 FEET
PAGE 53

N	X SUB(N) BAR FEET	Y SUB(N) BAR FEET	CABLE LENGTH FEET	MEAN TENSION LBS	THETA SUB(N) BAR DEGREES
0	0	306	6015	2159	1.8
1	100	303	5915	2157	1.6
2	500	287	5515	2119	2.2
3	1000	264	5016	2086	2.5
4	2000	215	4011	2042	2.8
5	3000	164	3006	1996	2.9
6	4000	111	2002	1946	2.9
7	5000	57	996	1898	3.0
8	5500	28	501	1853	3.7
9	5900	5	100	1809	3.8
10	6000	-0	-0	1770	3.2
ANCHOR				1769	3.8

CABLE MATERIAL NYLON
CURRENT PROFILE 2
T SUB(1) 720 LBS

CABLE DIAMETER 0.5 IN
OCEAN DEPTH 6000 FEET
PAGE 54

N	X SUB(N) BAR FEET	Y SUB(N) BAR FEET	CABLE LENGTH FEET	MEAN TENSION LBS	THETA SUB(N) BAR DEGREES
0	0	1055	6125	722	5.1
1	100	1046	6024	721	5.3
2	500	1008	5622	688	6.7
3	1000	923	5116	650	8.1
4	2000	783	4096	608	9.5
5	3000	630	3079	560	10.3
6	4000	463	2059	509	11.3
7	5000	287	1036	455	12.7
8	5500	156	522	420	13.8
9	5900	29	104	361	18.3
10	6000	-0	-0	347	20.2
ANCHOR				342	19.8

CABLE CONFIGURATIONS AND TENSIONS

CABLE MATERIAL NYLON
CURRENT PROFILE 3
T SUB(1) 3600 LBS

CABLE DIAMETER 0.5 IN
OCEAN DEPTH 6000 FEET
PAGE 55

N	X SUB(N) BAR FEET	Y SUB(N) BAR FEET	CABLE LENGTH FEET	MEAN TENSION LBS	THETA SUB(N) BAR DEGREES
0	0	4491	7587	3617	4.1
1	100	4484	7487	3607	4.1
2	500	4409	7077	3559	12.3
3	1000	4168	6527	3522	24.5
4	2000	3467	5312	3493	35.3
5	3000	2621	3996	3459	39.9
6	4000	1757	2667	3451	40.5
7	5000	880	1330	3397	40.8
8	5500	436	665	3367	41.2
9	5900	90	135	3349	41.5
10	6000	-0	-0	3337	42.2
ANCHOR				3333	42.1

CABLE MATERIAL NYLON
CURRENT PROFILE 3
T SUB(1) 2160 LBS

CABLE DIAMETER 0.5 IN
OCEAN DEPTH 6000 FEET
PAGE 56

N	X SUB(N) BAR FEET	Y SUB(N) BAR FEET	CABLE LENGTH FEET	MEAN TENSION LBS	THETA SUB(N) BAR DEGREES
0	0	9367	11270	2178	7.5
1	100	9355	11170	2162	6.5
2	500	9184	10749	2133	22.0
3	1000	8766	10111	2030	38.1
4	2000	7398	8417	2083	54.7
5	3000	5684	6432	2060	59.8
6	4000	3892	4376	2031	61.2
7	5000	2030	2264	1999	61.7
8	5500	1055	1172	1965	63.5
9	5900	206	228	1991	64.7
10	6000	-0	-0	1957	65.4
ANCHOR				1954	65.5

CABLE CONFIGURATIONS AND TENSIONS

CABLE MATERIAL NYLON
CURRENT PROFILE 3
T SUB(1) 1890 LBS

CABLE DIAMETER 0.5 IN
OCEAN DEPTH 6000 FEET
PAGE 57

N	X SUB(N) BAR FEET	Y SUB(N) BAR FEET	CABLE LENGTH FEET	MEAN TENSION LBS	THETA SUB(N) BAR DEGREES
0	0	36918	41734	1905	7.8
1	100	36877	41432	1891	7.8
2	500	36375	40132	1829	23.2
3	1000	34940	38065	1817	43.9
4	2000	29906	32213	1795	59.0
5	3000	23468	25105	1803	65.4
6	4000	16279	17304	1780	67.1
7	5000	8722	9180	1762	68.5
8	5500	4716	4936	1706	69.7
9	5900	935	1029	1714	70.9
10	6000	-0	-0	1702	72.1
ANCHOR				1717	72.3

CABLE MATERIAL NYLON
CURRENT PROFILE 4
T SUB(1) 3600 LBS

CABLE DIAMETER 0.5 IN
OCEAN DEPTH 6000 FEET
PAGE 58

N	X SUB(N) BAR FEET	Y SUB(N) BAR FEET	CABLE LENGTH FEET	MEAN TENSION LBS	THETA SUB(N) BAR DEGREES
0	0	6043	8574	3621	14.4
1	100	6017	8471	3598	14.5
2	500	5850	8038	3548	22.5
3	1000	5512	7437	3521	34.0
4	2000	4564	6060	3495	43.8
5	3000	3462	4575	3461	47.7
6	4000	2331	3063	3445	48.5
7	5000	1182	1540	3416	49.0
8	5500	591	774	3422	50.0
9	5900	122	158	3368	50.0
10	6000	-0	-0	3361	50.7
ANCHOR				3348	50.5

CABLE CONFIGURATIONS AND TENSIONS

CABLE MATERIAL NYLON
CURRENT PROFILE 4
T SUB(1) 2880 LBS

CABLE DIAMETER 0.5 IN
OCEAN DEPTH 6000 FEET
PAGE 59

N	X SUB(N) BAR FEET	Y SUB(N) BAR FEET	CABLE LENGTH FEET	MEAN TENSION LBS	THETA SUB(N) BAR DEGREES
0	0	8389	10403	2904	18.0
1	100	8356	10298	2877	18.2
2	500	8143	9846	2829	28.0
3	1000	7701	9178	2805	41.4
4	2000	6415	7550	2780	52.[illegible]
5	3000	4895	5731	2752	56.7
6	4000	3333	3875	2740	57.9
7	5000	1708	1974	2721	58.5
8	5500	876	1010	2719	59.4
9	5900	177	203	2696	60.2
10	6000	-0	-0	2662	60.6
ANCHOR				2664	60.7

CABLE MATERIAL NYLON
CURRENT PROFILE 4
T SUB(1) 2880 LBS

CABLE DIAMETER 0.5 IN
OCEAN DEPTH 6000 FEET
PAGE 60

N	X SUB(N) BAR FEET	Y SUB(N) BAR FEET	CABLE LENGTH FEET	MEAN TENSION LBS	THETA SUB(N) BAR DEGREES
0	0	8368	10383	2906	18.0
1	100	8335	10278	2879	18.2
2	500	8123	9826	2830	28.0
3	1000	7682	9158	2809	41.3
4	2000	6402	7535	2781	52.3
5	3000	4883	5717	2752	56.7
6	4000	3326	3865	2745	57.7
7	5000	1707	1967	2705	58.2
8	5500	877	1009	2681	59.1
9	5900	177	203	2696	60.2
10	6000	-0	-0	2662	60.6
ANCHOR				2657	60.6

CABLE CONFIGURATIONS AND TENSIONS

CABLE MATERIAL NYLON
CURRENT PROFILE 4
T SUB(1) 2140 LBS

CABLE DIAMETER 0.5 IN
OCEAN DEPTH 6000 FEET
PAGE 61

N	X SUB(N) BAR FEET	Y SUB(N) BAR FEET	CABLE LENGTH FEET	MEAN TENSION LBS	THETA SUB(N) BAR DEGREES
0	0	14922	16223	2174	24.2
1	100	14876	16113	2139	24.6
2	500	14576	15613	2090	36.8
3	1000	13925	14793	2068	52.5
4	2000	11864	12502	2065	64.2
5	3000	9298	9748	2036	68.9
6	4000	6447	6723	2018	70.3
7	5000	3452	3575	2042	71.7
8	5500	1770	1834	2022	73.6
9	5900	405	416	1974	74.2
10	6000	-0	-0	1984	75.4
ANCHOR				1973	75.4

CABLE MATERIAL NYLON
CURRENT PROFILE 3
T SUB(1) 3600 LBS

CABLE DIAMETER 0.5 IN
OCEAN DEPTH 1800 FEET
PAGE 62

N	X SUB(N) BAR FEET	Y SUB(N) BAR FEET	CABLE LENGTH FEET	MEAN TENSION LBS	THETA SUB(N) BAR DEGREES
0	0	921	2051	3600	2.3
1	30	920	2021	3598	2.3
2	150	909	1900	3571	5.3
3	300	880	1748	3555	10.8
4	600	781	1434	3498	18.0
5	900	636	1101	3472	26.0
6	1200	455	753	3454	31.8
7	1500	239	384	3418	35.8
8	1650	120	192	3393	38.2
9	1770	25	39	3378	39.7
10	1800	-0	-0	3357	40.5
ANCHOR				3362	40.6

CABLE CONFIGURATIONS AND TENSIONS

CABLE MATERIAL NYLON
CURRENT PROFILE 3
T SUB(1) 2160 LBS

CABLE DIAMETER 0.5 IN
OCEAN DEPTH 1800 FEET
PAGE 63

N	X SUB(N) BAR FEET	Y SUB(N) BAR FEET	CABLE LENGTH FEET	MEAN TENSION LBS	THETA SUB(N) BAR DEGREES
0	0	1780	2621	2166	3.6
1	30	1778	2591	2164	3.7
2	150	1760	2470	2137	8.8
3	300	1715	2313	2104	16.9
4	600	1542	1968	2057	29.1
5	900	1283	1569	2039	41.1
6	1200	934	1110	2025	49.5
7	1500	506	586	2003	55.0
8	1650	258	296	1964	58.8
9	1770	55	63	1977	60.4
10	1800	-0	-0	1955	61.6
ANCHOR				1964	61.7

CABLE MATERIAL NYLON
CURRENT PROFILE 3
T SUB(1) 1440 LBS

CABLE DIAMETER 0.5 IN
OCEAN DEPTH 1800 FEET
PAGE 64

N	X SUB(N) BAR FEET	Y SUB(N) BAR FEET	CABLE LENGTH FEET	MEAN TENSION LBS	THETA SUB(N) BAR DEGREES
0	0	3730	4312	1446	5.6
1	30	3727	4282	1443	5.7
2	150	3699	4159	1410	13.1
3	300	3628	3993	1381	25.2
4	600	3358	3588	1343	42.0
5	900	2877	3022	1332	57.2
6	1200	2225	2303	1331	66.4
7	1500	1318	1348	1342	72.5
8	1650	700	714	1319	75.9
9	1770	173	175	1289	77.8
10	1800	-0	-0	1300	79.9
ANCHOR				1294	79.9

CABLE CONFIGURATIONS AND TENSIONS

CABLE MATERIAL STEEL
CURRENT PROFILE 3
T SUB(1) 10000 LBS

CABLE DIAMETER 0.5 IN
OCEAN DEPTH 1800 FEET
PAGE 65

N	X SUB(N) BAR FEET	Y SUB(N) BAR FEET	CABLE LENGTH FEET	MEAN TENSION LBS	THETA SUB(N) BAR DEGREES
0	0	429	1858	10023	2.5
1	30	428	1828	10001	2.5
2	150	420	1708	9873	3.6
3	300	406	1558	9663	5.5
4	600	360	1252	9325	8.6
5	900	295	943	8904	12.2
6	1200	212	632	8467	15.3
7	1500	114	319	8050	18.1
8	1650	59	161	7706	19.6
9	1770	11	32	7515	21.2
10	1800	-0	-0	7385	21.8
ANCHOR				7367	21.9

CABLE MATERIAL STEEL
CURRENT PROFILE 3
T SUB(1) 6000 LBS

CABLE DIAMETER 0.5 IN
OCEAN DEPTH 1800 FEET
PAGE 66

N	X SUB(N) BAR FEET	Y SUB(N) BAR FEET	CABLE LENGTH FEET	MEAN TENSION LBS	THETA SUB(N) BAR DEGREES
0	0	888	2047	6034	4.0
1	30	886	2017	6013	4.1
2	150	873	1896	5884	6.0
3	300	848	1745	5674	9.3
4	600	770	1434	5343	15.0
5	900	650	1112	4919	21.7
6	1200	490	772	4497	28.4
7	1500	280	407	4068	35.1
8	1650	148	211	3774	41.1
9	1770	31	43	3562	44.6
10	1800	-0	-0	3448	47.0
ANCHOR				3430	47.4

CABLE CONFIGURATIONS AND TENSIONS

CABLE MATERIAL STEEL
CURRENT PROFILE 3
T SUB(1) 4858 LBS

CABLE DIAMETER 0.5 IN
OCEAN DEPTH 1800 FEET
PAGE 67

N	X SUB(N) BAR FEET	Y SUB(N) BAR FEET	CABLE LENGTH FEET	MEAN TENSION LBS	THETA SUB(N) BAR DEGREES
0	0	1596	2564	4894	5.0
1	30	1593	2534	4873	5.1
2	150	1578	2413	4746	7.5
3	300	1547	2260	4539	11.6
4	600	1444	1945	4198	18.9
5	900	1285	1606	3770	28.2
6	1200	1050	1223	3351	37.9
7	1500	707	769	2921	48.9
8	1650	453	478	2636	59.9
9	1770	145	147	2433	69.6
10	1800	-0	-0	2352	77.9
ANCHOR				2323	80.2

TABLES OF DYNAMIC TENSIONS

(3 pages)

(page 1 of 3)

Case	Page	Mat'l	Depth (ft)	$\bar{T}_1$ (lb)	Segments	Node	Rope Length (ft)	Wave Ht (ft)	Dynamic Tension in Pounds at Period in Seconds															
									Period (sec)	2.0	2.3	2.7	3.0	3.3	3.7	4.0	4.3	4.7	5.0	6	8	12	16	32
A	6	STL	10000	10000	10	1	23010	50													4000		1800	1500
						7	6625														2000		1730	1500
						10	0														3000		1150	1800
						1	23010	15		4000	3750	3500	2500	2000	1750	2000	2000	2000	2000		875		400	
						7	6625			2000	950	1500	1200	1000	600	1100	800	600	600		700		490	
						10	0			1400	750	850	850	850	800	1650	850	850	850		1000		700	
						1	23010	5		1100	1150	1400	950	500	500	750	1000	1000	900		130		110	
						7	6625			1155	1125	800	550	275	150	175	200	300	375		240		165	
						10	0			800	850	1000	900	775	750	800	825	950	950		360		240	
B	8	STL	18000	7634	10	1	18090	50													3400		2600	1800
						7	3267														3000		2200	1800
						10	0														1600		1500	1010
						1	18090	15								3000					575		500	
						7	3267									1700					800		600	
						10	0									1200					520		375	
						1	18090	5		1450	1800	1000	900	1200	1400	1250	1000	800	460		180		200	
						7	3267			1150	1000	1330	1000	1750	1000	800	1750	1550	2000		280		190	
						10	0			1360	1440	1300	1440	1520	1520	640	1000	960	800		190		160	
C	38	STL	6300	10000	4	1	6280	50													5500		6000	6000
						2	4710														6000		6000	6000
						3	3140														6500		6000	6500
						4	1570														6250		6000	6000
						1	6280	15		3200						1350				1300	1700	1700	1850	
						2	4710			1700						1550				1809	1800	1850	1800	
						3	3140			3100						2100				2100	1850	1900	1800	
						4	1570			3800						2300				2300	1850	1900	1800	
						1	6280	5								470					575	575		
						2	4710									625					575	575		
						3	3140									675					625	625		
						4	1570									775					650	800		
D	36	STL	6000	2838	10	1	6480	50															3000	1600
						7	1502																3250	1400
						10	0																2700	1300
						1	6480	40													4500			
						7	1502														4150			
						10	0														3500			
						1	6480	15				2600	2400	2000	1800	2000	2000	2100	2000	1600	1300	1800	700	
						7	1502					2650	2350	2100	2000	2050	2000	2000	1850	1700	1300	1000	650	
						10	0					2450	2250	2050	1950	1800	1900	1850	1800	1550	1125	950	500	
						1	6480	5								760					400		400	
						7	1502									650					425		250	
						10	0									520					320		200	
D	36	STL	6000	2838	4	1	6580	50													5250		5250	4750
						2	4935														5500		5250	4750
						3	3290														6000		5500	4750
						4	1645														6000		5250	4750
						1	6580	[illegible]		3400	2130	1460	1300			1350				1400	1450	1400	1400	
						2	4935			2600	1630	1740	1800			1800				1600	1700	1600		
						3	3290			2400	2730	2440	2200			[illegible]				1900	1850	1700		
						4	1645			[illegible]	[illegible]	2680	2500			[illegible]				[illegible]	1950	1600	1450	
						1	[illegible]									[illegible]					500		375	
						2	[illegible]									[illegible]					550		375	
						3	[illegible]									[illegible]					600		375	
						4	[illegible]									[illegible]					[illegible]		375	

(page 2 of 3)

Case	Page	Mat'l	Depth	T_1 (lb)	Segmts	Node	Rope Length (ft)	Wave Ht. (ft)	Period (sec)	2.0	2.3	2.7	3.0	3.3	3.7	4.0	4.3	4.7	5.0	6	8	12	16	32
									Dynamic Tension in Pounds at Period in Seconds															
E	65	STL	1800	10000	4	1	1860	25													10500		10000	9000
						2	1395														10500		10000	9000
						3	930														10500		10600	9250
						4	465														10500		9750	9000
						1	1860	15		4750	5050		5750		5750	5757			5750	6000	6000	6000	6000	
						2	1395			5750	5750		6000		6000	6000			6000	6000	6000	6000	6000	
						3	930			6750	6600		6750		6250	6500			6250	6250	6000	6250	6000	
						4	465			6750	6600		6250		6000				6250	6000	6000	6000	6000	
						1	1860	5		1850						1850					2000		2000	
						2	1395			2050						2050					2150		[illegible]	
						3	930			2300						2150					2150		[illegible]	
						4	465			2350						2150					2000		2000	
F	67	STL	1800	4858	4	1	2564	50															10000	5000
						2	1923																10000	5000
						3	1282																10000	5000
						4	641																10000	5000
						1	2564	15		4000	3600		4000		4000	4000			4000	3750	3500	2250	2300	
						2	1923			4500	4100		4250		4250	4250			4000	3750	3500	2250	2300	
						3	1282			5000	4850		4750		4500	4500			4250	4000	3600	2250	2300	
						4	641			5500	5200		4500		4500	4500			4250	4000	3600	2250	2300	
						1	2564	5		1300						1350					1050		800	
						2	1923			1550						1450					1100		750	
						3	1282			1700						1500					1150		600	
						4	641			1800						1450					1100		600	
G	23	NYL	18000	3600	10	1	23130	50													1350		575	280
						7	4026														70		130	140
						10	0														120		170	180
						1	23130	15								460					225		90	
						7	4026									35					48		50	
						10	0									70					72		60	
						1	23130	5		102			675			115			390	220	75		20	
						7	4026			20			60			20			25	52	25		15	
						10	0			18			65			52			70	75	45		18	
H	21	NYL	18000	460	10	1	22000	50													52		250	190
						7	6021														15		12	18
						10	0														5		8	20
						1	22000	15								20					90		45	
						7	6021									125					10		5	
						10	0									<1					2		5	
						1	22000	5								45					22		15	
						7	6021									125					8		5	
						10	0									<1					2		5	
I	55	NYL	6000	3600	10	1	7487	50													1400		500	400
						7	1330														450		440	400
						10	0														575		570	475
						1	7487	15				850		750	650	625	600	550	400	300	175	100	125	
						7	1330					95		170	190	200	200	200	190	170	180	150	150	
						10	0					300		300	280	280	230	230	250	210	250	150	150	
						1	7487	5								200					35		26	
						7	1330									120					62		62	
						10	0									150					75		45	

(page 3 of 3)

Case	Page	Mat'l.	Depth	$\bar{T}_1$ (lb)	Segmts	Node	Rope Length (ft)	Wave Ht. (ft)	Period (sec)	Dynamic Tension in Pounds at Period in Seconds 2.0	2.3	2.7	3.0	3.3	3.7	4.0	4.3	4.7	5.0	6	8	12	16	32
J	54	NYL	6000	720	10	1	6025	50															265	125
						7	1036																157	140
						10	0																180	150
						1	6025	46													663			
						7	1036														130			
						10	0														170			
						1	6025	15		220	180	130	120	90	80	295	60	70	80	70	140	20	30	
						7	1036			60	50	25	18	18	20	42	30	30	35	35	80	15	48	
						10	0			130	130	120	120	110	110	88	110	110	110	90	80	30	55	
						1	5025	5								51					30		8	
						7	1036									25					22		18	
						10	0									56					28		18	
K	62	NYL	1800	3600	4	1	2052	50													925		912	925
						2	1539														900		912	925
						3	1026														1012		938	925
						4	513														1050		938	925
						1	2052	15					480		325	285			270	265	280	305	310	
						2	1539						320		320	320			310	310	310	320	320	
						3	1026						475		440	410			388	375	355	338	330	
						4	513						500		475	450			400	375	345	312	320	
						1	2052	5		345						100					125		130	
						2	1539			148						132					135		135	
						3	1026			270						163					142		140	
						4	513			380						168					145		135	
L	64	NYL	1800	1440	4	1	4312	50													488		290	270
						2	3234														290		260	255
						3	2156														315		260	255
						4	1078														300		260	250
						1	4312	15					280		270	260			216	150	105	92	85	
						2	3234						180		155	140			126	90	80	80	75	
						3	2156						79		85	85			90	98	90	80	78	
						4	1078						125		130	138			136	119	92	90	78	
						1	4312	5		145						88					38		30	
						2	3234			78						49					29		26	
						3	2156			45						25					30		26	
						4	1078			50						49					30		25	

PLOTS OF DYNAMIC TENSIONS

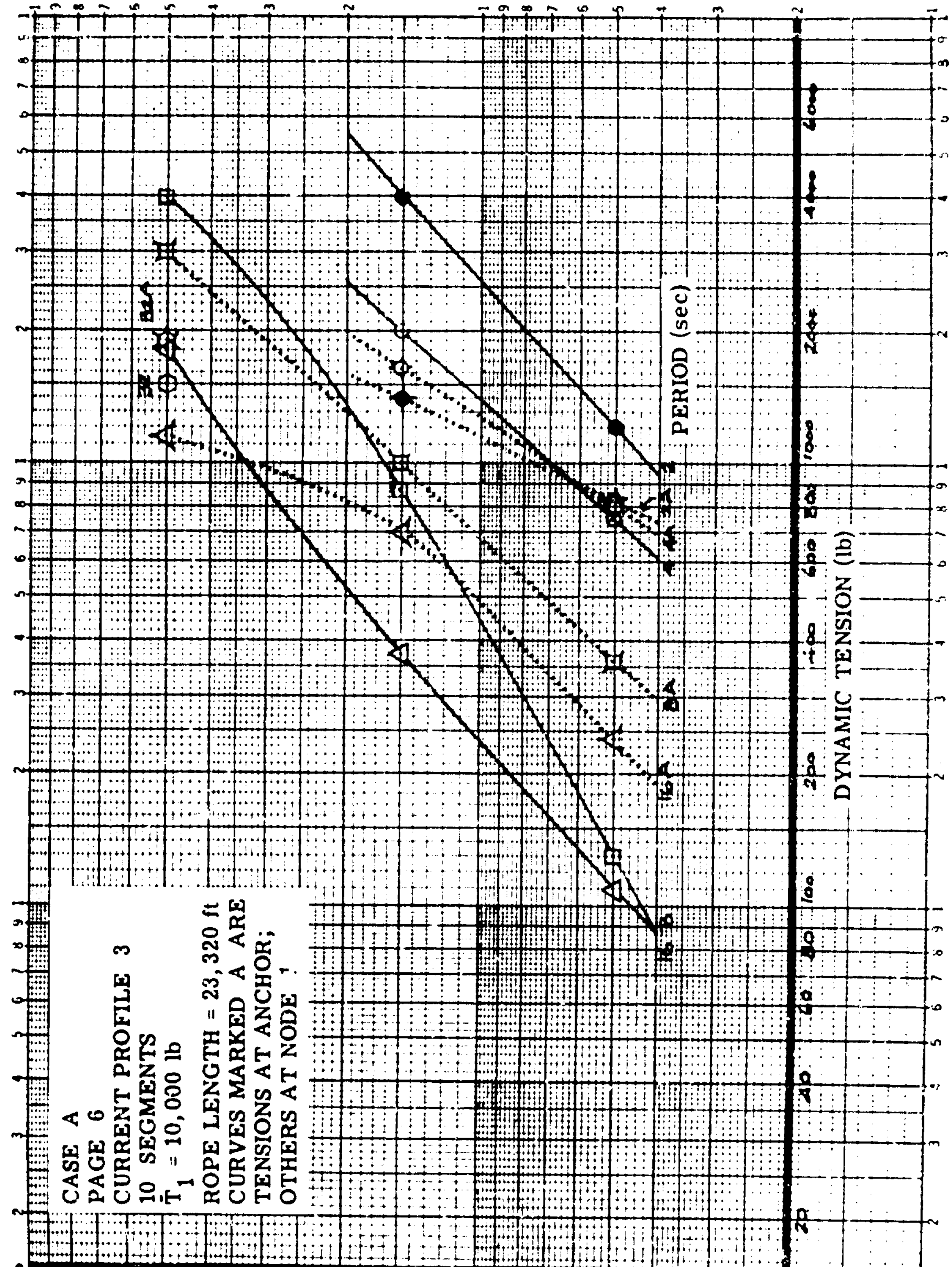
CASE A
PAGE 6
CURRENT PROFILE 3
10 SEGMENTS
T_1 = 10,000 lb
ROPE LENGTH = 23,320 ft
CURVES MARKED A ARE TENSIONS AT ANCHOR; OTHERS AT NODE 1
PERIOD (sec)
DYNAMIC TENSION (lb)
WAVE HEIGHT (ft)

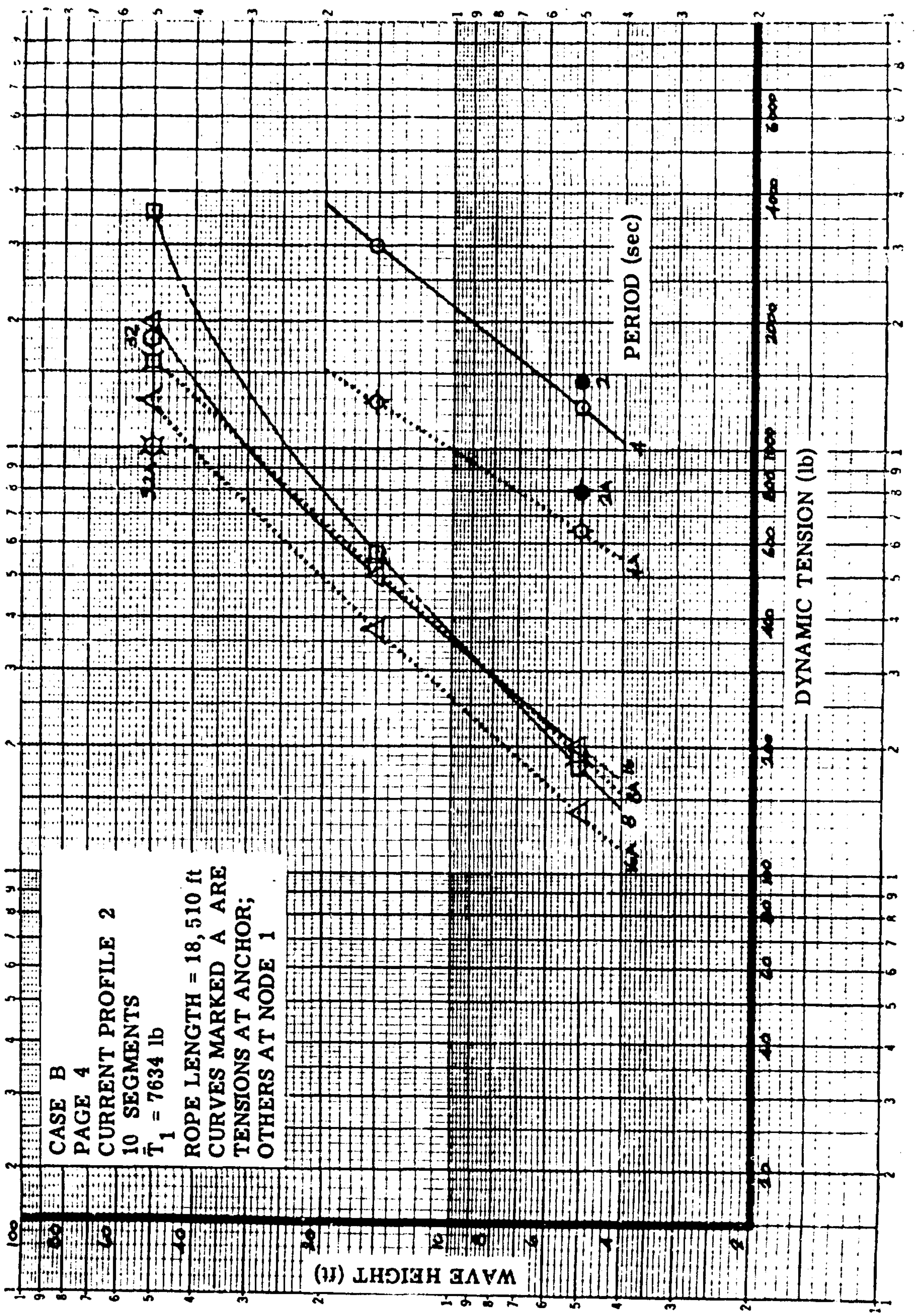
CASE B
PAGE 4
CURRENT PROFILE 2
10 SEGMENTS
T1 = 7634 lb
ROPE LENGTH = 18,510 ft
CURVES MARKED A ARE TENSIONS AT ANCHOR; OTHERS AT NODE 1
PERIOD (sec)
DYNAMIC TENSION (lb)
WAVE HEIGHT (ft)

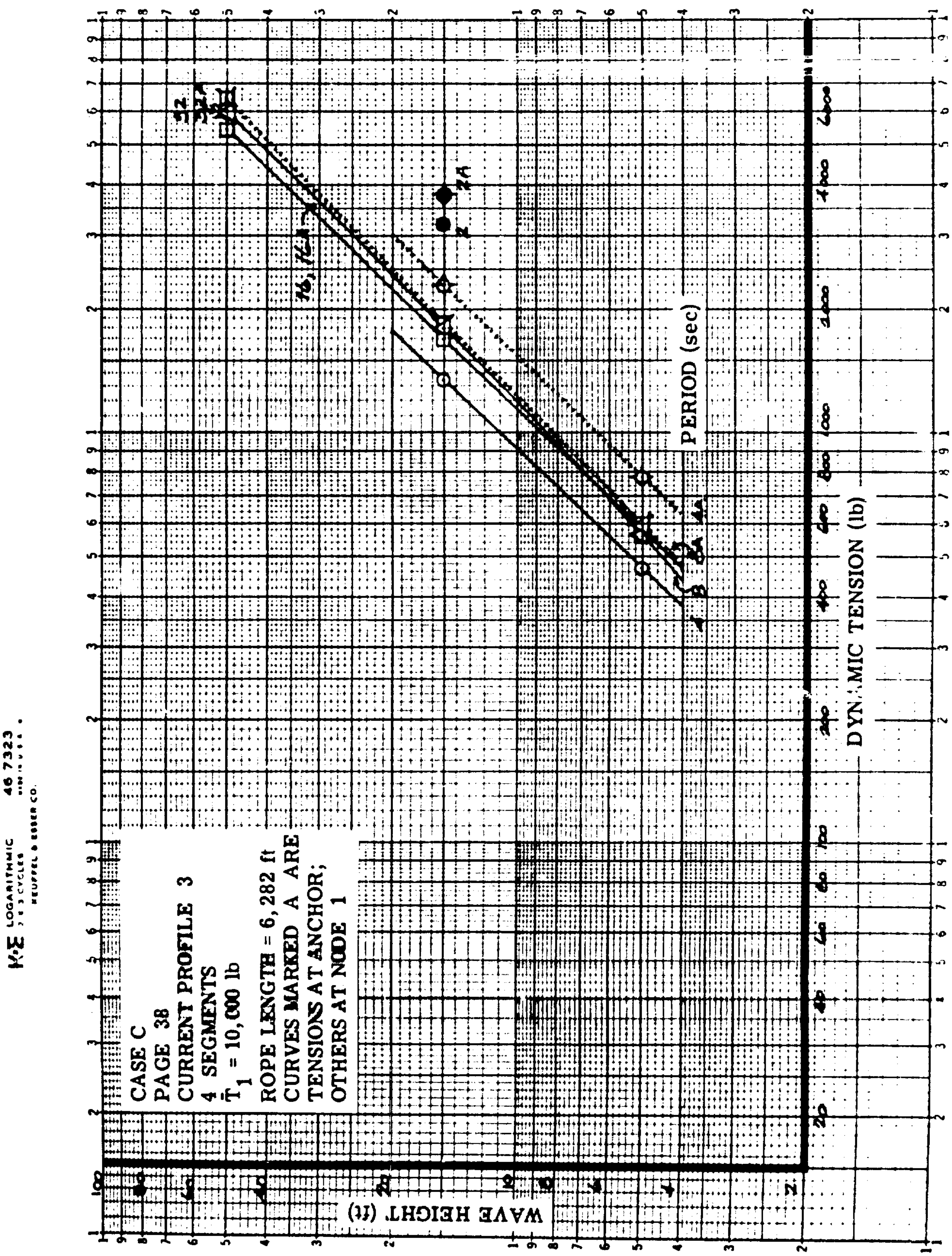
CASE C
PAGE 38
CURRENT PROFILE 3
4 SEGMENTS
$\bar{T}_1$ = 10,000 lb
ROPE LENGTH = 6,282 ft
CURVES MARKED A ARE
TENSIONS AT ANCHOR;
OTHERS AT NODE 1
PERIOD (sec)
DYN∴MIC TENSION (lb)
WAVE HEIGHT (ft)
K&E LOGARITHMIC 46 7323
KEUFFEL & ESSER CO.

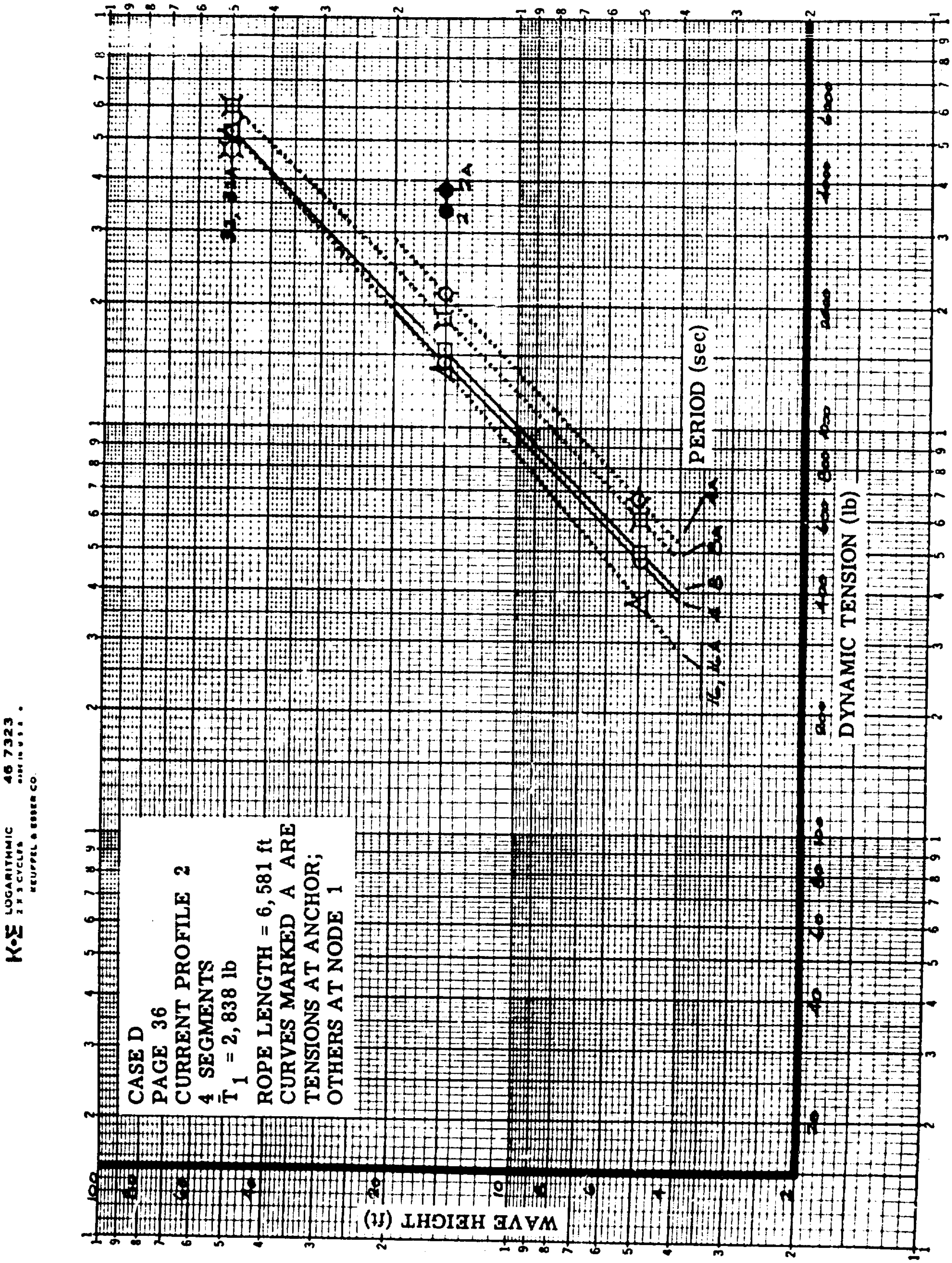
K•E LOGARITHMIC 2 X 3 CYCLES KEUFFEL & ESSER CO.
46 7323
CASE D
PAGE 36
CURRENT PROFILE 2
4 SEGMENTS
$\bar{T}_1$ = 2,838 lb
ROPE LENGTH = 6,581 ft
CURVES MARKED A ARE
TENSIONS AT ANCHOR;
OTHERS AT NODE 1
WAVE HEIGHT (ft)
DYNAMIC TENSION (lb)
PERIOD (sec)

K•E LOGARITHMIC 46 7323
2 X 3 CYCLES
KEUFFEL & ESSER CO.

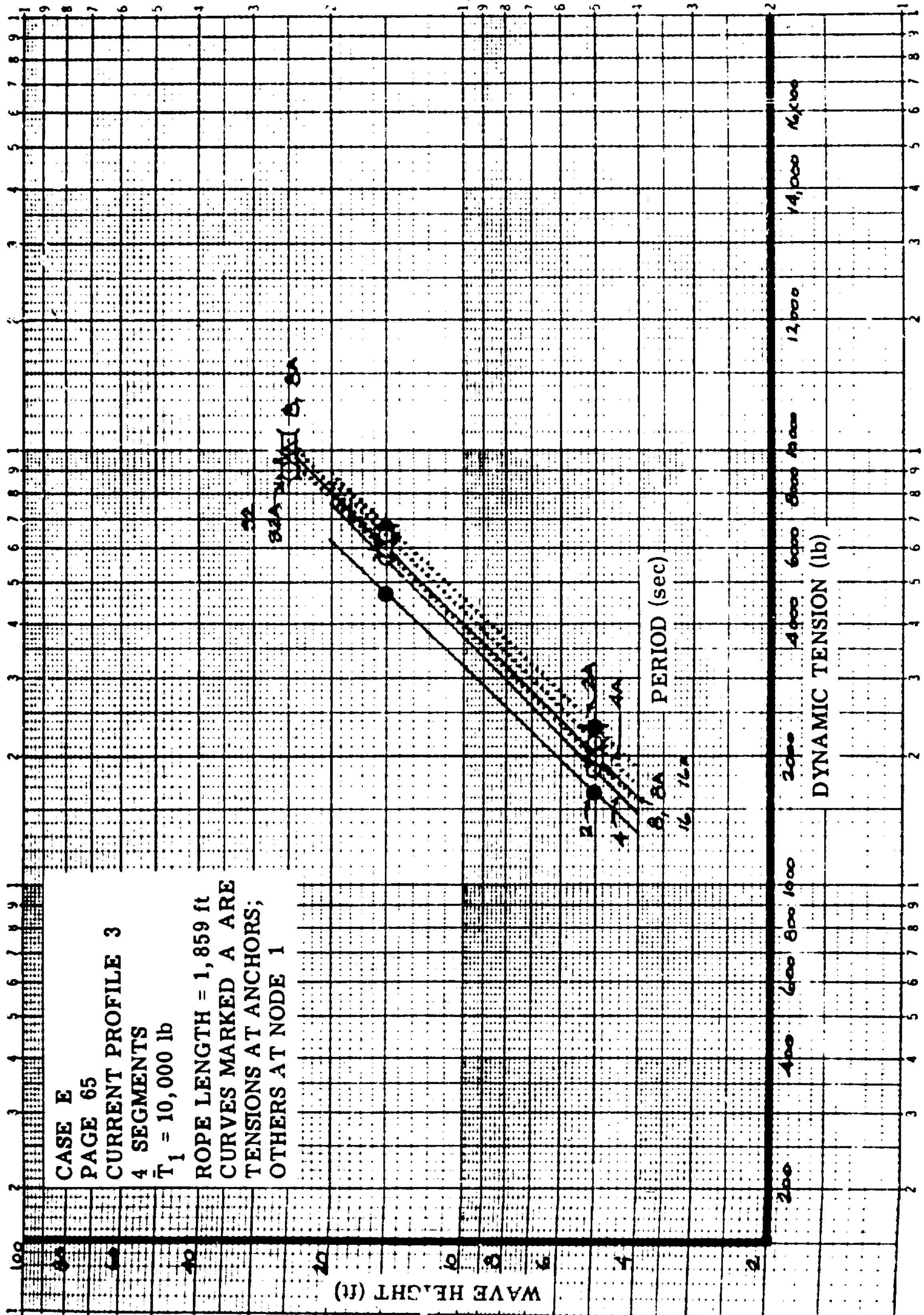

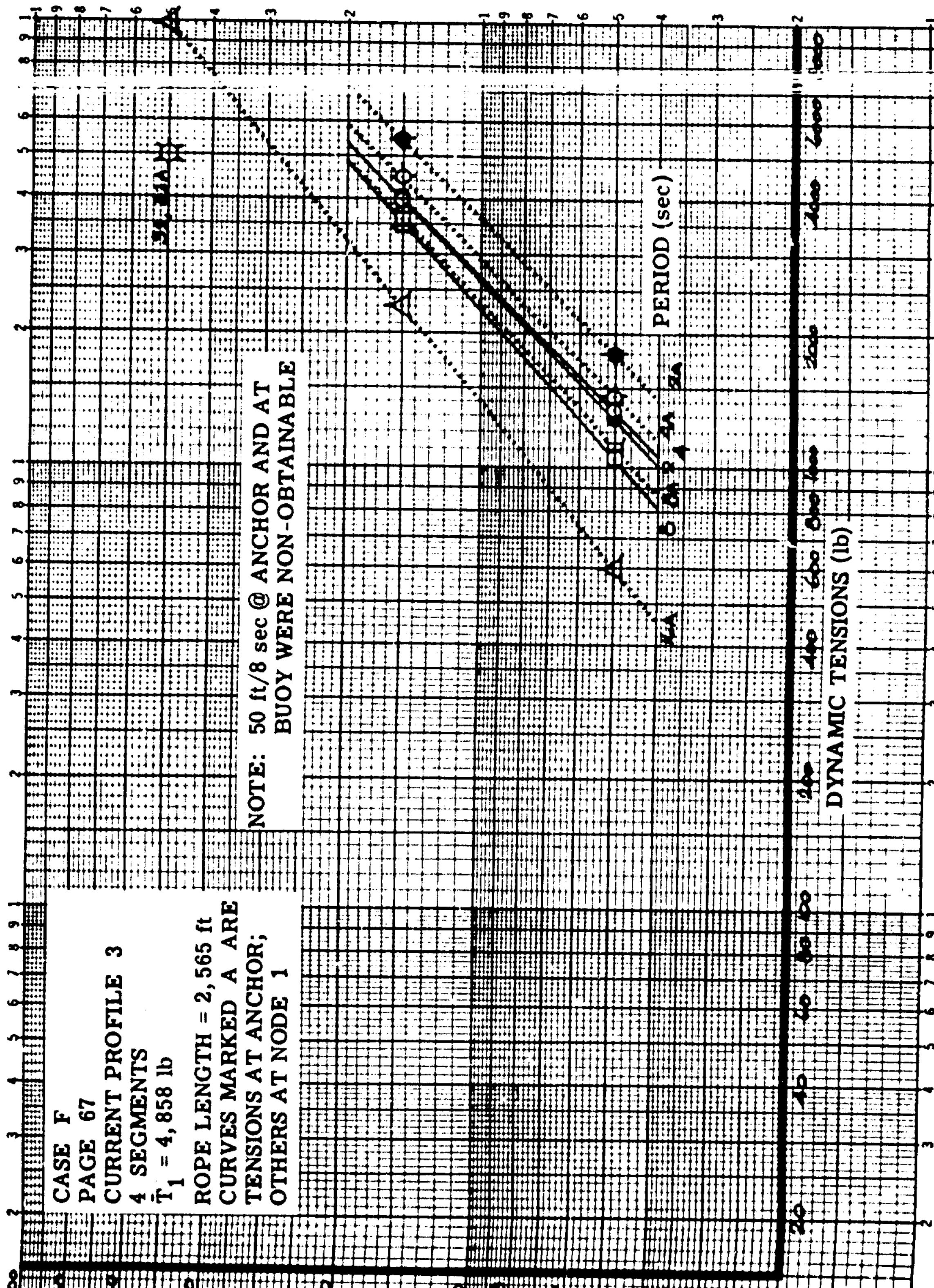
CASE F
PAGE 67
CURRENT PROFILE 3
4 SEGMENTS
$\bar{T}_1$ = 4,858 lb
ROPE LENGTH = 2,565 ft
CURVES MARKED A ARE TENSIONS AT ANCHOR; OTHERS AT NODE 1
NOTE: 50 ft/8 sec @ ANCHOR AND AT BUOY WERE NON-OBTAINABLE
PERIOD (sec)
DYNAMIC TENSIONS (lb)
WAVE HEIGHT (ft)

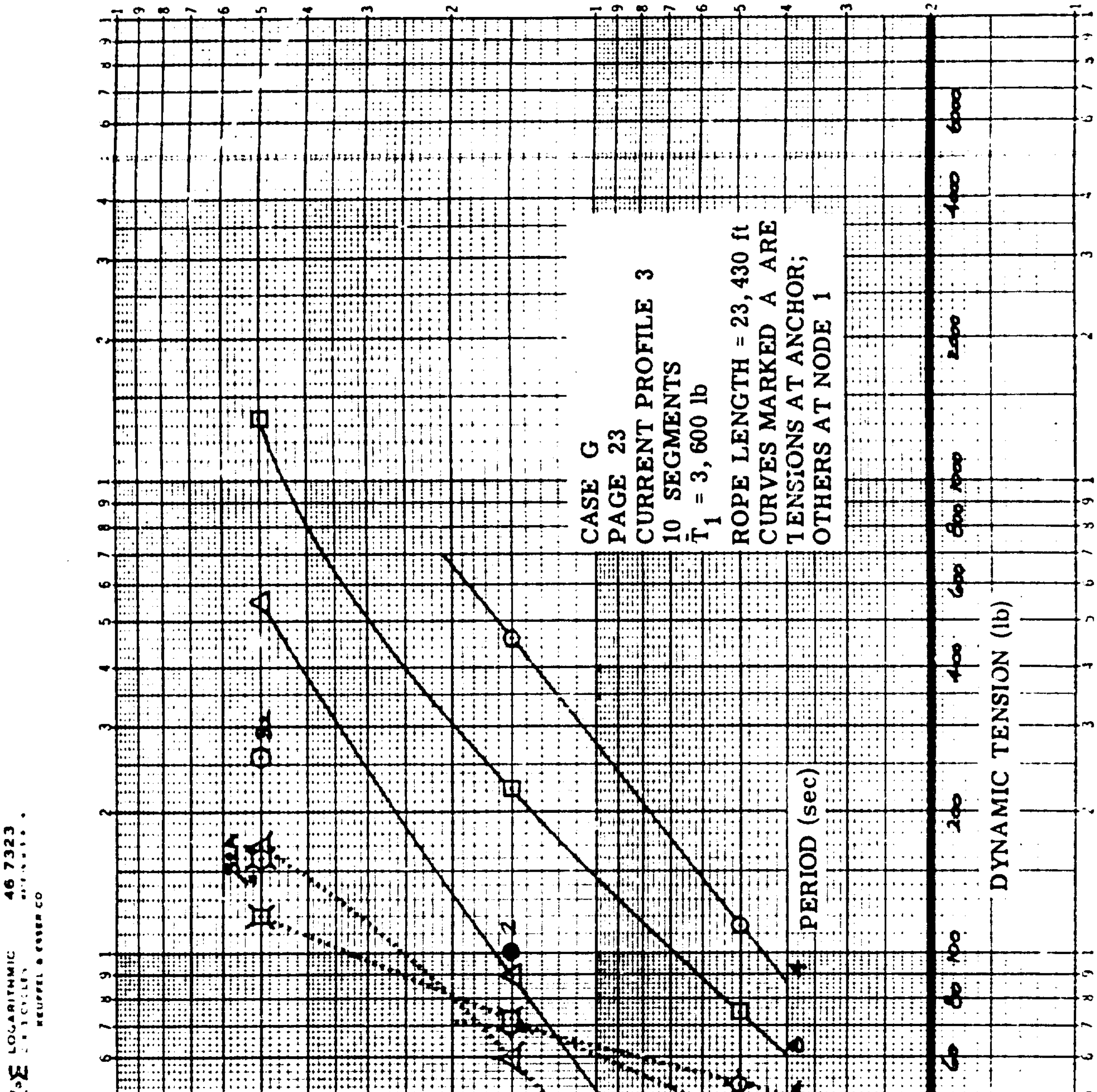
CASE G
PAGE 23
CURRENT PROFILE 3
10 SEGMENTS
$\bar{T}_1$ = 3, 600 lb
ROPE LENGTH = 23, 430 ft
CURVES MARKED A ARE TENSIONS AT ANCHOR; OTHERS AT NODE 1
PERIOD (sec)
DYNAMIC TENSION (lb)
WAVE HEIGHT (ft)

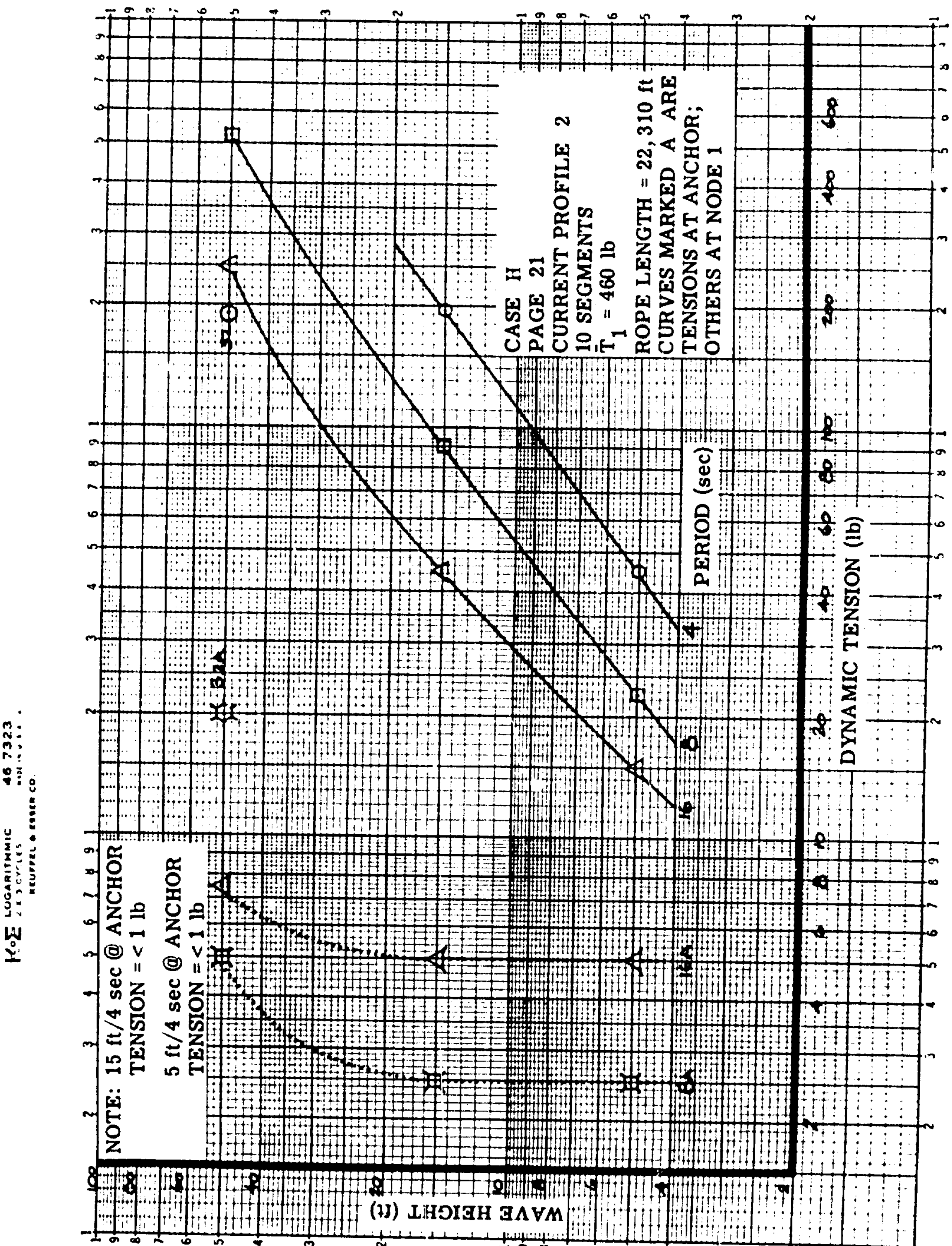
CASE H
PAGE 21
CURRENT PROFILE 2
10 SEGMENTS
$\bar{T}_1$ = 460 lb
ROPE LENGTH = 22, 310 ft
CURVES MARKED A ARE TENSIONS AT ANCHOR; OTHERS AT NODE 1
NOTE: 15 ft/4 sec @ ANCHOR TENSION = < 1 lb
5 ft/4 sec @ ANCHOR TENSION = < 1 lb
32A
16A
4
8
16
PERIOD (sec)
DYNAMIC TENSION (lb)
WAVE HEIGHT (ft)

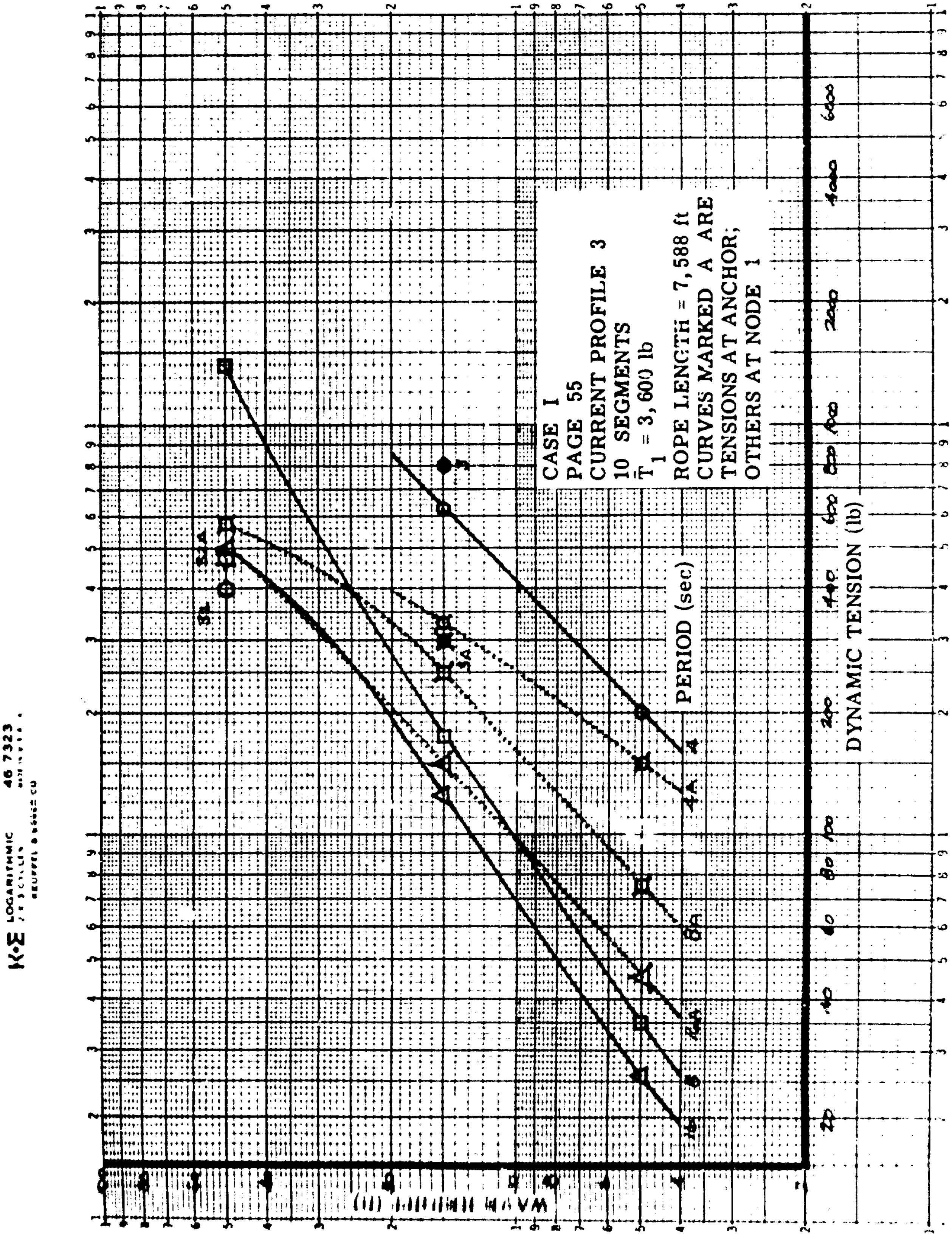
CASE I
PAGE 55
CURRENT PROFILE 3
10 SEGMENTS
$\bar{T}_1$ = 3,600 lb
ROPE LENGTH = 7,588 ft
CURVES MARKED A ARE
TENSIONS AT ANCHOR;
OTHERS AT NODE 1
PERIOD (sec)
DYNAMIC TENSION (lb)
WAVE HEIGHT (ft)
K-E LOGARITHMIC 46 7323

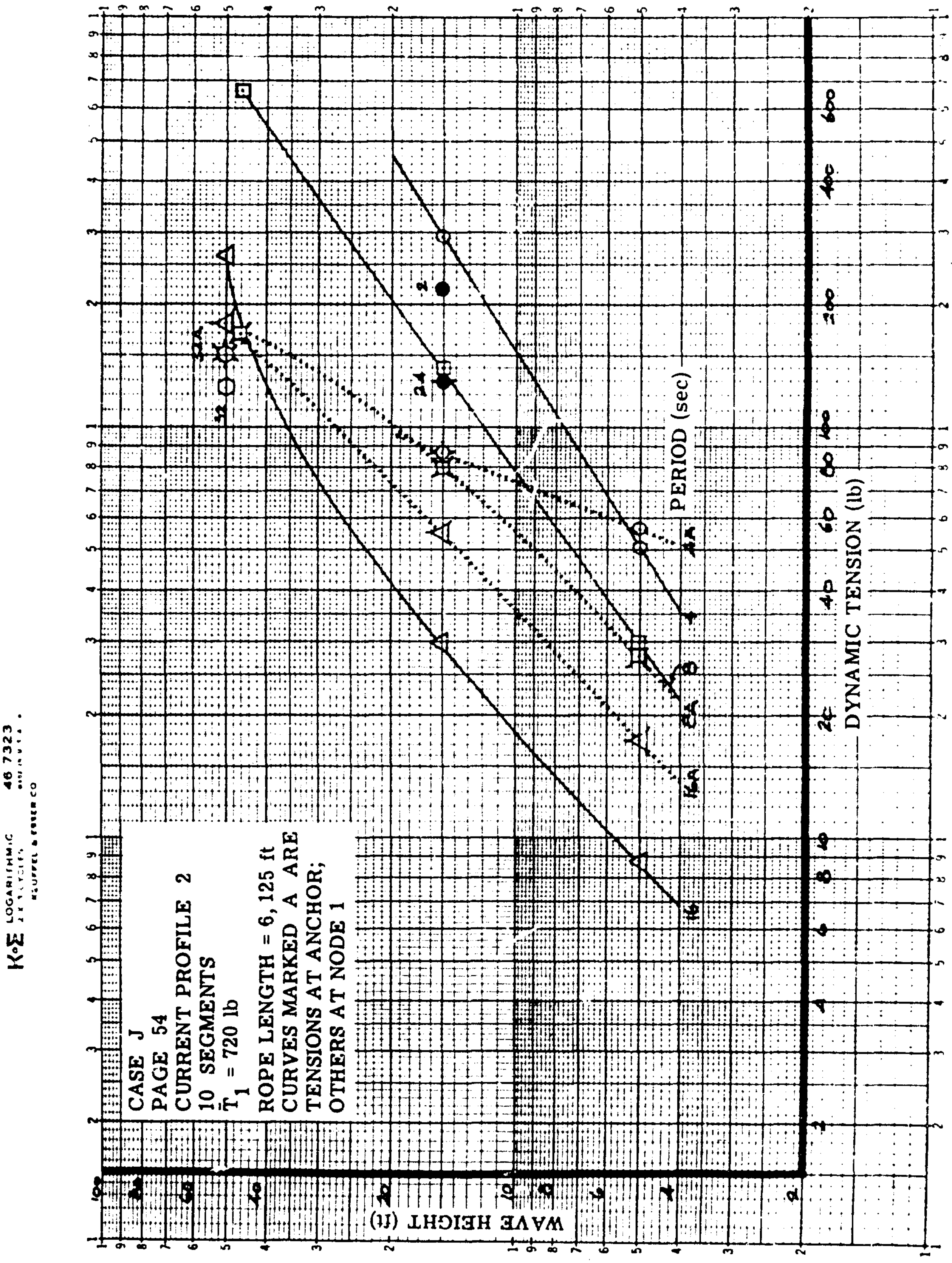
CASE J
PAGE 54
CURRENT PROFILE 2
10 SEGMENTS
T_1 = 720 lb
ROPE LENGTH = 6,125 ft
CURVES MARKED A ARE
TENSIONS AT ANCHOR;
OTHERS AT NODE 1
PERIOD (sec)
DYNAMIC TENSION (lb)
WAVE HEIGHT (ft)

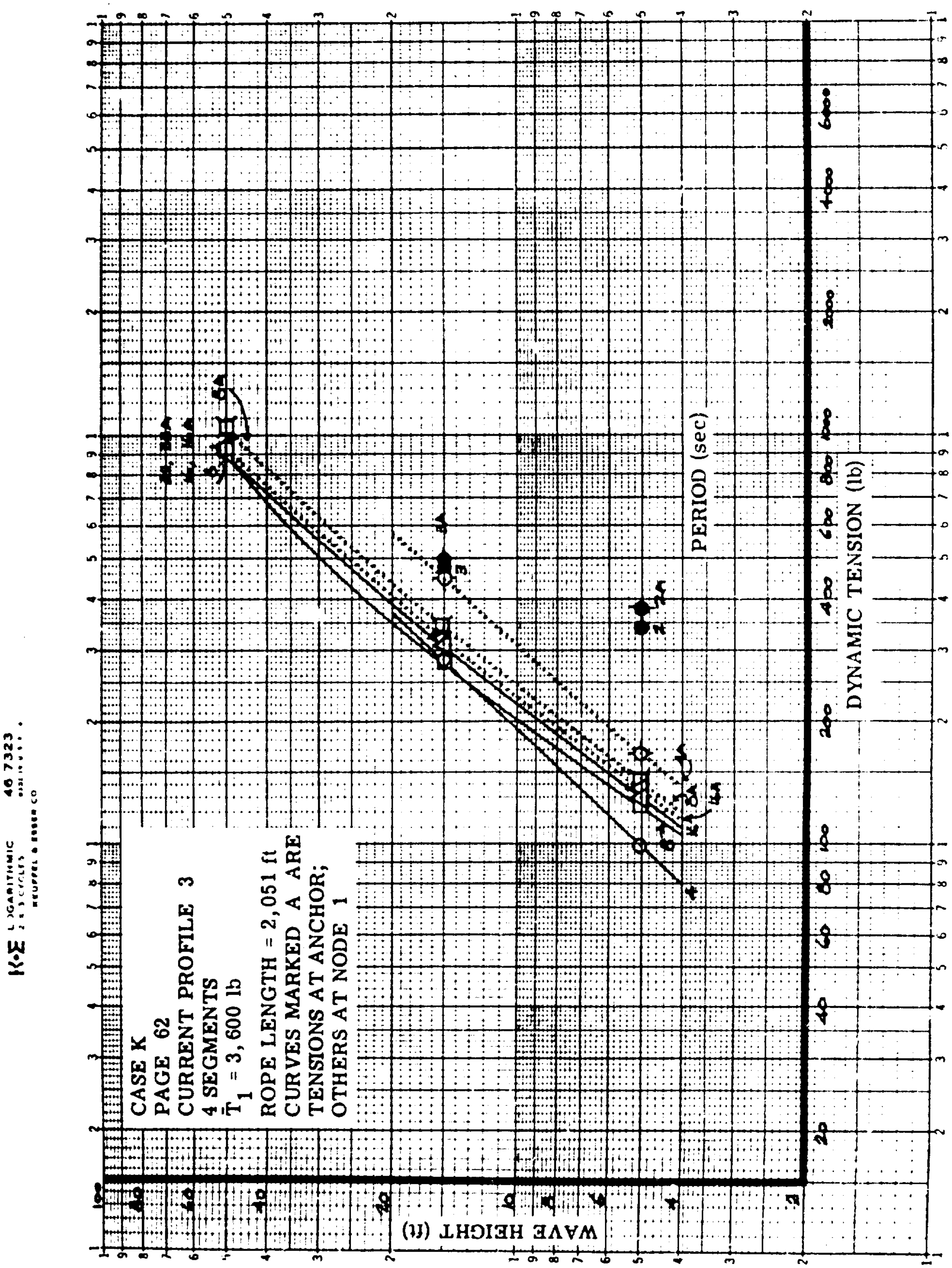
CASE K
PAGE 62
CURRENT PROFILE 3
4 SEGMENTS
$\bar{T}_1$ = 3,600 lb
ROPE LENGTH = 2,051 ft
CURVES MARKED A ARE TENSIONS AT ANCHOR; OTHERS AT NODE 1
PERIOD (sec)
DYNAMIC TENSION (lb)
WAVE HEIGHT (ft)

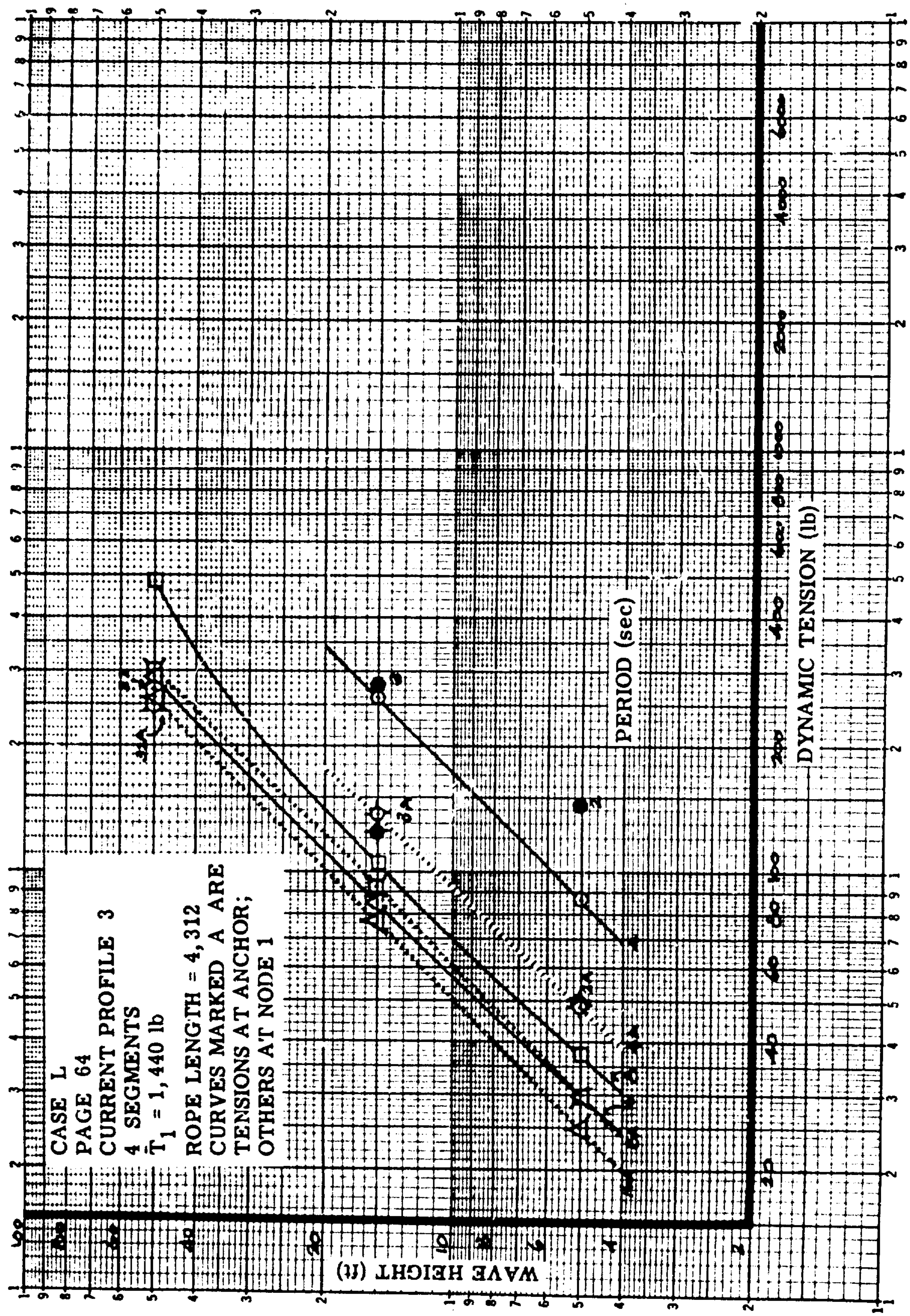
CASE L
PAGE 64
CURRENT PROFILE 3
4 SEGMENTS
$\bar{T}_1$ = 1, 440 lb
ROPE LENGTH = 4, 312
CURVES MARKED A ARE
TENSIONS AT ANCHOR;
OTHERS AT NODE 1
WAVE HEIGHT (ft)
PERIOD (sec)
DYNAMIC TENSION (lb)

MOTIONS OF NODES

MOTIONS OF NODES

Rope Material = Steel | Water Depth = 18,000 ft | Reference Page 6

Rope Diameter = 0.5 in. | $\overline{T}_1$ = 10,000 lb | Case A

Wave Height (ft)	Wave Period (sec)	n	Rope Angle (deg)	Major Axis Angle (deg)	Major Axis Length (ft)	Minor Axis Length (ft)	CW*
50	32	1	7.8	0	50.0	3.2	
		2	14.3	3.5	47.0	10.0	
		3	18.3	17.5	43.2	9.4	
		4	21.4	19.0	37.6	7.3	
		5	25.9	20.0	31.2	8.6	
		6	32.9	22.5	25.0	10.0	
		7	43.3	6.0	19.0	10.6	
		8	56.4	-5.0	14.6	9.2	
		9	71.7	-10.0	14.5	4.5	
50	16	1	7.8	3.0	50.0	2.0	
		2	14.3	8.0	48.0	6.0	
		3	18.3	18.0	45.4	4.5	
		4	21.4	21.3	40.2	3.7	
		5	25.9	24.0	34.6	5.0	
		6	32.9	30.5	27.8	6.4	
		7	43.3	39.5	19.4	8.0	
		8	56.4	54.0	13.8	7.2	
		9	71.7	-10.5	8.2	5.0	
50	8	1	7.8	3.5	49.8	1.0	
		2	14.3	8.0	47.4	2.0	
		3	18.3	15.5	45.0	1.6	
		4	21.4	22.0	42.4	1.0	
		5	25.9	23.5	39.0	1.8	
		6	32.9	31.5	33.0	3.0	
		7	43.3	41.0	24.2	4.2	
		8	56.4	55.0	18.0	3.0	
		9	71.7	52.0	7.4	5.0	

* Rotation of nodes counterclockwise except when X is shown in this column.

MOTIONS OF NODES

Rope Material = Steel | Water Depth = 6,000 ft | Reference Page 6

Rope Diameter = 0.5 in. | $\bar{T}_1$ = 10,000 lb | Case A

Wave Height (ft)	Wave Period (sec)	n	Rope Angle (deg)	Major Axis Angle (deg)	Major Axis Length (ft)	Minor Axis Length (ft)	CW
15	16	1	7.8	4.0	15.0	0.6	
		2	14.3	5.5	14.6	3.0	
		3	18.3	19.0	13.7	2.4	
		4	21.4	22.0	12.1	2.0	
		5	25.9	26.0	10.6	2.6	
		6	32.9	30.0	8.6	3.2	
		7	43.3	30.0	6.2	3.8	
		8	56.4	31.5	4.2	2.6	
		9	71.7	-9.0	3.4	1.6	
15	8	1	7.8				
		2	14.3	6.0	15.4	0.2	
		3	18.3	16.5	15.0	0.8	
		4	21.4	21.5	14.8	0.4	
		5	25.9	25.5	12.8	1.1	
		6	32.9	33.0	10.6	1.6	
		7	43.3	43.5	8.1	2.4	
		8	56.4	54.0	3.1	2.1	
		9	71.7	-8.5	2.6	2.1	
15	4	1	7.8	5.0	14.9	0.3	
		2	14.3	9.0	13.3	1.5	
		3	18.3	17.0	11.6	0.5	
		4	21.4	19.0	8.8	0.5	
		5	25.9	21.0	10.0	0.2	
		6	32.9	30.0	12.5	0.2	
		7	43.3	42.5	11.6	1.0	
		8	56.4	60.0	9.2	0.3	
		9	71.7	69.0	3.8	1.6	

MOTIONS OF NODES

Rope Material = Steel | Water Depth = 6,000 ft | Reference Page 6

Rope Diameter = 0.5 in. | $\bar{T}_1$ = 10,000 lb | Case A

Wave Height (ft)	Wave Period (sec)	n	Rope Angle (deg)	Major Axis Angle (deg)	Major Axis Length (ft)	Minor Axis Length (ft)	CW
5	16	1	7.8	4.0	5.0	0.2	
		2	14.3	-3.0	5.0	1.1	
		3	18.3	18.5	4.3	1.6	
		4	21.4	21.5	4.0	1.0	
		5	25.9	25.0	3.5	1.4	
		6	32.9	33.0	2.9	1.8	
		7	43.3	-32.0	2.5	1.9	
		8	56.4	22.0	1.6	1.0	
		9	71.7	-12.5	1.4	0.5	
5	8	1	7.8	5.5	5.0	0	
		2	14.3	3.5	5.2	0	
		3	18.3	19.0	5.2	0.3	
		4	21.4	22.5	5.1	0.2	
		5	25.9	28.5	4.7	0.5	
		6	32.9	36.0	3.9	0.8	
		7	43.3	49.0	2.8	1.3	
		8	56.4	60.0	2.2	1.1	
		9	71.7	-12.0	1.1	0.8	
5	4	1	7.8	5.0	4.8	0.2	
		2	14.3	13.0	4.1	1.0	
		3	18.3	21.0	3.2	0.4	
		4	21.4	13.5	2.3	0.2	
		5	25.9	19.0	4.1	0	
		6	32.9	30.0	5.7	0.2	
		7	43.3	45.0	5.4	0.5	
		8	56.4	63.0	4.3	0.2	
		9	71.7	71.5	1.8	0.5	
5	2	1	7.8	5.5	5.2	0	
		2	14.3	8.0	5.1	0.4	
		3	18.3	19.0	4.2	0.2	
		4	21.4	20.0	3.2	0.1	
		5	25.9	27.0	4.7	0.1	
		6	32.9	34.0	2.9	0.4	
		7	43.3	35.5	3.5	0	
		8	56.4	51.5	4.2	0	
		9	71.7	72.0	1.9	0.4	

MOTIONS OF NODES

Rope Material = Steel — Water Depth = 18,000 ft — Reference Page 4

Rope Diameter = 0.5 in. — $\bar{T}_1$ = 7,634 lb — Case B

Wave Height (ft)	Wave Period (sec)	n	Rope Angle (deg)	Major Axis Angle (deg)	Major Axis Length (ft)	Minor Axis Length (ft)	CW
50	32	1	1.6	-1.0	50.0	0	
		2	1.9	-3.5	41.8	3.0	
		3	2.0	1.5	45.0	3.5	
		4	2.6	-0.5	39.4	3.0	
		5	3.7	-1.5	34.6	3.2	
		6	5.8	-4.5	31.4	3.6	
		7	10.0	-10.5	30.0	3.4	
		8	20.0	-25.5	35.0	7.2	
		9	45.8	-25.0	35.0	1.0	
50	16	1	1.6	0.5	50.0	0	
		2	1.9	2.5	47.5	2.0	
		3	2.0	2.5	44.5	1.2	
		4	2.6	3.0	37.0	2.2	
		5	3 7	3.0	29.5	2.5	
		6	5.8	4.0	22.0	2.9	
		7	10.0	-8.5	17.2	3.3	
		8	20.0	-26.5	18.5	8.3	
		9	45.8	-25.0	20.5	1.4	
50	8	1	1.6	1.0	49.5	0	
		2	1.9	1.0	48.8	0.8	
		3	2.0	1.5	47.0	0.4	
		4	2.6	3.0	40.0	0.8	
		5	3.7	3.5	32.5	1.0	
		6	5.8	5.5	24.0	1.8	
		7	10.0	9.5	14.4	2.8	
		8	20.0	39.5	10.4	6.2	
		9	45.8	-24.0	12.2	1.4	

MOTIONS OF NODES

Rope Material = Steel — Water Depth = 18,000 ft — Reference Page 4

Rope Diameter = 0.5 in. — $\bar{T}_1$ = 7,634 lb — Case B

Wave Height (ft)	Wave Period (sec)	n	Rope Angle (deg)	Major Axis Angle (deg)	Major Axis Length (ft)	Minor Axis Length (ft)	CW
15	16	1	1.6	0	15.0	0	
		2	1.9	-2.0	14.4	0.3	
		3	2.0	3.0	13.4	0.8	
		4	2.6	1.5	11.6	0.9	
		5	3.7	0	10.0	1.2	
		6	5.8	-2.5	8.7	1.4	
		7	10.0	-12.5	8.2	1.4	
		8	20.0	-26.5	9.4	2.4	
		9	45.8	-25.5	9.4	0.4	
15	8	1	1.6	1.0	15.0	0	
		2	1.9	-0.5	14.8	0.4	
		3	2.0	2.5	13.9	0.2	
		4	2.6	4.0	12.0	0.3	
		5	3.7	3.5	10.0	0.6	
		6	5.8	4.0	7.6	1.0	
		7	10.0	-1.5	5.3	1.4	
		8	20.0	-25.0	4.6	3.0	
		9	45.8	-25.0	4.9	0.5	
15	4	1	1.6	1.5	15.0	0	
		2	1.9	0	14.8	0.8	
		3	2.0	2.0	16.0	0.8	
		4	2.6	2.0	18.8	0	
		5	3.7	3.5	18.8	0.8	
		6	5.8	6.5	15.2	0.4	
		7	10.0	10.0	8.2	1.2	
		8	20.0	50.0	4.9	0.4	
		9	45.8	-26.0	5.0	1.1	

MOTIONS OF NODES

Rope Material = Steel | Water Depth = 18,000 ft | Reference Page 4

Rope Diameter = 0.5 in. | $\bar{T}_1$ = 7,634 lb | Case B

Wave Height (ft)	Wave Period (sec)	n	Rope Angle (deg)	Major Axis Angle (deg)	Major Axis Length (ft)	Minor Axis Length (ft)	CW
5	16	1	1.6	0	5.0	0	
		2	1.9	0	4.9	0.1	
		3	2.0	2.5	4.6	0.4	
		4	2.6	2.0	4.2	0.4	
		5	3.7	0	3.9	0.6	
		6	5.8	-5.0	3.8	0.8	
		7	10.0	-17.5	3.8	0.7	
		8	20.0	-26.5	4.3	0.7	
		9	45.8	-24.5	4.2	0.1	
5	8	1	1.6	1.0	5.0	0	
		2	1.9	-4.0	5.0	0	
		3	2.0	4.0	4.6	0.1	
		4	2.6	3.0	4.0	0.1	
		5	3.7	4.5	3.5	0.3	
		6	5.8	3.0	2.9	0.5	
		7	10.0	-7.0	2.4	0.8	
		8	20.0	-33.0	2.7	1.1	
		9	45.8	-25.0	2.8	0.2	
5	4	1	1.6	1.0	5.2	0	
		2	1.9	0.5	5.7	0.1	
		3	2.0	2.0	7.0	0	
		4	2.6	1.5	8.8	0	
		5	3.7	4.0	8.8	0.1	
		6	5.8	7.0	7.2	0.3	
		7	10.0	8.5	4.0	0.8	
		8	20.0	64.0	3.4	0.8	
		9	45.8	-26.5	3.2	0.6	
5	2	1	*				
		2					
		3					
		4					
		5					
		6					
		7					
		8					
		9					

* (x) and (y) sweeps not obtainable

MOTIONS OF NODES

Rope Material = Steel | Water Depth = 6,000 ft | Reference Page 38

Rope Diameter = 0.5 in. | $\bar{T}_1$ = 10,000 lb | Case C

Wave Height (ft)	Wave Period (sec)	n	Rope Angle (deg)	Major Axis Angle (deg)	Major Axis Length (ft)	Minor Axis Length (ft)	CW
50	32	1	12.9	8.5	37.5	17.0	
		2	18.8	18.0	25.0	18.0	
		3	20.6	-63.0	14.8	12.0	
50	16	1	12.9	11.5	37.2	10.0	
		2	18.8	20.0	24.8	10.0	
		3	20.6	20.0	12.5	8.2	
50	8	1	12.9	12.5	38.4	3.8	
		2	18.8	20.5	26.8	3.6	
		3	20.6	23.5	13.5	3.0	
15	16	1	12.9	13.0	11.2	2.1	
		2	18.8	16.0	7.4	3.8	
		3	20.6	39.0	3.8	3.2	
15	8	1	12.9	13.0	11.4	1.1	
		2	18.8	25.0	7.6	1.8	
		3	20.6	31.0	4.0	1.4	
15	4	1	12.9	12.6	12.5	0.4	
		2	18.8	21.0	9.0	0.6	
		3	20.6	25.0	4.9	0.5	
5	16	1	12.9	12.0	3.8	0.8	
		2	18.8	-10.0	2.4	2.4	
		3	20.6	-73.0	2.0	1.2	
5	8	1	12.9	13.0	3.8	0.4	
		2	18.8	31.0	2.6	0.8	
		3	20.6	46.0	1.4	0.6	
5	4	1	12.9	12.6	4.1	0.2	
		2	18.8	23.5	3.0	0.2	
		3	20.6	28.5	1.6	0.2	

MOTIONS OF NODES

Rope Material = Steel
Rope Diameter = 0.5 in.

Water Depth = 6,000 ft
$\bar{T}_1$ = 2,838 lb

Reference Page 36
Case D

Wave Height (ft)	Wave Period (sec)	n	Rope Angle (deg)	Major Axis Angle (deg)	Major Axis Length (ft)	Minor Axis Length (ft)	CW
50	32	1	5.7	-6.5	42.5	9.0	
		2	8.8	-18.0	37.6	11.0	
		3	25.9	-48.0	57.5	10.0	
50	16	1	5.7	1.5	39.0	7.0	
		2	8.8	-4.0	28.5	9.5	
		3	25.9	-50.0	34.0	11.6	
50	8	1	5.7	6.0	39.0	3.6	
		2	8.8	7.0	27.0	5.2	
		3	25.9	-25.0	15.0	12.0	
15	16	1	5.7	-3.5	12.4	3.0	
		2	8.8	-15.0	11.0	3.8	
		3	25.9	50.0	16.9	3.2	
15	8	1	5.7	6.0	11.6	1.7	
		2	8.8	4.5	8.0	2.6	
		3	25.9	-54.0	7.8	4.0	
15	4	1	5.7	6.0	12.4	0.6	
		2	8.8	9.0	9.1	1.2	
		3	25.9	10.0	5.2	4.1	
5	16	1	5.7	-7.5	4.6	1.0	
		2	8.8	-14.5	4.6	1.4	
		3	25.9	7.5	8.0	0.8	
5	8	1	5.7	4.0	4.0	0.8	
		2	8.8	-2.0	3.1	1.3	
		3	25.9	-53.0	4.4	1.3	
5	4	1	5.7	5.5	4.1	0.2	
		2	8.8	10.0	2.9	0.5	
		3	25.9	-54.0	2.2	1.5	

MOTIONS OF NODES

Rope Material = Steel — Water Depth = 1,800 ft — Reference Page 65

Rope Diameter = 0.5 in. — $\bar{T}_1$ = 10,000 — Case E

Wave Height (ft)	Wave Period (sec)	n	Rope Angle (deg)	Major Axis Angle (deg)	Major Axis Length (ft)	Minor Axis Length (ft)	CW
25	32	1	8.6	-47.5	26.5	14.5	
		2	13.8	-66.0	31.2	11.0	
		3	18.2	-66.0	25.0	5.2	
25	16	1	8.6	-11.5	19.6	12.0	
		2	13.8	-76.0	17.6	12.0	
		3	18.2	-73.0	14.8	6.0	
25	8	1	8.6	5.0	19.0	6.0	
		2	13.8	6.0	12.5	8.0	
		3	18.2	-60.5	7.0	6.0	
15	16	1	8.6	-11.0	11.6	7.0	
		2	13.8	-55.0	9.6	7.2	
		3	18.2	-64.0	7.9	3.6	
15	8	1	8.6	5.0	11.2	3.6	
		2	13.8	10.0	7.5	4.4	
		3	18.2	-40.0	4.0	3.7	
15	4	1	8.6	7.5	11.4	1.8	
		2	13.8	14.0	7.8	2.1	
		3	18.2	18.0	4.0	2.0	
5	16	1	8.6	-10.0	3.9	2.3	
		2	13.8	-51.0	3.1	2.4	
		3	18.2	-64.0	2.6	1.2	
5	8	1	8.6	5.5	3.7	1.2	
		2	13.8	14.0	2.5	1.4	
		3	18.2	-54.0	1.3	1.2	
5	4	1	8.6	8.5	3.8	0.6	
		2	13.8	14.0	2.6	0.7	
		3	18.2	19.0	1.3	0.7	
5	2	1	8.6	9.0	4.0	0.3	
		2	13.8	15.5	2.8	0.4	
		3	18.2	22.0	1.5	0.4	

MOTIONS OF NODES

Rope Material = Steel — Water Depth = 1,800 ft — Reference Page 67

Rope Diameter = 0.5 in. — $\bar{T}_1$ = 4,858 lb — Case F

Wave Height (ft)	Wave Period (sec)	n	Rope Angle (deg)	Major Axis Angle (deg)	Major Axis Length (ft)	Minor Axis Length (ft)	CW
50	32	1	23.8	-16.5	54.0	8.0	
		2	41.5	-19.5	55.0	8.5	
		3	59.3	-19.5	60.0	4.0	
50	16	1	23.8	-16.0	49.5	16.0	
		2	41.5	-19.0	43.0	15.0	
		3	59.3	-21.0	42.5	8.5	
50	8	1	*				
		2					
		3					
15	16	1	23.8	-7.0	14.4	3.1	
		2	41.5	-14.5	15.0	3.4	
		3	59.3	-21.0	19.2	1.8	
15	8	1	23.8	-1.8	12.6	4.4	
		2	41.5	-15.0	11.6	5.1	
		3	59.3	-22.0	12.8	3.0	
15	4	1	23.8	-29.5	7.0	3.8	
		2	41.5	29.5	7.6	5.2	
		3	59.3	28.0	7.0	3.8	
15	2	1	23.8	21.0	12.2	1.8	
		2	41.5	41.5	8.8	3.9	
		3	59.3	59.5	4.8	3.6	
5	16	1	23.8	-5.0	4.9	0.8	
		2	41.5	-7.5	4.7	1.1	
		3	59.3	-20.5	7.5	0.5	
5	8	1	23.8	1.0	4.3	1.1	
		2	41.5	-4.0	3.9	1.4	
		3	59.3	-21.5	6.0	0.9	
5	4	1	23.8	13.0	3.9	1.1	
		2	41.5	8.0	2.8	1.6	
		3	59.3	-27.0	3.5	1.2	
5	2	1	23.8	21.0	4.0	0.6	
		2	41.5	37.0	2.8	1.1	
		3	59.3	-46.0	2.0	1.4	

* (x) and (y) sweeps not available

MOTIONS OF NODES

Rope Material = Nylon — Water Depth = 18,000 ft — Reference Page 23

Rope Diameter = 0.5 in. — $\bar{T}_1$ = 3,600 lb — Case G

Wave Height (ft)	Wave Period (sec)	n	Rope Angle (deg)	Major Axis Angle (deg)	Major Axis Length (ft)	Minor Axis Length (ft)	CW
50	32	1	17.1	14.0	50.0	1.6	
		2	32.7	25.5	46.0	4.2	
		3	38.6	40.0	42.0	2.4	
		4	39.6	40.0	35.0	0.8	
		5	40.4	40.0	27.0	0	
		6	40.8	40.0	19.0	1.8	
		7	41.6	40.0	10.0	0.4	X
		8	42.2	78.0	6.0	0.1	X
		9	42.8	37.0	1.0	0.4	
50	16	1	17.1	15.5	50.0	1.0	
		2	32.7	24.5	43.5	2.2	
		3	38.6	39.0	38.0	1.0	
		4	39.6	39.0	31.5	0.4	
		5	40.4	41.0	24.0	0	
		6	40.8	43.5	18.5	1.0	
		7	41.6	33.0	11.0	0.4	
		8	42.2	68.0	6.0	1.6	
		9	42.8	30.0	1.2	0.2	X
50	8	1	17.1	15.0	48.0	1.0	
		2	32.7	27.5	35.6	2.0	
		3	38.6	40.0	25.6	0	
		4	39.6	37.0	17.0	0	
		5	40.4	40.0	14.4	0	
		6	40.8	40.0	10.8	0.8	
		7	41.6	40.0	6.6	0.2	
		8	42.2	50.0	4.0	1.0	
		9	42.8	0	0	0	

MOTIONS OF NODES

Rope Material = Nylon — Water Depth = 18,000 ft — Reference Page 23

Rope Diameter = 0.5 in. — $\overline{T}_1$ = 3,600 lb — Case G

Wave Height (ft)	Wave Period (sec)	n	Rope Angle (deg)	Major Axis Angle (deg)	Major Axis Length (ft)	Minor Axis Length (ft)	CW
15	16	1	17.1	16.0	15.2	0.2	
		2	32.7	25.0	14.4	0.9	
		3	38.6	40.0	13.3	0.6	
		4	39.6	41.0	11.7	?	
		5	40.4	42.0	9.6	0.2	X
		6	40.8	43.5	6.8	0.5	
		7	41.6	40.0	3.7	0	
		8	42.2	70.0	2.2	0.6	X
		9	42.8	32.5	0.4	0	X
15	8	1	17.1	16.0	14.8	0.2	
		2	32.7	25.0	12.6	0.8	
		3	38.6	41.0	10.8	0.1	
		4	39.6	39.5	9.6	0.1	
		5	40.4	41.5	9.0	0	
		6	40.8	41.5	4.0	0.2	
		7	41.6	?	6.0	?	
		8	42.2	40.5	2.4	1.0	
		9	42.8	42.0	0.6	0	
15	4	1	17.1	15.5	14.6	0.2	
		2	32.7	27.5	11.4	0.7	
		3	38.6	39.0	8.2	0.1	
		4	39.6	40.0	4.7	0	
		5	40.4	40.0	4.8	0	
		6	40.3	46.0	3.3	0.2	
		7	41.6	42.0	3.4	0	
		8	42.2	42.0	2.2	0.4	
		9	42.8	43.0	0.4	0	

* (x) and (y) sweeps not obtainable

MOTIONS OF NODES

Rope Material = Nylon | Water Depth = 18,000 ft | Reference Page 23

Rope Diameter = 0.5 in. | $\bar{T}_1$ = 3,600 lb | Case G

Wave Height (ft)	Wave Period (sec)	n	Rope Angle (deg)	Major Axis Angle (deg)	Major Axis Length (ft)	Minor Axis Length (ft)	CW
5	16	1	17.1	15.0	5.1	0.1	
		2	32.7	20.5	5.0	0.7	
		3	38.6	41.5	4.4	0.4	
		4	39.6	40.5	3.9	0	
		5	40.4	43.0	3.?	?	
		6	40.8	44.0	2.2	0.3	
		7	41.6	43.0	1.2	0.1	X
		8	42.2	82.0	0.8	0.1	X
		9	42.8	37.0	0.2	0	
5	8	1	17.1	15.5	5.0	0	
		2	32.7	23.0	4.7	0.4	
		3	38.6	41.0	4.7	0.1	
		4	39.6	40.0	5.4	0.1	
		5	40.4	40.6	5.2	0.1	X
		6	40.8	46.0	4.3	0.2	
		7	41.6	41.5	2.6	0.1	
		8	42.2	56.5	1.5	0.7	X
		9	*				
5	4	1	17.1	15.5	5.0	0	
		2	32.7	21.0	4.7	0.4	
		3	38.6	39.0	3.8	0.1	
		4	39.6	38.0	2.8	0	
		5	40.4	40.0	2.4	0.1	
		6	40.8	46.5	2.2	0.1	
		7	41.6	41.5	2.5	0	
		8	42.2	40.0	1.8	0.4	X
		9	42.8	41.0	0.3	0	

* (x) and (y) sweeps not obtainable

MOTIONS OF NODES

Rope Material = Nylon | Water Depth = 18,000 ft | Reference Page 21

Rope Diameter = 0.5 in. | $\overline{T}_1$ = 460 lb | Case H

Wave Height (ft)	Wave Period (sec)	n	Rope Angle (deg)	Major Axis Angle (deg)	Major Axis Length (ft)	Minor Axis Length (ft)	CW
50	32	1	10.4	11.0	48.0	0	X
		2	12.8	11.5	40.0	2.0	
		3	15.2	12.0	35.0	0.8	
		4	18.1	17.5	25.0	0.5	
		5	24.0	21.0	23.0	1.0	
		6	31.5	34.0	18.0	2.0	
		7	41.8	41.0	13.0	1.5	
		8	55.8	55.0	9.0	0	
		9	71.1	75.0	4.0	0.8	
50	16	1	10.4	10.0	46.2	0	
		2	12.8	12.5	33.0	1.4	
		3	15.2	16.0	25.0	0.6	
		4	18.1	16.5	17.0	0	
		5	24.0	20.0	13.5	0.4	
		6	31.5	31.0	10.0	1.0	
		7	41.8	36.0	7.0	0.6	
		8	55.8	52.0	5.0	0.2	
		9	71.1	72.5	1.5	0	
50	8	1	10.4	11.0	45.0	0	
		2	12.8	13.0	24.0	0.5	
		3	15.2	15.5	14.0	0.3	
		4	18.1	16.0	6.5	0	
		5	24.0	22.0	9.0	0	
		6	31.5	37.0	4.0	0.4	
		7	41.8	38.0	3.4	0	
		8	55.8	54.0	3.0	0	
		9	71.1	70.0	0.4	0	

MOTIONS OF NODES

Rope Material = Nylon Water Depth = 18,000 ft Reference Page 21

Rope Diameter = 0.5 in. $\bar{T}_1$ = 460 lb Case H

Wave Height (ft)	Wave Period (sec)	n	Rope Angle (deg)	Major Axis Angle (deg)	Major Axis Length (ft)	Minor Axis Length (ft)	CW
15	16	1	10.4	10.0	14.4	0	
		2	12.8	13.0	12.0	0.2	
		3	15.2	13.0	10.6	0.4	
		4	18.1	17.0	9.0	0.2	
		5	24.0	21.5	7.9	0.2	
		6	31.5	31.0	6.4	0.6	
		7	41.8	41.0	4.8	0.4	
		8	55.8	55.0	3.2	0.2	
		9	71.1	71.5	1.2	0.1	
15	8	1	10.4	10.0	14.2	0	
		2	12.8	13.5	10.6	0.1	
		3	15.2	15.0	7.5	0.2	
		4	18.1	18.0	4.2	0	
		5	24.0	23.0	5.4	0.1	
		6	31.5	36.0	3.1	0.3	
		7	41.8	37.0	2.8	0.1	
		8	55.8	55.0	2.0	0	
		9	71.1	73.0	0.2	?	
15	4	1	10.4	10.0	14.3	0	
		2	12.8	13.0	7.2	0	
		3	15.2	14.0	4.5	0	
		4	18.1	15.0	1.7	0.1	
		5	24.0	19.0	0.6	0.1	
		6	31.5	38.0	0.2	0	
		7	41.8	36.0	0.2	0	
		8	55.8	50.0	0.2	0	
		9	71.1	?	?	?	

MOTIONS OF NODES

Rope Material = Nylon — Water Depth = 18,000 ft — Reference Page 21

Rope Diameter = 0.5 in. — $\bar{T}_1$ = 460 lb — Case H

Wave Height (ft)	Wave Period (sec)	n	Rope Angle (deg)	Major Axis Angle (deg)	Major Axis Length (ft)	Minor Axis Length (ft)	CW
5	16	1	10.4	11.0	4.9	0	
		2	12.8	12.5	4.6	0	
		3	15.2	12.5	4.3	0.2	
		4	18.1	17.0	4.4	0.2	
		5	24.0	23.0	4.4	0.1	
		6	31.5	31.5	3.9	0.4	
		7	41.8	41.0	3.0	0.4	
		8	55.8	46.0	2.1	0.3	
		9	71.1	?	?	?	
5	8	1	10.4	8.0	5.0	0	
		2	12.8	13.0	4.5	0	
		3	15.2	15.5	3.5	0.1	
		4	18.1	16.0	2.4	0	
		5	24.0	13.0	3.4	0.1	
		6	31.5	32.0	1.8	0.2	
		7	41.8	40.0	2.0	0.1	
		8	55.8	60.0	1.5	0.1	
		9	71.1	80.0	0.8	?	
5	4		*				

* (x) and (y) sweeps not obtainable

MOTIONS OF NODES

Rope Material = Nylon Water Depth = 6,000 ft Reference Page 55

Rope Diameter = 0.5 in. $\bar{T}_1$ = 3,600 lb Case I

Wave Height (ft)	Wave Period (sec)	n	Rope Angle (deg)	Major Axis Angle (deg)	Major Axis Length (ft)	Minor Axis Length (ft)	CW
50	32	1	8.2	0	49.6	0.2	
		2	18.4	11.0	47.8	5.5	
		3	29.9	30.0	43.0	2.5	
		4	37.4	37.0	35.0	2.5	
		5	40.0	39.0	26.0	2.8	
		6	40.6	43.0	18.0	1.5	
		7	41.0	51.0	9.0	0.4	
		8	41.4	72.0	6.0	0.8	
		9	41.8	9.0	1.6	0.4	
50	16	1	8.2	0	50.0	0	
		2	18.4	16.0	49.0	3.4	
		3	29.9	30.0	45.2	1.2	
		4	37.4	37.0	37.4	1.4	
		5	40.0	39.0	28.4	1.8	
		6	40.6	41.5	19.6	0.4	
		7	41.0	45.0	10.0	0.8	X
		8	41.4	73.0	6.0	0.2	
		9	41.8	6.5	2.0	0.1	
50	8	1	8.2	0	50.0	0.8	
		2	18.4	17.0	49.0	1.4	
		3	29.9	29.0	45.0	0.6	
		4	37.4	36.0	39.0	0.6	
		5	40.0	40.0	31.2	0.8	
		6	40.6	41.0	23.0	0.2	
		7	41.0	38.0	12.0	0.4	
		8	41.4	68.0	7.0	1.6	
		9	41.8	10.0	1.4	0.2	

MOTIONS OF NODES

Rope Material = Nylon | Water Depth = 6,000 ft | Reference Page 55

Rope Diameter = 0.5 in. | $\bar{T}_1$ = 3,600 lb | Case I

Wave Height (ft)	Wave Period (sec)	n	Rope Angle (deg)	Major Axis Angle (deg)	Major Axis Length (ft)	Minor Axis Length (ft)	CW
15	16	1	8.2	1.0	15.0	0	
		2	18.4	18.0	14.7	1.0	
		3	29.9	30.0	13.8	0.4	
		4	37.4	37.0	11.2	0.4	
		5	40.0	39.0	8.6	0.8	
		6	40.6	43.0	6.0	0.2	
		7	41.0	50.0	3.4	0.2	X
		8	41.4	?	2.0	?	X
		9	41.8	39.0	0.5	0.1	
15	8	1	8.2	2.5	15.0	0.3	
		2	18.4	20.0	15.4	0	
		3	29.9	30.0	14.6	0.1	
		4	37.4	37.0	12.8	0.2	
		5	40.0	40.0	10.4	0.4	
		6	40.6	41.5	7.8	0.2	
		7	40.0	40.0	4.2	0.4	
		8	41.4	86.0	1.8	0.2	X
		9	41.8	31.0	5.4	0.2	
15	4	1	8.2	4.0	14.9	0.4	
		2	18.4	18.0	14.7	0.1	
		3	29.9	29.5	14.0	0	
		4	37.4	37.0	13.4	0	
		5	40.0	40.5	13.0	0.1	
		6	40.6	41.0	10.0	0	
		7	41.0	39.0	5.6	0.2	
		8	41.4	62.0	3.4	1.8	X
		9	41.8	20.0	0.6	0	

MOTIONS OF NODES

Rope Material = Nylon   Water Depth = 6,000 ft   Reference Page 55

Rope Diameter = 0.5 in. $\bar{T}_1$ = 3,600 lb   Case I

Wave Height (ft)	Wave Period (sec)	n	Rope Angle (deg)	Major Axis Angle (deg)	Major Axis Length (ft)	Minor Axis Length (ft)	CW
5	16	1	8.2	1.5	5.2	0	
		2	18.4	17.5	5.0	0 3	
		3	29.9	30.0	4.8	0.1	
		4	37.4	38.0	3.4	0.3	
		5	40.0	45.5	2.2	0.2	
		6	40.6	38.0	4.2	0.1	
		7	41.0	52.0	1.6	0.2	
		8	41.4	?	1.0	?	
		9	41.8	37.0	0.4	0	
5	8	1	8.2	2.5	5.0	0.1	
		2	18.4	20.5	5.2	0.1	
		3	29.9	30.0	5.0	0	
		4	37.4	38.5	4.4	0.1	
		5	40.0	41.0	3.7	0.2	
		6	40.6	41.0	2.5	0	
		7	41.0	41.0	1.7	0.2	
		8	41.4	?	?	?	
		9	41.8	39.0	0.4	0	
5	4	1	8.2	5.0	5.2	0.1	
		2	18.4	18.0	5.6	0.1	
		3	29.9	30.0	6.1	0	
		4	37.4	37.0	6.6	0	
		5	40.0	40.0	6.5	0	
		6	40.6	41.0	5.0	0	
		7	41.0	39.0	3.0	0.1	
		8	41.4	51.0	1.7	0.7	
		9	41.8	28.0	0.4	0	

MOTIONS OF NODES

Rope Material = Nylon | Water Depth = 6,000 ft | Reference Page 54

Rope Diameter 0.5 in. | $\overline{T}_1$ = 720 lb | Case J

Wave Height (ft)	Wave Period (sec)	n	Rope Angle (deg)	Major Axis Angle (deg)	Major Axis Length (ft)	Minor Axis Angle (ft)	CW
50	32	1	6.0	2.5	49.5	1.0	
		2	7.4	18.5	48.0	0.8	
		3	8.8	8.0	44.0	0.5	
		4	9.9	9.5	36.0	0.5	
		5	10.8	12.0	27.0	2.2	
		6	12.0	13.0	18.0	2.4	
		7	13.2	10.0	11.0	0	
		8	16.0	70.0	7.0	1.2	
		9	19.3	0	1.1	0	
50	16	1	6.0	4.0	49.5	1.0	
		2	7.4	10.5	47.5	4.0	
		3	8.8	6.5	45.0	0	
		4	9.9	10.0	38.0	0.8	
		5	10.8	12.0	30.0	1.0	
		6	12.0	12.5	20.0	1.2	
		7	13.2	11.0	12.0	0.6	
		8	16.0	60.0	6.0	2.6	
		9	19.3	0	1.6	0	
46	8	1	6.0	5.0	46.0	0.6	
		2	7.4	7.0	39.0	2.2	
		3	8.8	7.5	35.0	0.8	
		4	9.9	9.0	30.0	0	
		5	10.8	11.5	25.0	0.2	
		6	12.0	13.0	19.0	0.2	
		7	13.2	14.0	11.0	0.2	
		8	16.0	22.0	6.0	2.7	X
		9	19.3	-5.0	1.0	0	

MOTIONS OF NODES

Rope Material = Nylon
Rope Diameter = 0.5 in.

Water Depth 6,000 ft
$\overline{T}_1$ = 720 lb

Reference Page 54
Case J

Wave Height (ft)	Wave Period (sec)	n	Rope Angle (deg)	Major Axis Angle (deg)	Major Axis Length (ft)	Minor Axis Length (ft)	CW
15	16	1	6.0	3.5	14.8	0.3	
		2	7.4	11.0	14.6	1.0	
		3	8.8	4.5	14.0	0.1	
		4	9.9	11.0	11.6	0.4	
		5	10.8	13.0	9.2	0.5	
		6	12.0	15.0	6.2	0.7	
		7	13.2	6.0	3.8	0.3	
		8	16.0	55.0	2.6	0.8	X
		9	19.3	-62.0	1.0	0.3	
15	8	1	6.0	5.5	15.3	0.2	
		2	7.4	7.0	15.0	1.0	
		3	8.8	8.0	14.8	0.4	
		4	9.9	10.0	14.0	0	
		5	10.8	11.0	11.8	0.1	
		6	12.0	12.5	8.8	0.2	
		7	13.2	12.5	5.2	0.2	
		8	16.0	31.0	3.2	1.6	X
		9	19.3	-21.0	0.6	0.1	X
15	4	1	6.0	6.0	14.8	0.1	
		2	7.4	7.0	12.7	0.4	
		3	8.3	8.5	10.8	0.2	
		4	9.9	9.5	8.5	0	
		5	10.8	10.0	8.4	0	
		6	12.0	12.0	7.8	0	
		7	13.2	13.5	5.2	0	
		8	16.0	13.0	3.0	0.9	X
		9	19.3	0	0.6	0	

MOTIONS OF NODES

Rope Material = Nylon | Water Depth 6,000 ft | Reference Page 54

Rope Diameter = 0.5 in. | $\overline{T}_1$ = 720 lb | Case J

Wave Height (ft)	Wave Period (sec)	n	Rope Angle (deg)	Major Axis Angle (deg)	Major Axis Length (ft)	Minor Axis Length (ft)	CW
5	16	1	6.0	4.5	5.0	0.1	
		2	7.4	10.0	4.9	0.3	
		3	8.8	4.0	4.6	0.2	
		4	9.9	11.0	?	?	
		5	10.8	11.0	?	?	
		6	12.0	17.0	2.3	0.4	
		7	13.2	-1.0	1.4	0	
		8	16.0	64.0	1.0	0.3	
		9	19.3	-63.0	0.4	0.1	
5	8	1	6.0	5.5	5.2	0.1	
		2	7.4	7.5	5.3	0.3	
		3	8.8	8.5	5.5	0.2	
		4	9.9	10.0	10.5	0.1	
		5	10.8	11.0	?	?	
		6	12.0	15.0	?	?	
		7	13.2	14.0	1.9	0.2	
		8	16.0	51.0	1.4	0.9	X
		9	19.3	34.0	0.4	0.1	X
5	4	1	6.0	5.5	5.1	0	
		2	7.4	7.0	4.5	0.1	X
		3	8.8	10.0	4.0	0.1	
		4	9.9	12.0	?	?	
		5	10.8	10.0	?	?	
		6	12.0	12.0	4.9	0	
		7	13.2	13.5	3.3	0	
		8	16.0	9.0	1.9	0.6	
		9	19.3	1.0	0.4	0	

MOTIONS OF NODES

Rope Material = Nylon　　Water Depth = 1,800 ft　　Reference Page 62

Rope Diameter = 0.5 in.　　$\overline{T}_1$ = 3,600 lb　　Case K

Wave Height (ft)	Wave Period (sec)	n	Rope Angle (deg)	Major Axis Angle (deg)	Major Axis Length (ft)	Minor Axis Length (ft)	CW
50	32	1	18.6	15.0	37.4	5.8	
		2	29.2	29.0	25.0	5.5	
		3	35.6	33.0	12.5	3.8	
50	16	1	18.6	17.0	37.5	3.1	
		2	29.2	29.0	25.0	2.9	
		3	35.6	35.0	12.5	2.0	
50	8	1	18.6	17.5	39.2	1.4	
		2	29.2	29.0	27.3	1.3	
		3	35.6	36.0	14.2	1.1	
15	16	1	18.6	17.0	56.0	5.0	
		2	29.2	28.0	37.8	5.0	
		3	35.6	36.5	18.7	2.4	
15	8	1	18.6	17.5	58.0	2.5	
		2	29.2	29.0	40.5	2.6	
		3	35.6	36.0	20.0	1.2	
15	4	1	18.6	17.5	66.0	1.0	
		2	29.2	29.0	49.0	1.3	
		3	35.6	37.0	26.0	0.8	
5	16	1	18.6	16.5	37.0	4.3	
		2	29.2	29.0	25.0	3.9	
		3	35.6	34.5	12.5	2.8	
5	8	1	18.6	18.0	38.4	2.1	
		2	29.2	29.0	26.0	2.0	
		3	35.6	36.0	13.0	1.3	
5	4	1	18.6	18.5	42.0	0.9	
		2	29.2	28.5	30.0	1.0	
		3	35.6	35.5	15.5	1.0	
5	2	1	18.6	18.0	62.0	0	
		2	29.2	28.5	59.0	0.6	
		3	35.6	35.5	35.4	0.7	

MOTIONS OF NODES

Rope Material = Nylon | Water Depth = 1,800 ft | Reference Page 64

Rope Diameter 0.5 in. | $\overline{T}_1$ = 1,440 lb | Case L

Wave Height (ft)	Wave Period (sec)	n	Rope Angle (deg)	Major Axis Angle (deg)	Major Axis Length (ft)	Minor Axis Length (ft)	CW
50	32	1	52.6	51.0	30.0	3.0	
		2	68.8	67.5	19.5	2.2	
		3	75.1	75.5	10.0	1.7	
50	16	1	52.6	51.5	30.0	1.8	
		2	68.8	68.5	19.8	1.5	
		3	75.1	75.0	10.0	1.3	
50	8	1	52.6	51.5	31.0	0.8	
		2	68.8	69.0	21.5	0.7	
		3	75.1	75.5	11.5	0.6	
15	16	1	52.6	51.0	45.0	2.4	
		2	68.8	68.0	30.0	1.8	
		3	75.1	75.0	15.0	1.4	
15	8	1	52.6	51.5	47.5	1.0	
		2	68.8	68.5	34.5	1.0	
		3	75.1	75.0	18.1	0.9	
15	4	1	52.6	51.4	43.0	0.2	
		2	68.8	68.5	38.4	0.1	
		3	75.1	76.0	26.3	0.6	
5	16	1	52.6	51.5	30.0	1.5	
		2	68.8	68.0	19.8	1.4	
		3	75.1	75.0	10.1	1.0	
5	8	1	52.6	52.0	31.7	0.7	
		2	68.8	68.5	22.0	0.7	
		3	75.1	75.0	12.0	0.5	
5	4	1	52.6	52.0	31.5	0	
		2	68.8	68.5	28.0	0.4	
		3	75.1	75.0	18.5	0.3	
5	2	1	52.6	51.5	26.6	0	
		2	68.8	67.0	12.5	0	
		3	75.1	75.5	15.8	0	

APPENDIX
DETAILS OF THE COMPUTER STUDY

INTRODUCTION

This study was accomplished in two phases. Phase I consisted of finding the static deflection curves of buoy mooring ropes for a wide range of combinations of system parameters, including buoy drag, current profile, rope tension at the surface, rope material, rope diameter, and water depth. Phase II consisted of a perturbation analysis of rope motions resulting from time-varying buoy displacements. The data required for Phase II was obtained from the static deflection curves of Phase I.

In both cases the mooring rope was represented by a lumped parameter model, and a set of finite-difference differential equations was derived. These were solved on an analog computer. Both the static deflection and dynamic solutions were checked by comparing results with those obtained by Wilson[1,2] and Whicker.[3]

SOLUTION OF THE EQUILIBRIUM CURVE OF A BUOY MOORING ROPE

Method of Solution

The basic problem solved during Phase I may be stated as follows:

Find the equilibrium curve and tensions of a buoy mooring rope anchored to the sea bed when given the following:

1. Rope weight per unit length in water
2. Rope diameter
3. Depth of water
4. Current velocity profile as a function of depth
5. Buoy drag
6. Rope tension at the surface

The principal advantage of this formulation of the problem is that the investigator is free to choose in advance the tension in the rope at the surface as well as the surface drag, both of which are important mooring design parameters. In contrast, Wilson, whose approach to the problem involves a different method of computation, specifies as input parameters two angles: the angle of the rope at the anchor and the angle of the rope at the height above the sea bed where current velocity becomes non-zero.

In this study the basic problem formulated above was solved by approximating the distributed parameter system with a lumped parameter model, as shown in Figure 20. Rope mass and external forces were assumed to be concentrated at the indicated nodes, with each mass joined to the two adjacent ones by a laterally rigid but longitudinally extensible member which was free to pivot about the nodal points. The depth of each node was forced to remain constant, and the vertical separation between nodes was made smaller at both ends of the rope, where large curvature was anticipated, to obtain a better approximation of rope shape in those regions.

The use of the lumped-parameter-rope model facilitates the inclusion of loads due to objects attached to the rope, such as current meters. Often it is desirable to affix current meters to the mooring line in such a way that after the rope has assumed its steady state configuration, the current meters are at predetermined depths of particular interest. By using the method described in this report, the effect on rope shape of current meters located at any discrete depth may be handled by assigning a node to that depth. The drag and weight of the current meters can than be combined with the forces on the rope when obtaining the static deflection curve. Total weight at a node is obtained by adding the weights of the current meter and the two adjacent half-lengths of rope. The method used to obtain current meter drag is explained in Derivation of Equations.

Motion of the assumed lumped parameter model of the mooring rope can be described by a set of differential equations in x and y, solvable by the method of finite differences (Refs. 4, 5, and 6). In essence, the method used to find the

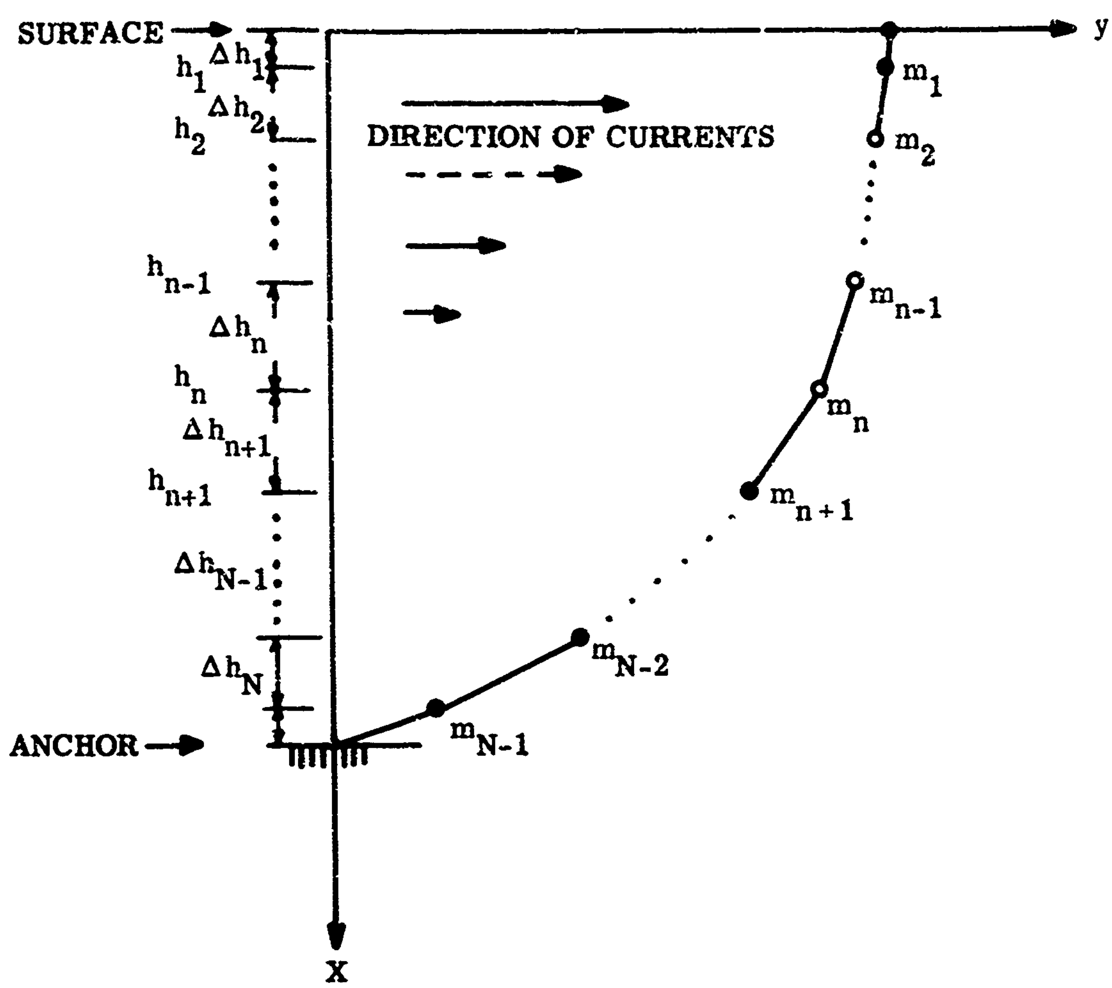

Figure 20 Lumped Parameter Model of Mooring Rope

equilibrium curve of the rope is based on the solution of these equations of motion. To solve the equations, the forces acting on each nodal mass must first be computed. If the summation of such forces is not zero, the resultant force unbalance causes motion at the node until the rope assumes a shape in which the forces are balanced. The final configuration of the rope for which the sum of the x and y forces on each nodal mass is zero is, by definition, the static deflection curve of the rope.

Since only the steady state solution is of interest, the general equations of motion can be greatly simplified because, under the final condition of equilibrium, forces arising from accelerations and velocities vanish. Thus, such quantities as added liquid mass and drag due to rope motion in the fluid medium may be ignored.

The forces considered to act on each nodal mass, including tension, weight, and hydrodynamic drag due to currents, were confined to a vertical plane. The positive buoyancy of the surface buoy was assumed to be equal at all times to the vertical component of line tension at the surface.

Derivation of Equations

The n^{th} finite difference differential equations for motion in the x and y directions may be derived by consideration of Figure 21, which shows a more detailed representation of the n^{th} node. Thus,

$$m_n \frac{d^2 y_n}{dt^2} = T_n \sin \theta_n - T_{n+1} \sin \theta_{n+1} + Q_{yn} \tag{1}$$

and

$$m_n \frac{d^2 x_n}{dt^2} = -T_n \cos \theta_n + T_{n+1} \cos \theta_{n+1} + W_n + Q_{xn} \tag{2}$$

where Q_{yn} and Q_{xn} are the horizontal and vertical drag forces at Node n, T_n is the tension in the rope segment joining m_{n-1} and m_n (i.e., s_n), θ_n is the angle between the vertical and s_n, and W_n is the weight concentrated at Node n.

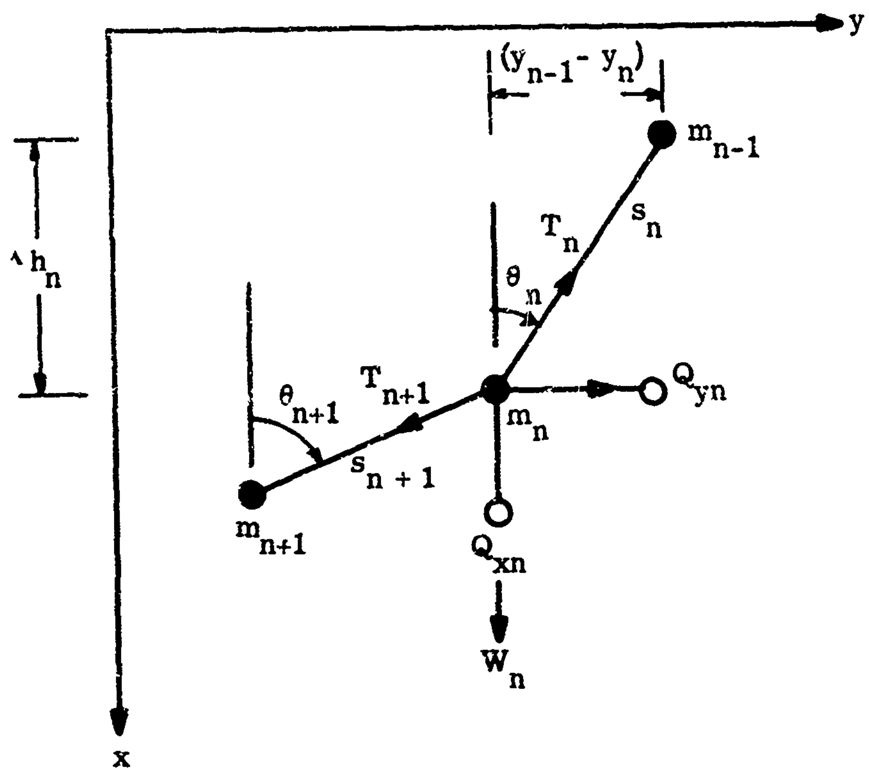

Figure 21 Detailed Representation of n^{th} Node

If the rope is divided into n segments, there will be $n + 1$ pairs of equations to be solved simultaneously. Since Δh_n is constrained to be a constant, $d^2x_n/dt^2 = 0$, and Equation (2) becomes

$$T_{n+1} \cos \theta_{n+1} = T_n \cos \theta_n - W_n - Q_{xn} \tag{3}$$

Multiplying both sides of Equation (3) by $\tan \theta_{n+1}$ yields

$$T_{n+1} \sin \theta_{n+1} = \left[T_n \cos \theta_n - W_n - Q_{xn}\right] \tan \theta_{n+1} \tag{4}$$

If one tension, T_n for instance, is chosen arbitrarily, then the vertical and horizontal components of tension at all other nodes can be found by successive applications of Equation (3) and (4), provided that θ_n , W_n , and Q_{xn} are known. These last three quantities, together with Q_{yn} , can, in fact, be found since they may each be expressed in terms of y_n , and y_n is determined by the indirect solution of Equation (1).

The indirect solution of the differential equation on the analog computer is done by assuming that the dependent variable (in this case, y_n) and all but its highest derivative are available at the output of some computer element, such as an operational amplifier. In addition, all forcing functions are assumed to be available. The equation is rearranged with the highest derivative appearing alone on one side. This derivative is then obtained by simple summation of the terms on the other side of the equation. By successive integrations with respect to time, all lower derivatives of the dependent variable are found. The basic problem is thus reduced to one of expressing the forces at the n^{th} node (i.e., the right-hand terms of Equations (1) and (2) as functions of y-coordinates of the nodes).

Examination of Figure 21 reveals that $\tan \theta_n$ is simply

$$\tan \theta_n = \frac{y_{n-1} - y_n}{\Delta h_n} \tag{5}$$

The term W_n is found by assuming that the weight concentrated at Node n consists of the sum of the weights of the two rope half-segments adjacent to Node n plus the weight of any other object which might be attached to the rope at the n^{th} node. Thus, for a uniform rope,

$$W_n = 1/2\,(s_n + s_{n+1})\,w_n + W'_n \tag{6}$$

where s_n is the length of rope between nodes n and n-1, w_n is the weight per unit length of the rope in water, and W'_n is the weight in water of an object attached to the rope at the n^{th} node. The quantity s_n is computed from the relationship

$$s_n = \sqrt{(\Delta h_n)^2 + (y_{n-1} - y_n)^2} \tag{7}$$

In deriving the drag forces Q_{yn} and Q_{xn}, the component of drag tangential to the rope is assumed to be negligible compared to the normal drag component.* Figure 22 shows the normal drag forces on the n^{th} and $(n+1)^{th}$ segments. For each segment the total drag D_n has been divided into two parts. The drag on the upper half of s_n is $\alpha_n D_n$; that on the lower half is $(1 - \alpha_n)\,D_n$ where

$$\alpha_n \triangleq \frac{\text{drag on the upper half of } s_n}{D_n} \tag{8}$$

The total horizontal and vertical drags at the n^{th} node were defined as

$$\left.\begin{aligned} Q_{yn} &= (1 - \alpha_n) D_n \cos\theta_n + \alpha_{n+1} D_{n+1} \cos\theta_{n+1} \\ &\text{and} \\ Q_{xn} &= (1 - \alpha_n) D_n \sin\theta_n + \alpha_{n+1} D_{n+1} \sin\theta_{n+1} \end{aligned}\right\} \tag{9}$$

* The tangential drag coefficient is about 2 percent of the normal drag coefficient; hence this assumption is obviously valid for angles up to 45 degrees. Since the larger angles occur near the sea floor where water velocities are small, little error in rope shape results.

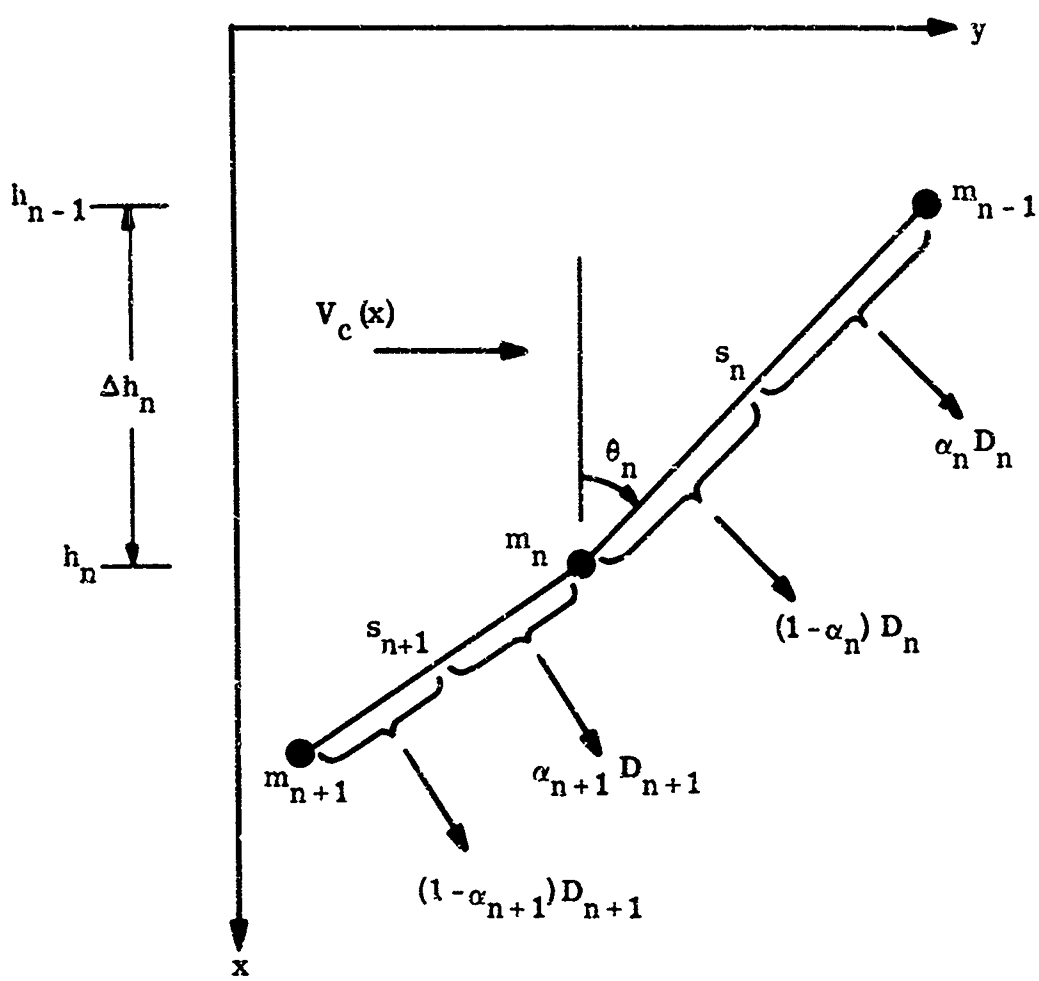

Figure 22 Drag Forces on Rope Segments, s_n and s_{n+1}

If the current velocity V_c varies as a function of x, then

$$D_n = \int_{h_{n-1}}^{h_n} 1/2\,\rho \left[V_c(x) \cos\theta_n\right]^2 \, d\, C_D \frac{dx}{\cos\theta_n} \tag{10}$$

which may be written

$$D_n = (\cos\theta_n) \int_{h_{n-1}}^{h_n} 1/2\,\rho \left[V_c(x)\right]^2 \, d\, C_D \, dx \tag{11}$$

where d is the rope diameter, C_D is the normal drag coefficient, and ρ is the water density.

The integral in Equation (11) is merely the total drag on s_n when this segment of the rope is vertical; i.e., when $\theta_n = 0$. The value of the integral is a constant and may be evaluated if the function $V_c(x)$ is known. Labeling the drag of the vertical rope as D_n',

$$D_n = D_n' \cos\theta_n \tag{12}$$

and Equation (9) becomes

$$\left.\begin{aligned} Q_{yn} &= (1-\alpha_n)\, D_n' \cos^2\theta_n + \alpha_{n+1} D_{n+1}' \cos^2\theta_{n+1} \\ Q_{xn} &= (1-\alpha_n)\, D_n' \sin\theta_n \cos\theta_n + \alpha_{n+1} D_{n+1}' \sin\theta_{n+1} \cos\theta_{n+1} \end{aligned}\right\} \tag{13}$$

To determine α_n, the integration of Equation (11) must be done over the two intervals

$$h_{n-1} \leq x \leq h_n - \frac{\Delta h_n}{2}$$

and

$$h_n - \frac{\Delta h_n}{2} \leq x \leq h_n$$

As a final step the $\sin\theta_n$ and $\cos\theta_n$ terms appearing in Equation (13) can be expressed in terms of the nodal coordinates and the rope lengths, yielding

$$\left.\begin{aligned} Q_{yn} &= (1-\alpha_n) D'_n \left(\frac{\Delta h_n}{s_n}\right)^2 + \alpha_{n+1} D'_{n+1} \left(\frac{\Delta h_{n+1}}{s_{n+1}}\right)^2 \\ Q_{xn} &= (1-\alpha_n) D'_n \frac{(y_{n-1}-y_n)\,\Delta h_n}{s_n^2} + \alpha_{n+1} D'_{n+1} \frac{(y_n - y_{n+1})\,\Delta h_{n+1}}{s_{n+1}^2} \end{aligned}\right\} \tag{14}$$

If current meters are attached to the mooring rope, the resultant drag can be calculated and combined with that of the rope. It was assumed that half the drag of a current meter was associated with the upper and lower ends of segment s_n, as shown in Figure 23. From the figure,

$$\left.\begin{aligned} D^+_{nCM} &= 1/2\,\rho\,(V_{c(n-1)}\cos\theta_n)^2\, C_D \frac{\ell}{2}\, d_{CM} \\ &\text{and} \\ D^-_{nCM} &= 1/2\,\rho\,(V_{cn}\cos\theta_n)^2\, C_D \frac{\ell}{2}\, d_{CM} \end{aligned}\right\} \tag{15}$$

From the standpoint of computer implementation it is desirable to simplify Equation (15) to the form of Equation (12); that is,

$$D^{\pm}_{nCM} = (\text{constant}) \cos\theta_n$$

The current meter drag can then be combined with cable drag to yield a new set of equations of the form given by Equation (13). By approximating $\cos^2\theta_n$ as $(.866)\cos\theta_n$, Equation (15) may be written

$$\left.\begin{aligned} D^+_{nCM} &= \left(D^+_{nCM}\right)^1 \cos\theta_n \\ D^-_{nCM} &= \left(D^-_{nCM}\right)^1 \cos\theta_n \end{aligned}\right\}$$

where

$$\left(D^+_{nCM}\right)^1 = 1/2\,\rho\,(.866)\, V^2_{c(n-1)}\, C_D \frac{\ell}{2}\, d_{CM}$$

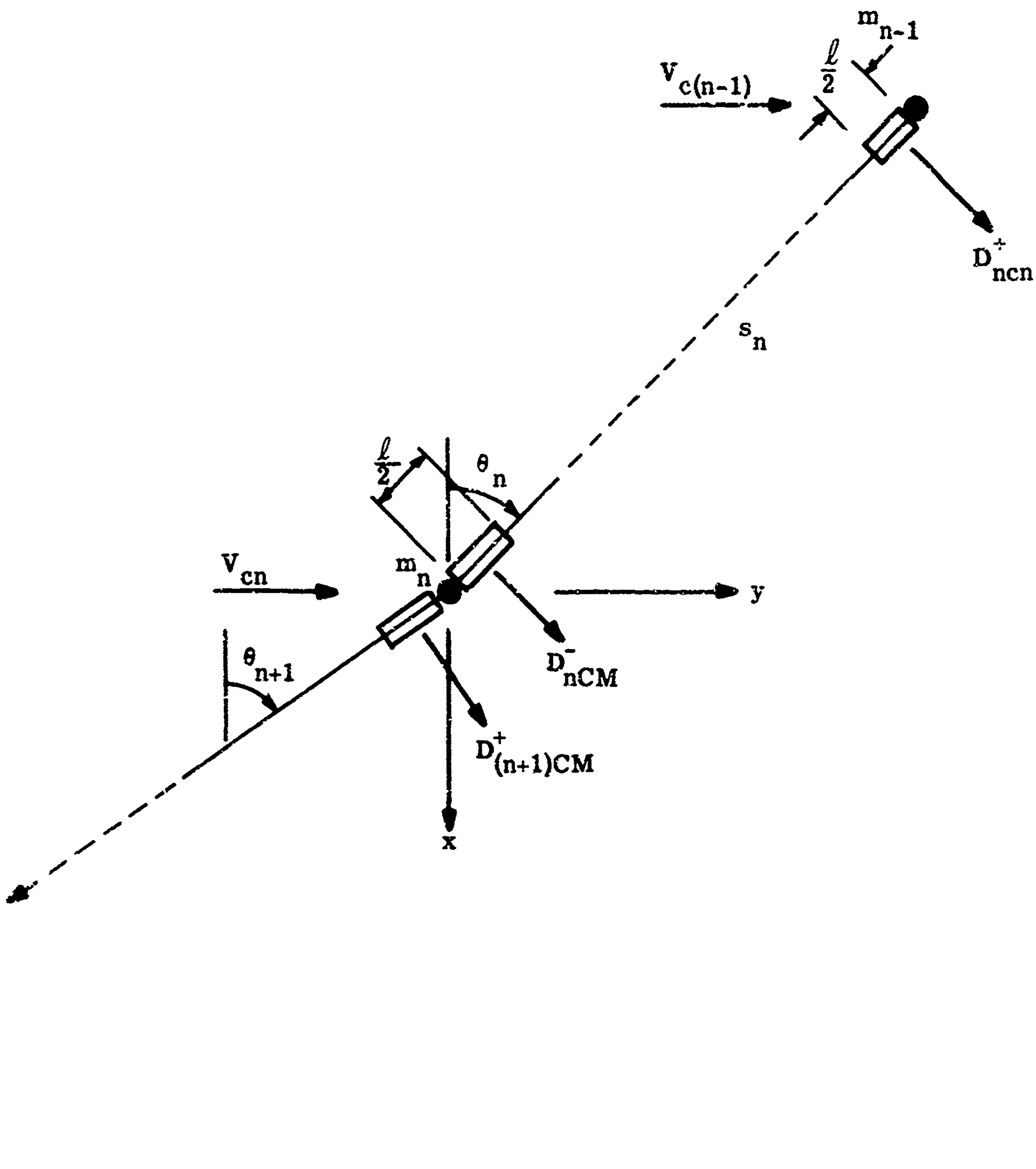

Figure 23 Sketch Showing Method of Calculating Current Meter Drag

and

$$\left(D^-_{nCM}\right)^1 = 1/2\, \rho\, (.866)\, V^2_{cn}\, C_D\, \frac{\ell}{2}\, d_{CM}$$

The magnitude of 30 degrees chosen for θ_n is a compromise which gives a fairly accurate value for the current meter drag at the top of the mooring line where current meter drag may be significant compared to rope drag since the lengths of the rope segments are small. For $0^\circ \leq \theta \leq 40^\circ$ the maximum error in D^+_{nCM} or D^-_{nCM} due to the approximation above is 13%. For $\theta > 40^\circ$, the accuracy of the current meter approximation falls off; but when this happens rope segments either have become longer, where the contribution of current meter drag to total drag becomes less, or they are near bottom where the current is weaker.

The total normal drag on s_n may be written

$$\left[D_n\right]_{total} = \left[D'_n + \left(D^+_{nCM}\right)^1 + \left(D^-_{nCM}\right)^1\right] \cos\theta_n$$

$$= \left[D'_n\right]_{total} \cos\theta_n$$

and Equation (13) becomes, when current meter drag is included,

$$\left.\begin{aligned} Q_{yn} &= (1-\alpha_n)\left[D'_n\right]_{total} \cos^2\theta_n + \alpha_{n+1}\left[D'_{n+1}\right]_{total} \cos^2\theta_{n+1} \\ Q_{xn} &= (1-\alpha_n)\left[D'_n\right]_{total} \sin\theta_n \cos\theta_n + \alpha_{n+1}\left[D'_{n+1}\right]_{total} \sin\theta_{n+1}\cos\theta_{n+1} \end{aligned}\right\}$$

where

$$\alpha n = \frac{\displaystyle\int_{h_{n-1}}^{h_{n-1}+\frac{\Delta h_n}{2}} 1/2\,\rho\left[V_c(x)\right]^2 d\, C_D\, dx + \left[D^+_{nCM}\right]^1}{\displaystyle\int_{h_{n-1}}^{h_n} 1/2\,\rho\left[V_c(x)\right]^2 d\, C_D\, dx + \left(D^+_{nCM}\right)^1 + \left(D^-_{nCM}\right)^1}$$

Computer Implementation

During a computer run the accelerations a   ocities of the nodes are unimportant because these quantities vanish when steady state is achieved. However, it is desirable to obtain a well-damped, rapidly converging solution. The damping characteristic can be modified by the addition of a rate damping term in Equation (1). Thus,

$$m_n \ddot{y}_n = T_n \sin \theta_n - T_{n+1} \sin \theta_{n+1} + Q_{yn} - K_R \dot{y}_n$$

where K_R can be adjusted until desired damping characteristics are obtained. Rapidity of solution is determined by the choice of m_n which can be interpreted as a force scale factor. Although the value of m_n has no effect on the final shape of the mooring rope, this is not true of the term W_n in Equation (2) which must be computed from Equation (6).

Figure 24 is a block diagram showing how the foregoing equations were implemented on the analog computer for the upper two nodes (n = 0, and n = 1). As previously stated, if one tension is known then all other tensions are determined from Equations (3) and (4). The tension that was arbitrarily chosen for the Phase I study was T_1. The angle θ_1 was obtained with a servo resolver by inverse resolution of $(y_o - y_1)$ and Δh_1, the two components of s_1. One cup of this resolver was then used to multiply the selected T_1 by the sine and cosine of θ_1. The extra drag force D_B which acts on the surface node corresponds to buoy drag.

The tension T_1, chosen arbitrarily, does not represent the tension at the buoy but rather the tension in the cable at the midpoint of cable segment s_1. To obtain a better approximation of tension magnitude and direction at the buoy, it is necessary to consider the forces on the isolated system composed of the upper half of s_1 and the buoy (Fig. 25). The weight of the indicated section of rope is W_o, the horizontal and vertical drag forces acting on the segment are Q_{yo} and Q_{xo}, B is the buoyant force acting on the buoy, and D_B is buoy drag. Since this system is in equilibrium, the summation of the vertical forces and the summation of the horizontal forces are equal to zero. Thus,

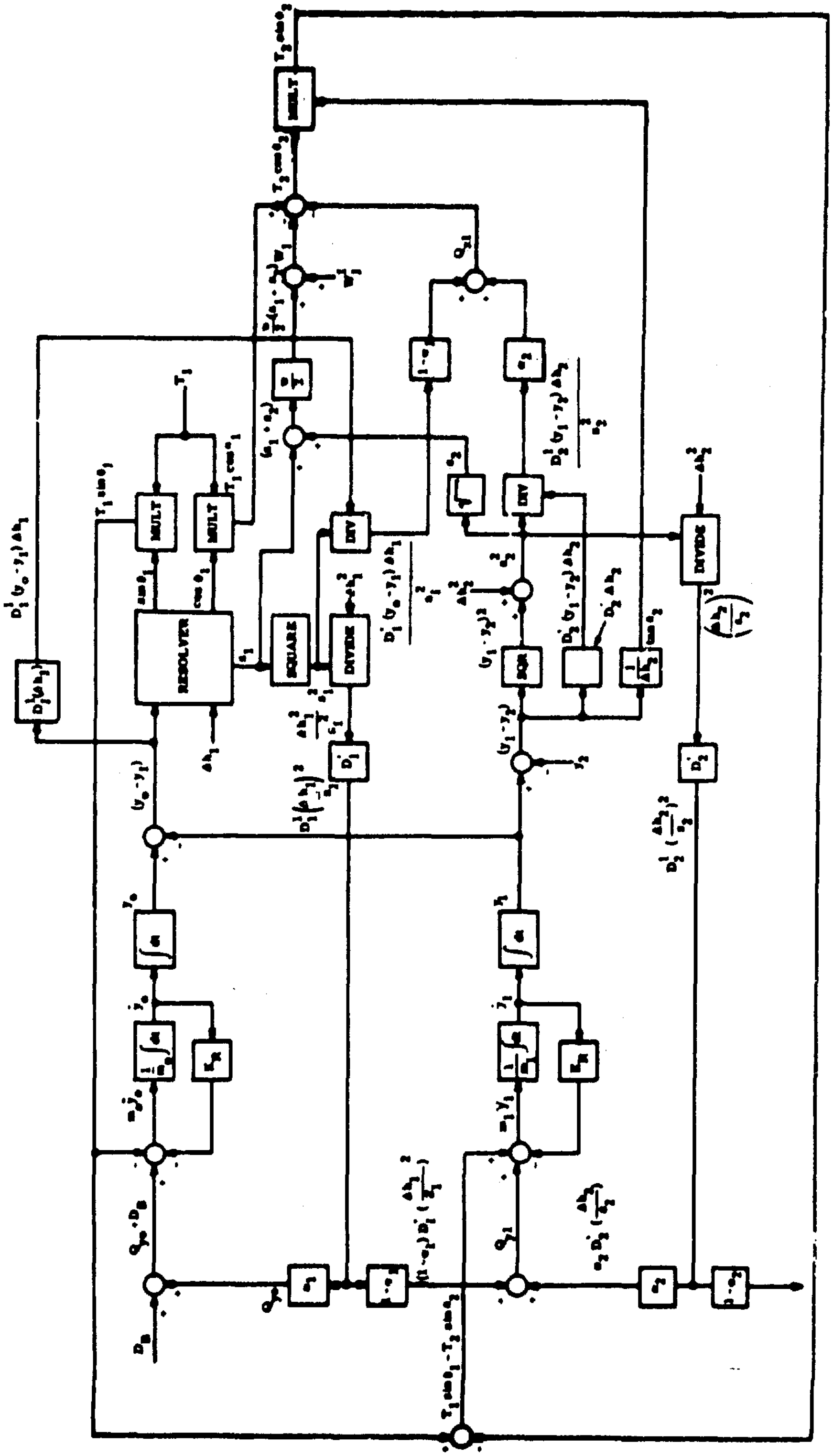

Figure 24 Block Diagram Showing Implementation of Phase I Equations for $n = 0$ and $n = 1$

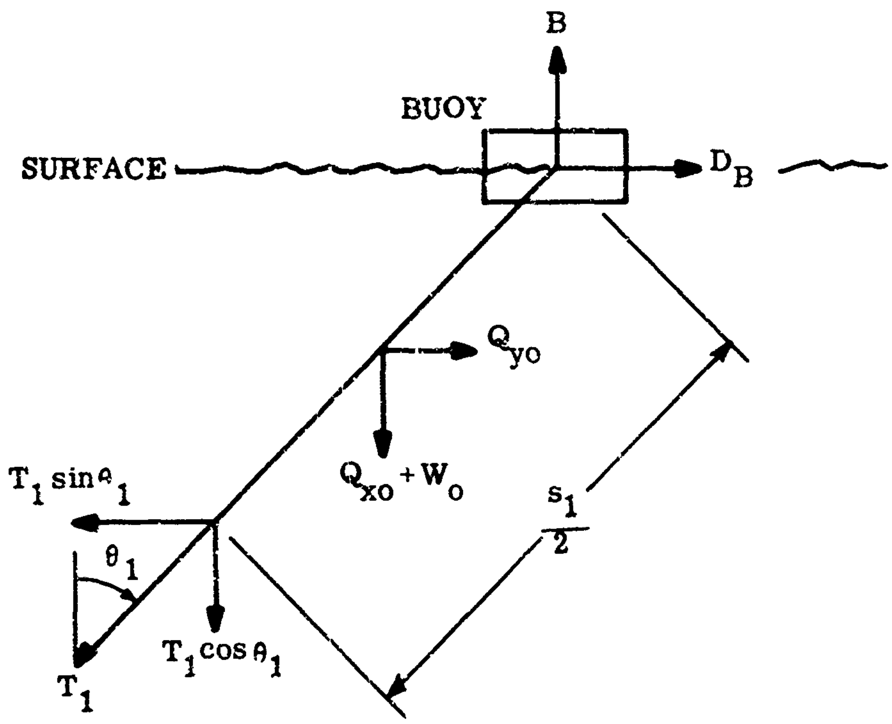

(a) Upper Half-Segment of Cable and Buoy

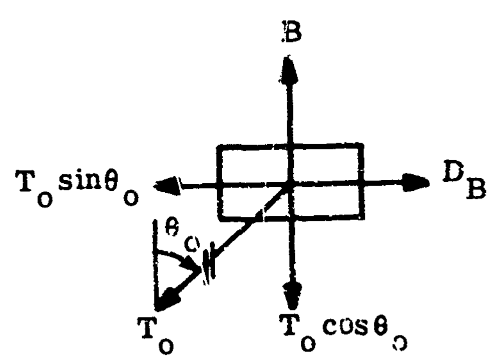

(b) Buoy

Figure 25 Forces Near the Buoy

$$\left.\begin{aligned} &T_1 \cos \theta_1 + Q_{xo} + W_o - B = 0 \\ \text{and} \\ &-T_1 \sin \theta_1 + Q_{yo} + D_B = 0 \end{aligned}\right\} \quad (16)$$

Let us now isolate the buoy, labeling the magnitude of rope tension at the buoy as T_o and the angle of the rope at the buoy as θ_o (see Figure 5b). Since the buoy is in equilibrium,

$$\left.\begin{aligned} &-T_o \sin \theta_o + D_B = 0 \\ \text{and} \\ &T_o \cos \theta_o - B = 0 \end{aligned}\right\} \quad (17)$$

Combining Equations (16) and (17) gives the following relationship:

$$\left.\begin{aligned} &T_o \sin \theta_o = D_B = T_1 \sin \theta_1 - Q_{yo} \\ &T_o \cos \theta_o = B = T_1 \cos \theta_1 + Q_{xo} + W_o \\ &\theta_o = \tan^{-1} \frac{D_B}{T_1 \cos \theta_1 + Q_{xo} + W_o} \end{aligned}\right\} \quad (18)$$

from which T_o and θ_o can be calculated.

In like manner it can be shown that the components of tension at the anchor are

$$T_A \sin \theta_A = T_{10} \sin \theta_{10} + Q_{y10} = H \quad (19)$$

and

$$T_A \cos \theta_A = T_{10} \cos \theta_{10} - (Q_{x10} + W_{10}) = U \quad (20)$$

where H and U are the required holding power and negative buoyancy of the anchor.

PERTURBATION ANALYSIS OF THE MOTION OF A BUOY MOORING ROPE

Method of Solution

Phase II consisted of a perturbation study of the motion of a buoy mooring rope resulting from time-varying buoy displacements. The unperturbed rope shapes were obtained from the Phase I data. The dynamic analysis was carried out on an analog computer, using a lumped parameter model of the rope similar to that of Phase I. For Phase II, however, both horizontal and vertical nodal motions were considered, and the rope was considered to be elastic.

Although developed independently, the equations used here are similar to those of Walton and Polachek[4, 5] and of Polachek, et al.[6] Our method, however, contains additional simplifying assumptions necessary to adapt the equations to an analog computer.

When writing the equations of motion of the rope, account must be taken (as was done in Refs. 4 and 5) of the hydrodynamic reaction forces which occur when the rope is accelerated laterally. The water entrained by the moving rope is moved only by the normal component of motion. Hence, to handle the so-called virtual mass, accelerations must be resolved both normal and tangential to the rope. The resulting inertial force must then be resolved again along the x and y axes. The method of resolution of these forces is shown in Figure 26. The acceleration at the n^{th} node normal to segment s_n is

$$a^-_{Nn} = \ddot{y}_n \cos\theta_n + \ddot{x}_n \sin\theta_n \tag{21}$$

The reaction force is proportional to the normal acceleration; thus

$$F^-_{Nn} = 1/2\, m^v_{n-1/2}\, a^+_N \tag{22}$$

where F^-_{Nn} represents the reaction force at node n due to lateral acceleration of that half of segment s_n adjacent to m_n. The term $m^v_{n-1/2}$ is the virtual mass of the fluid entrained by s_n. Resolving F^-_{Nn} into its horizontal and vertical components gives

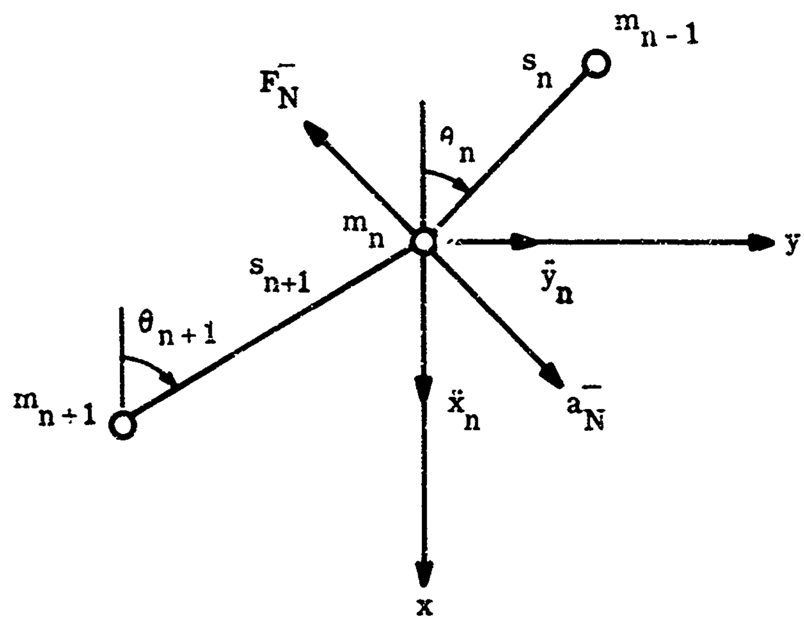

Figure 26 Sketch Showing Method of Resolution of Hydrodynamic Reaction Forces

$$F_{yn}^{-} = - F_{Nn}^{-} \cos \theta_n \tag{23}$$

and

$$F_{xn}^{-} = - F_{Nn}^{-} \sin \theta_n \tag{24}$$

By combining Equations (21), (22), (23) and (24), we obtain the following equations:

$$F_{yn}^{-} = - 1/2 \, m_{n-1/2}^{v} (\ddot{y}_n \cos^2 \theta_n + \ddot{x}_n \sin \theta_n \cos \theta_n) \tag{25}$$

$$F_{xn}^{-} = - 1/2 \, m_{n-1/2}^{v} (\ddot{y}_n \sin \theta_n \cos \theta_n + \ddot{x}_n \sin^2 \theta_n) \tag{26}$$

In a similar manner the x and y components of the reaction force at Node n due to lateral acceleration of the adjacent half of segment s_{n+1} can be found. Thus,

$$F_{yn}^{+} = - 1/2 \, m_{n+1/2}^{v} (\ddot{y}_n \cos^2 \theta_{n+1} + \ddot{x}_n \sin \theta_{n+1} \cos \theta_{n+1}) \tag{27}$$

$$F_{xn}^{+} = - 1/2 \, m_{n+1/2}^{v} (\ddot{y}_n \sin \theta_{n+1} \cos \theta_{n+1} + \ddot{x}_n \sin^2 \theta_{n+1}) \tag{28}$$

The total horizontal and vertical components of reaction force are found by combining the forces of Equations (25), (26), (27) and (28), giving

$$F_{xn}^{v} = F_{xn}^{-} + F_{xn}^{+} \tag{29}$$

and

$$F_{yn}^{v} = F_{yn}^{-} + F_{yn}^{+} \tag{30}$$

The equations of motion of the n^{th} mass may now be written as follows:

$$m_n \ddot{y}_n = \sum F_n^y + F_{yn}^v \tag{31}$$

$$m_n \ddot{x}_n = \sum F_n^x + F_{xn}^v \tag{32}$$

where m_n is the mass concentrated at Node n, and $\sum F_n^y$ and $\sum F_n^x$ represent the summation of all horizontal and vertical external forces other than the hydrodynamic reaction forces.

After combining Equations (25) through (32) and collecting terms, the equations of motion can be written in matrix notation, yielding

$$\begin{bmatrix} I_n & K_n \\ K_n & J_n \end{bmatrix} \begin{bmatrix} \ddot{x}_n \\ \ddot{y}_n \end{bmatrix} = \begin{bmatrix} \sum F_n^x \\ \sum F_n^y \end{bmatrix} \tag{33}$$

where

$$\left.\begin{aligned} I_n &= m_n + 1/2\, m^v_{n-1/2} \sin^2 \theta_n + 1/2\, m_{n+1/2} \sin^2 \theta_{n+1} \\ J_n &= m_n + 1/2\, m^v_{n-1/2} \cos^2 \theta_n + 1/2\, m^v_{n+1/2} \cos^2 \theta_{n+1} \\ K_n &= 1/2\, m^v_{n-1/2} \sin \theta_n \cos \theta_n + 1/2\, m^v_{n+1} \sin \theta_{n+1} \cos \theta_{n+1} \end{aligned}\right\} \tag{34}$$

The term m_n includes not only the average mass of the two adjacent rope segments, but also the mass of any additional object, such as a current meter which may be attached to the rope at the n^{th} node. Furthermore, if such objects are symmetrical with respect to the rope, their virtual mass can be included in the term $m^v_{n\pm 1/2}$.

The $\sum F_n^y$ and $\sum F_n^x$ forces correspond to the terms on the right-hand sides of Equations (1) and (2) (see Fig. 2). Thus,

$$\sum F_n^y = T_n \sin \theta_n - T_{n+1} \sin \theta_{n+1} + Q_{yn}$$

$$\sum F_n^x = - T_n \cos \theta_n + T_{n+1} \cos \theta_{n+1} + W_n + Q_{xn}$$

And Equation (33) may be rewritten

$$\begin{bmatrix} I_n & K_n \\ K_n & J_n \end{bmatrix} \begin{bmatrix} \ddot{x}_n \\ \ddot{y}_n \end{bmatrix} = \begin{bmatrix} -T_n \cos\theta_n + T_{n+1}\cos\theta_{n+1} - W_n + Q_{xn} \\ T_n \sin\theta_n - T_{n+1}\sin\theta_{n+1} + Q_{yn} \end{bmatrix} \tag{35}$$

To simplify scaling and, in particular, to obtain a higher degree of accuracy in the calculation of tensions, recourse is now made to the perturbation technique. If the amplitude of the surface buoy displacement is small compared to the length of the rope, then the shape of the rope at any time will differ only slightly from that at static equilibrium and the resulting relative displacements of each node will be small compared to the static displacements.

Applying the perturbation technique, we define the variables x_n and y_n as follows:

$$\left.\begin{aligned} x_n &= \bar{x}_n + x_n' \\ y_n &= \bar{y}_n + y_n' \end{aligned}\right\} \tag{36}$$

where $\bar{x}_n$ and $\bar{y}_n$ are the vertical and horizontal displacements at $t = 0$ (i.e., static equilibrium), and x_n' and y_n' are the displacements resulting from buoy motion. Since T_n, θ_n, Q_{xn}, Q_{yn}, I_n, J_n, and K_n are functions of x_n and y_n, these parameters must be similarly defined. Thus,

$$\left.\begin{aligned} T_n &= \bar{T}_n + T_n' \\ \theta_n &= \bar{\theta}_n + \theta_n' \\ Q_{xn} &= \bar{Q}_{xn} + Q_{xn}' \\ Q_{yn} &= \bar{Q}_{yn} + Q_{yn}' \\ I_n &= \bar{I}_n + I_n' \\ J_n &= \bar{J}_n + J_n' \\ K_n &= \bar{K}_n + K_n' \end{aligned}\right\} \tag{37}$$

Substituting Equations (36) and (37) into (35) gives

$$\begin{bmatrix} \left(\overline{I}_n + I'_n\right) & \left(\overline{K}_n + K'_n\right) \\ \left(\overline{K}_n + K'_n\right) & \left(\overline{J}_n + J'_n\right) \end{bmatrix} \begin{bmatrix} \left(\ddot{\overline{x}}_n + \ddot{x}'_n\right) \\ \left(\ddot{\overline{y}} + \ddot{y}'_n\right) \end{bmatrix} = \tag{38}$$

$$\begin{bmatrix} -\left(\overline{T}_n + T'_n\right) \cos\left(\overline{\theta}_n + \theta'_n\right) + \left(\overline{T}_{n+1} + T'_{n+1}\right) \cos\left(\overline{\theta}_{n+1} + \theta'_{n+1}\right) + W_n + \overline{Q}_{xn} + Q'_{xn} \\ \left(\overline{T}_n + T'_n\right) \sin\left(\overline{\theta}_n + \theta'_n\right) - \left(\overline{T}_{n+1} + T'_{n+1}\right) \sin\left(\overline{\theta}_{n+1} + \theta'_{n+1}\right) + \overline{Q}_{yn} + Q'_{yn} \end{bmatrix}$$

In the absence of buoy motion, all the primed quantities are zero; in addition,

$$\left.\begin{aligned} -\overline{T}_n \cos\overline{\theta}_n + \overline{T}_{n+1} \cos\overline{\theta}_{n+1} + W_n + \overline{Q}_{xn} &= 0 \\ \overline{T}_n \sin\overline{\theta}_n - \overline{T}_{n+1} \sin\overline{\theta}_{n+1} + Q_{yn} &= 0 \end{aligned}\right\} \tag{39}$$

from the condition of static equilibrium.

The assumption is now made that θ'_n is a small angle, thus

$$\sin\theta'_n \simeq \theta'_n \text{ and } \cos\theta'_n \simeq 1$$

On this basis the right-hand matrix of Equation (38) becomes

$$\begin{bmatrix} \underline{-\overline{T}_n \cos\overline{\theta}_n} + \theta'_n \overline{T}_n \sin\overline{\theta}_n - T'_n(\cos\overline{\theta}_n - \theta'_n \sin\overline{\theta}_n) + \underline{\overline{T}_{n+1}\cos\overline{\theta}_{n+1}} - \theta'\overline{T}_{n+1}\sin\overline{\theta}_{n+1} + \\ \underline{\overline{T}_n \sin\overline{\theta}_n} + \overline{T}_n \theta'_n \cos\overline{\theta}_n + T'_n(\sin\overline{\theta}_n + \theta'_n \cos\overline{\theta}_n) \underline{- \overline{T}_{n+1}\sin\overline{\theta}_{n+1}} - \overline{T}_{n+1}\theta'_{n+1}\cos\overline{\theta}_{n+1} - \end{bmatrix}$$

$$\begin{bmatrix} T'_{n+1} (\cos\overline{\theta}_{n+1} - \theta'_{n+1} \sin\overline{\theta}_{n+1}) + \underline{W_n} + \underline{\overline{Q}_{xn}} + Q'_{xn} \\ T'_{n+1} (\sin\overline{\theta}_{n+1} + \theta'_{n+1} \cos\overline{\theta}_{n+1}) + \underline{Q_{yn}} + Q'_{yn} \end{bmatrix}$$

But the sum of the underlined terms is zero (Eq. 39) and, in general, the higher-order products of the primed quantities can be neglected. Equation (38) may therefore be simplified to

$$\begin{bmatrix} \left(\bar{I}_n + I'_n\right) & \left(\bar{K}_n + K'_n\right) \\ \left(\bar{K}_n + K'_n\right) & \left(\bar{J}_n + J'_n\right) \end{bmatrix} \begin{bmatrix} \ddot{x}'_n \\ \ddot{y}'_n \end{bmatrix} = \tag{40}$$

$$\begin{bmatrix} \theta'_n \bar{T}_n \sin\bar{\theta}_n - T'_n \cos\bar{\theta}_n - \theta' \bar{T}_{n+1} \sin\bar{\theta}_{n+1} + T'_{n+1} \cos\bar{\theta}_{n+1} + Q'_{xn} \\ \bar{T}_n \theta'_n \cos\bar{\theta}_n + T'_n \sin\bar{\theta}_n - \bar{T}_{n+1}\, \theta'_{n+1} \cos\bar{\theta}_{n+1} - T'_{n+1} \sin\bar{\theta}_{n+1} + Q'_{yn} \end{bmatrix}$$

The y differential equation that was used for Node 1 differed from Equation (40); that is, the higher-order term $T'_1 \; \theta'_1 \cos\bar{\theta}_1$ was retained, since in most cases $\bar{\theta}_1$ was a small angle.

Expressions will now be developed for the quantities of Equation (40) in terms of x_n and y_n.

Assuming Hooke's law for steel cables, we can express the tension in any segment as a function of the elongation of that segment. Thus,

$$\frac{T_n}{A} = E \, \frac{s_n - s_{no}}{s_{no}}$$

where A is the effective cross-sectional area; E is the effective value of Young's Modulus, and s_{no} is an unstretched reference length. Applying incremental substitution gives

$$\left(\bar{T}_n + T'_n\right) = AE\left(\frac{\bar{s}_n - s_{no}}{s_{no}} + \frac{s'_n}{s_{no}}\right)$$

The nominal equation is

$$\overline{T}_n = AE\left(\frac{\overline{s}_n - s_{no}}{s_{no}}\right) \tag{41}$$

and the perturbation equation is

$$T_n' = AE\,\frac{s_n'}{s_{no}} \tag{42}$$

Solving Equation (41) for s_{no} gives

$$s_{no} = \frac{\overline{s}_n}{1 + \frac{\overline{T}_n}{AE}} \tag{43}$$

For all steel ropes considered in this study

$$\frac{\overline{T}_n}{AE} \ll 1$$

Thus,

$$s_{no} \cong \overline{s}_n$$

and

$$T_n' \cong AE\,\frac{s_n'}{\overline{s}_n} \tag{44}$$

The nominal tension $\overline{T}_n$ is not, of course, obtained from Equation (41) but from the Phase I data.

For nylon the function relating stress and strain is more complicated, so that a "dynamic spring constant," μ was therefore determined experimentally.

$$\left[T_n'\right]_{nylon} = \mu\,\frac{s_n'}{\overline{s}_n} \tag{45}$$

As shown in Figure 7, the value of μ is a function not only of $\overline{T}_n$ but also of $s_n'/\overline{s}_n$, the variation of μ with $s_n'/\overline{s}_n$ becoming more pronounced at the higher static tensions. To obtain an approximate solution to this problem, the value of μ chosen for each computer run was that one determined by the given static tension and the average value of the anticipated perturbation strain variation.

To find the changes in tension from Equations (42) and (45), the change in length s_n' must be determined. Consider Figure 27, which shows the configuration of the n^{th} rope segment before and after a small displacement. From the figure

$$(\overline{s}_n + s_n')^2 = (\overline{s}_n \sin \overline{\theta}_n + y_{n-1}' - y_n')^2 + (\overline{s}_n \cos \overline{\theta}_n + x_n' - x_{n-1}')^2$$

Solving for s_n'

$$s_n' = \frac{2\,\overline{s}_n(y_{n-1}' - y_n') \sin \overline{\theta}_n + (y_{n-1}' - y_n')^2 + 2\,\overline{s}_n(x_n' - x_{n-1}') \cos \overline{\theta}_n + (x_n' - x_{n-1}')^2}{2\,\overline{s}_n} \tag{46}$$

If we assume that

$$(y_{n-1}' - y_n') \ll 2\,\overline{s}_n \sin \overline{\theta}_n$$

and (47)

$$(x_n' - x_{n-1}') \ll 2\,\overline{s}_n \cos \overline{\theta}_n$$

then the higher-order terms can be neglected and Equation (44) reduces to

$$s_n' \cong (y_{n-1}' - y_n') \sin \overline{\theta}_n + (x_n' - x_{n-1}') \cos \overline{\theta}_n \tag{48}$$

For $n = 1$, the higher-order term $(y_{n-1}' - y_n')/2\,\overline{s}_n$ was retained, since it was not obvious that the first inequality of Equation (47) would be valid because of the smallness of $\overline{\theta}_1$ in some cases.

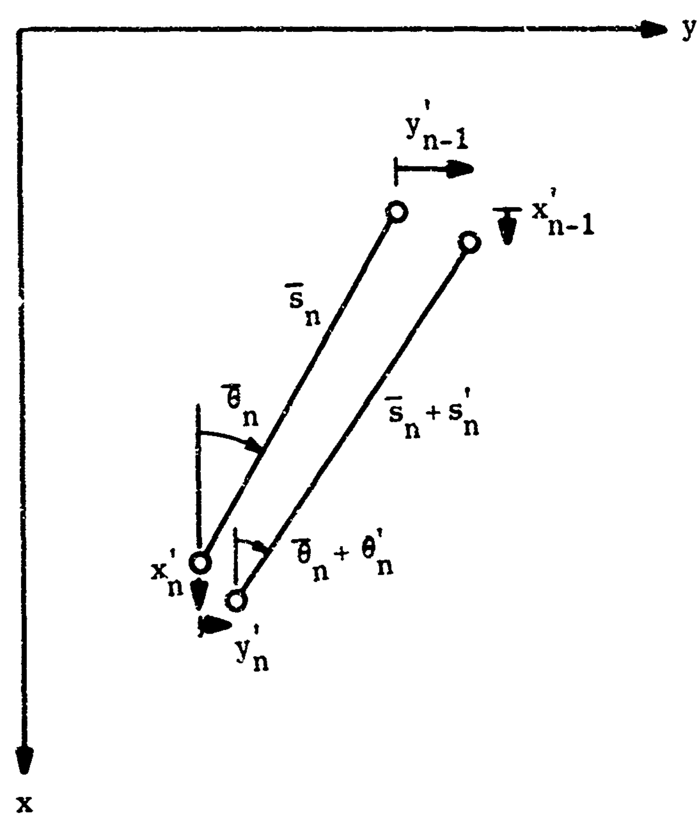

Figure 27 Configuration of n^{th} Rope Segment Before and After a Small Displacement

The final expression for T_n' is obtained by combining either Equation (42) or (45) with Equation (48); thus

$$\left.\begin{aligned}
&\text{(for steel)}\\
&T_n' = \frac{AE}{\bar{s}_n}\left[(y_{n-1}' - y_n')\sin\bar{\theta}_n + (x_n' - x_{n-1}')\cos\bar{\theta}_n\right]\\
&\text{(for nylon)}\\
&T_n' = \frac{\mu}{\bar{s}_n}\left[(y_{n-1}' - y_n')\sin\bar{\theta}_n + (x_n' - x_{n-1}')\cos\bar{\theta}_n\right]
\end{aligned}\right\} \quad (49)$$

The value of θ_n' can also be found by referring to Figure 27. From the figure,

$$\tan(\bar{\theta}_n + \theta_n') = \frac{\bar{s}_n \sin\bar{\theta}_n + y_{n-1}' - y_n'}{\bar{s}_n \cos\bar{\theta}_n + x_n' - x_{n-1}'}$$

Expanding the left side of the equation by the formula for the tangent of the sum of two angles and solving for θ_n' gives

$$\tan\theta_n' = \frac{(y_{n-1}' - y_n')\cos\bar{\theta}_n - (x_n' - x_{n-1}')\sin\bar{\theta}_n}{\bar{s}_n + s_n'}$$

With the assumption that θ_n' is a small angle, and that $s_n' << \bar{s}_n$, the expression for θ_n' becomes

$$\theta_n' \simeq \frac{(y_{n-1}' - y_n')\cos\bar{\theta}_n - (x_n' - x_{n-1}')\sin\bar{\theta}_n}{\bar{s}_n} \quad (50)$$

By the use of Equations (49) and (50), the tension forces of Equation (40) can be computed.

The method of calculating the drag force of Equation (40) is based on the representation of the rope shown in Figure 28. Drag forces are computed in orthogonal-axis systems, one axis of which is assumed to be tangent to the rope at Node n. The angle with the vertical made by this axis is defined as ψ_n where

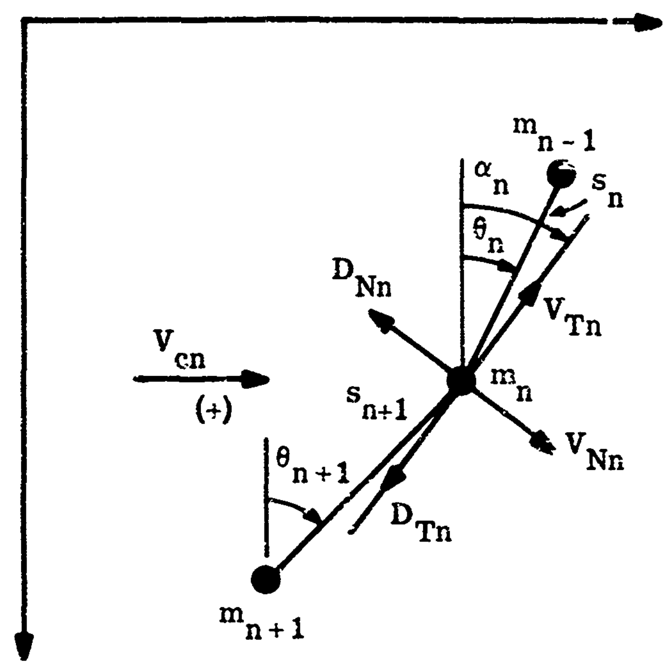

Figure 28 Representation of Rope for Purpose of Computing Drag Forces

$$\psi_n \triangleq \bar{\theta}_n + \frac{\bar{\theta}_{n+1} - \bar{\theta}_n}{2}$$

or

$$\psi_n \triangleq \frac{\bar{\theta}_n + \bar{\theta}_{n+1}}{2} \tag{51}$$

Because of the relatively small amplitudes of surface buoy displacement, the angle ψ_n was assumed to be constant.

A tangential drag and a normal drag are computed, and the forces so obtained are then resolved back into the x-, y-axis system. Thus, if D_{Tn} and D_{Nn} are the tangential and normal drag forces, then

$$\left.\begin{aligned} Q_{xn} &= - D_{Nn} \sin \psi_n + D_{Tn} \cos \psi_n \\ &\text{and} \\ Q_{yn} &= - D_{Nn} \cos \psi_n - D_{Tn} \sin \psi_n \end{aligned}\right\} \tag{52}$$

The normal drag D_{Nn} is defined as

$$\left.\begin{aligned} D_{Nn} &\triangleq k_{Nn} \left|V_{Nn}\right| V_{Nn} \\ k_{Nn} &= 1/2\, \rho\, C_D\, d \left(\frac{\bar{s}_n + \bar{s}_{n+1}}{2}\right) \end{aligned}\right\} \tag{53}$$

where ρ is the fluid mass density, C_D the dimensionless normal drag coefficient, and d is rope diameter.

Equation (53) is a good approximation if $\theta_{n+1} - \theta_n$ is a small angle and $(\bar{s}_n + \bar{s}_{n+1}) >> s'_n + s'_{n+1}$. Similarly, D_{Tn} is defined as

$$D_{Tn} = \gamma k_{Nn} \left|V_{Tn}\right| V_{Tn} \tag{54}$$

where γ is the ratio of the dimensionless tangential drag coefficient to the dimensionless normal drag coefficient. (A numerical value of .02 was used for γ.)

The tangential and normal velocity components V_{Tn} and V_{Nn} are found by resolving the x and y velocity components of m_n with respect to the surrounding fluid onto the tangential and normal axes. Thus,

$$\left.\begin{aligned} V_{Tn} &= (\dot{y}_n - V_{cn}) \sin \psi_n - \dot{x}_n \cos \psi_n \\ V_{Nn} &= (\dot{y}_n - V_{cn}) \cos \psi_n + \dot{x}_n \sin \psi_n \end{aligned}\right\} \quad (55)$$

where V_{cn} is the current velocity at the depth of Node n.

By the use of incremental substitution, the following nominal and perturbation equations are obtained from Equation (55):

$$\left.\begin{aligned} \overline{V}_{Tn} &= - V_{cn} \sin \psi_n \\ V'_{Tn} &= \dot{y}'_n \sin \psi_n - \dot{x}'_n \cos \psi_n \end{aligned}\right\} \quad (56)$$

$$\left.\begin{aligned} \overline{V}_{Nn} &= - V_{cn} \cos \psi_n \\ V'_{Nn} &= \dot{y}'_n \cos \psi_n + \dot{x}'_n \sin \psi_n \end{aligned}\right\} \quad (57)$$

In addition, Equation (52) can be written

$$\left.\begin{aligned} Q'_{xn} &= - D_{Nn} \sin \psi_n + D_{Tn} \cos \psi_n - \overline{Q}_{xn} \\ Q'_{yn} &= - D_{Nn} \cos \psi_n - D_{Tn} \sin \psi_n - \overline{Q}_{yn} \end{aligned}\right\} \quad (58)$$

Combining Equations (54) through (58) gives

$$\left.\begin{aligned} Q'_{xn} = & -k_{Nn} \left|V_{Nn}\right| V_{Nn} \sin \psi_n + \gamma k_{Nn} \left|V_{Tn}\right| V_{Tn} \cos \psi_n \\ & + k_{Nn} \left|\overline{V}_{Nn}\right| \overline{V}_{Nn} \sin \psi_n - \gamma k_{Nn} \left|\overline{V}_{Tn}\right| \overline{V}_{Tn} \cos \psi_n \\ Q'_{yn} = & -k_{Nn} \left|V_{Nn}\right| V_{Nn} \cos \psi_n - \gamma k_{Nn} \left|V_{Tn}\right| V_{Tn} \sin \psi_n \\ & + k_{Nn} \left|\overline{V}_{Nn}\right| \overline{V}_{Nn} \cos \psi_n + \gamma k_{Nn} \left|\overline{V}_{Tn}\right| \overline{V}_{Tn} \sin \psi_n \end{aligned}\right\} \quad (59)$$

where

$$\left.\begin{aligned} V_{Tn} &= (\dot{y}'_n - V_{cn}) \sin \psi_n - \dot{x}'_n \cos \psi_n \\ &\text{and} \\ V_{Nn} &= (\dot{y}'_n - V_{cn}) \cos \psi_n + \dot{x}'_n \sin \psi_n \end{aligned}\right\} \tag{60}$$

The drag forces Q'_{xn} and Q'_{yn} of Equation (40) were computed from Equations (59) and (60).

To compute the mass matrix of Equation (40) it was assumed that

$$I'_n << \overline{I}_n$$

$$J'_n << \overline{J}_n$$

$$K'_n << \overline{K}_n$$

Under these conditions the terms of the matrix become

$$\overline{I}_n + I'_n \cong \overline{I}_n = m_n + 1/2\, m^v_{n-1/2} \sin^2 \overline{\theta}_n + 1/2\, m^v_{n+1/2} \sin^2 \overline{\theta}_{n+1} \tag{61a}$$

$$\overline{J}_n + J'_n \cong \overline{J}_n = m_n + 1/2\, m^v_{n-1/2} \cos^2 \overline{\theta}_n + 1/2\, m^v_{n+1/2} \cos^2 \overline{\theta}_{n+1} \tag{61b}$$

$$\overline{K}_n + K'_n \cong \overline{K}_n = 1/2\, m^v_{n-1/2} \sin \overline{\theta} \cos \overline{\theta} + 1/2\, m^v_{n+1/2} \sin \overline{\theta}_{n+1} \cos \overline{\theta}_{n+1} \tag{61c}$$

Equations (61) are obtained by neglecting θ'_n in the terms $\sin^2 (\overline{\theta}_n + \theta'_n)$, $\cos^2 (\overline{\theta}_n + \theta'_n)$, and $\sin (\overline{\theta}_n + \theta'_n) \cos (\overline{\theta}_n + \theta'_n)$. To find the resultant error, consider the exact expansion of these terms:

$$\sin^2 (\overline{\theta}_n + \theta'_n) = \sin^2 \overline{\theta}_n \cos^2 \theta'_n \left[1 + 2 \frac{\tan \theta'_n}{\tan \overline{\theta}_n} + \sin^2 \theta'_n \cos^2 \overline{\theta}_n\right] \tag{62}$$

$$\cos^2 (\overline{\theta}_n + \theta'_n) = \cos^2 \overline{\theta}_n \cos^2 \theta'_n \left[1 - 2 \tan \overline{\theta}_n \tan \theta'_n + \tan^2 \theta'_n \tan^2 \overline{\theta}_n\right] \tag{63}$$

$$\begin{aligned} \sin (\overline{\theta}_n + \theta'_n) \cos (\overline{\theta}_n + \theta'_n) = \sin \overline{\theta}_n \cos \overline{\theta}_n \cos^2 \theta'_n \Bigg[1 = \frac{\tan \theta'_n}{\tan \overline{\theta}_n} - \\ \tan \overline{\theta}_n \tan \theta'_n - \tan^2 \theta'_n\Bigg] \end{aligned} \tag{64}$$

For all cases examined, θ_n' was sufficiently small to justify neglecting the last term in the brackets and approximating $\cos^2 \theta_n'$ by unity and $\tan \theta_n'$ by θ_n'. With these approximations, Equations (62), (63), and (64) become

$$\sin^2 (\overline{\theta}_n + \theta_n') \simeq \sin^2 \overline{\theta}_n \left[1 + 2 \frac{\theta_n'}{\tan \overline{\theta}_n}\right] \tag{65}$$

$$\cos^2 (\overline{\theta}_n + \theta_n') \simeq \cos^2 \overline{\theta}_n \left[1 - 2 (\tan \overline{\theta}_n) \theta_n'\right] \tag{66}$$

$$\sin (\overline{\theta}_n + \theta_n') \cos (\overline{\theta}_n + \theta_n') \simeq \sin \overline{\theta}_n \cos \overline{\theta}_n \left[1 + \frac{\theta_n'}{\tan \overline{\theta}_n} - (\tan \overline{\theta}_n) \theta_n'\right] \tag{67}$$

If, in Equation (65), the second term in the bracket is not much less than unity, then $\overline{\theta}_n$ must be a small angle. But if both θ_n' and $\overline{\theta}_n$ are small angles, then $1/2\ m^v_{n-1/2} \sin^2 (\overline{\theta}_n + \theta_n')$ is much less than m_n in Equation (61a) and neglecting θ_n' does not lead to a significant overall percentage error in I_n. In a similar manner it can be shown that neglecting θ_n' in Equation (66) results in no significant overall error in J_n. For the great majority of the cases examined, the last two terms in the bracket of Equation (67) were small compared to unity; but for the most violent excitation conditions (50-ft amplitude and 1,800-ft depth), the neglecting of θ' did lead to appreciable error in the value of K_n at the top of the rope. In only two runs, however, did this error exceed 20 percent. These were Case F (50-ft wave height, 16-sec period) and Case E (25-ft wave height, 32-sec period), which had maximum errors in K_n of 24 percent and 34 percent.

Computer Implementation

To simplify analog computer programing, the tension forces at Node n were expressed as a function of y_n' and x_n' in pairs. From Equation (40) the x and y tension forces on m_n are

$$T_{xn} = \theta_n' \overline{T}_n \sin \overline{\theta}_n - T_n' \cos \overline{\theta}_n - \theta_n' \overline{T}_{n+1} \sin \overline{\theta}_{n+1} + T_{n+1}' \cos \overline{\theta}_{n+1} \tag{68}$$

and

$$T_{yn} = \overline{T}_n \theta_n' \cos \overline{\theta}_n + T_n' \sin \overline{\theta}_n - \overline{T}_{n+1} \theta_{n+1}' \cos \overline{\theta}_{n+1} - T_{n+1}' \sin \overline{\theta}_{n+1} \tag{69}$$

Substitution of the values of T_n' and θ_n' from Equations (49) and (50) into (68) and (69) gives the following equations:

$$T_{xn} = \left[(\overline{T}_n - \mu)\frac{\sin\overline{\theta}_n \cos\overline{\theta}_n}{\overline{s}_n}\right](y_{n-1} - y_n) - \left[(\overline{T}_{n+1} - \mu)\frac{\sin\overline{\theta}_{n+1}\cos\overline{\theta}_{n+1}}{\overline{s}_{n+1}}\right]$$

$$(y_n - y_{n+1}) - \left[\frac{\overline{T}_n \sin^2\overline{\theta}_n + \mu\cos^2\overline{\theta}_n}{\overline{s}_n}\right](x_n - x_{n-1}) +$$

$$\left[\frac{\overline{T}_{n+1}\sin^2\overline{\theta}_{n+1} + \mu\cos^2\overline{\theta}_{n+1}}{\overline{s}_{n+1}}\right](x_{n+1} - x_n) \tag{70}$$

$$T_{yn} = \left[\frac{\overline{T}_n \cos^2\overline{\theta}_n + \mu\sin^2\overline{\theta}_n}{\overline{s}_n}\right](y_{n-1} - y_n) - \left[\frac{\overline{T}_{n+1}\cos^2\overline{\theta}_{n+1} + \mu\sin^2\overline{\theta}_{n+1}}{\overline{s}_{n+1}}\right]$$

$$(y_n - y_{n+1}) - \left[\frac{\left(\overline{T}_n - \mu\right)\sin\overline{\theta}_n\cos\overline{\theta}_n}{\overline{s}_n}\right](x_n - x_{n-1}) +$$

$$\left[\frac{\left(\overline{T}_{n+1} - \mu\right)\sin\overline{\theta}_{n+1}\cos\overline{\theta}_{n+1}}{\overline{s}_{n+1}}\right](x_{n+1} - x_n) \tag{71}$$

And now the following "tension coefficients" are defined:

$$\left.\begin{aligned} a_n &= \frac{\overline{T}_n\cos^2\overline{\theta}_n + \mu\sin^2\overline{\theta}_n}{\overline{s}_n} \\ b_n &= \frac{\left(\overline{T}_n - \mu\right)\sin\overline{\theta}_n\cos\overline{\theta}_n}{\overline{s}_n} \\ c_n &= \frac{\overline{T}_n\sin^2\overline{\theta}_n + \mu\cos^2\overline{\theta}_n}{\overline{s}_n} \end{aligned}\right\} \tag{72}$$

For each given rope configuration, these coefficients are constants. In terms of the tension coefficients, Equations (70) and (71) become

$$T_{xn} = b_n(y_{n-1} - y_n) - b_{n+1}(y_n - y_{n+1}) - c_n(x_n - x_{n-1}) + c_{n+1}(x_{n+1} - x_n) \tag{73}$$

$$T_{yn} = a_n(y_{n-1} - y_n) - a_{n+1}(y_n - y_{n+1}) - b_n(x_n - x_{n-1}) + b_{n+1}(x_{n+1} - x_n) \tag{74}$$

Equations (73) and (74) were used to obtain the tension forces on the analog computer.

A computer diagram showing the implementation of the n^{th} nodal equations is given in Figure 29.

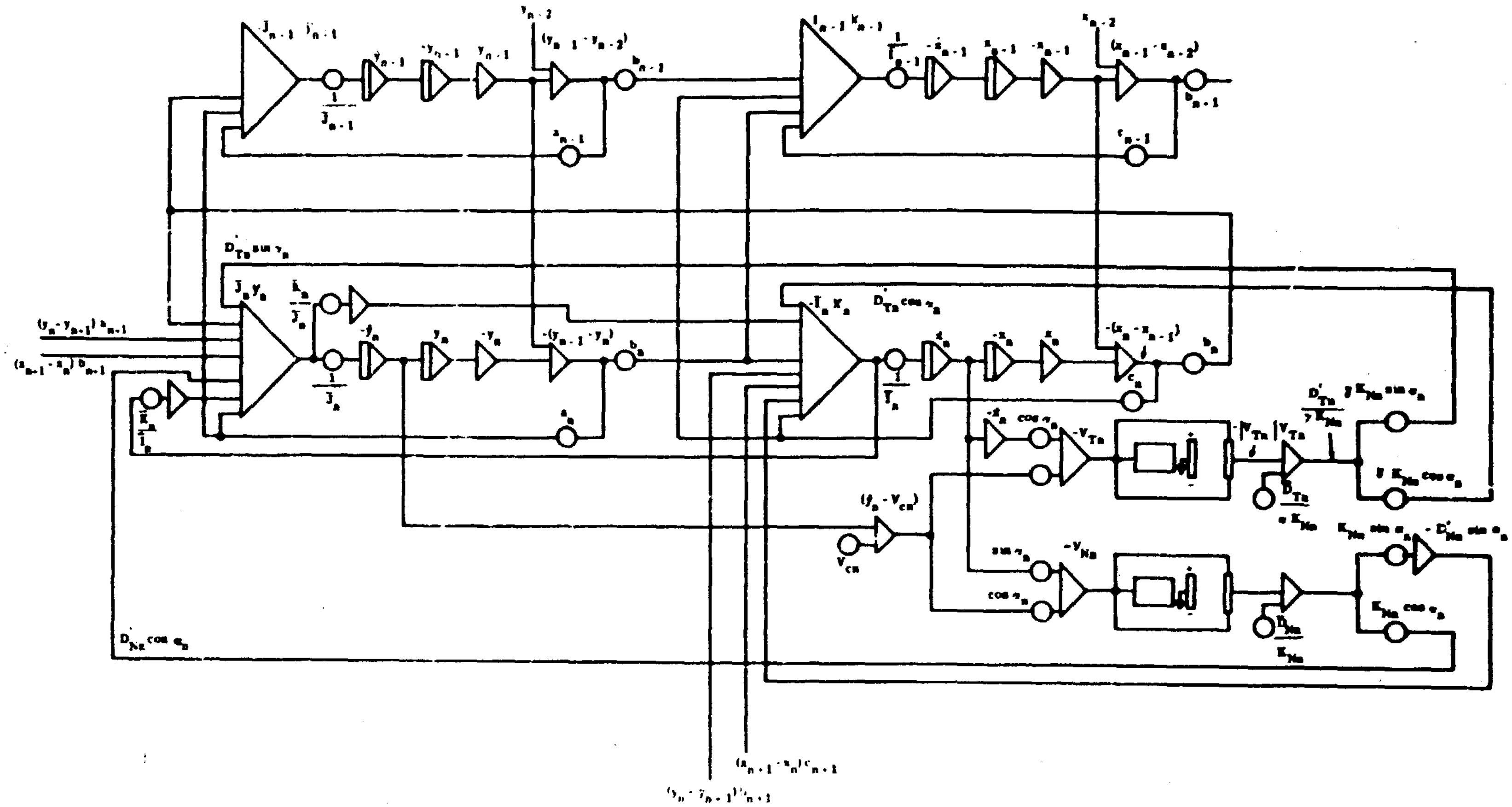

Figure 29 Analog Computer Circuit Diagram Showing Implementation of Perturbation Equations for n^{th} Node

LITERATURE CITED

(1) Wilson, B. W., Characteristics of Anchor Cables in Uniform Ocean Currents, The A. and M. College of Texas Department of Oceanography and Meterology Technical Report No. 204-1 (Apr 1960) 149 pp.

(2) Wilson, B. W., Characteristics of Deep-Sea Anchor Cables in Strong Ocean Currents, The A. and M. College of Texas Technical Reports Nos. 204-3 and 204-3A (2 vols.), (Feb 1961 and Mar 1961, respectively) 89 and 266 pp. (Note: 204-3 is ASTIA AD-259379)

(3) Whicker, L. F., Theoretical Analysis of the Effect of Ship Motion on Mooring Cables in Deep Water, U.S. Navy David Taylor Model Basin Report 1221, (Mar 1958) 24 pp.

(4) Walton, T.S. and H. Polachek, Calculation of Non-Linear Transient Motions of Cables, U.S. Navy David Taylor Model Basin Report No. 1279 (Jul 1959), 50 pp. (DDC No. AD418603)

(5) Walton, T.S. and H. Polachek, Calculation of Transient Motion of Submerged Cables, Mathematical Tables and Aids to Computation 14, 27-46 (1960)

(6) Polachek, H., T.S. Walton, R. Mejia, and C. Dawson, Transient Motion of an Elastic Cable Immersed in a Fluid, Mathematics of Computation, Jan 1963, pp. 60-63

(7) Walton, T.S., Personal communication to R.P. Brumbach, (Sept 1965)

(8) Johnson, H. and F. Lampietti, in "Experimental Drilling in Deep Water at La Jolla and Guadalupe Sites" AMSOC Committee Report, National Academy of Sciences – National Research Council Pub. No. 914 (1961), p. 58

(9) Rather, R.L., Vil Goerland, J.B. Hersey, A.C. Vine, and F. Dakin, 1965, Improved towline design for oceanography, Undersea Technology 6 (5), 57-63(1965)

(10) Hakkarinen, W., The World of NOMAD-1, Buoy Technology, Marine Technology Society, Trans. 1964 Buoy Technology Symposium 24-25 Mar 1965, Washington, D.C., 1, 443-456

(11) Roberts, E.B., Roberts Radio Current Meter Mod II Operating Manual, U.S. Dept. Commerce, Coast and Geodetic Survey, Washington, D.C., 1952, 33 pp. (The NOMAD hull is almost identical to a scaled-up Roberts Current Meter Buoy)

LITERATURE CITED (Cont.)

(12) Geodyne Corporation, Waltham, Mass., Bull. No. S-32 7/24/63 and DWG A-92 of 3/7/63 describing Model A-92 Instrument Buoy

(13) Isaacs, J.D., J.L. Faughn, G.B. Schick, and M.C. Sargent, Deep-Sea Mooring, Bull. Scripps Inst. Oceanography 8 (3), 271-312 (1963)

(14) Vinogradov, V.V., Russian Naval Hydrographic Service Foam Buoy, Okeanologiya 2 (2), 346-352 (1962), transl. in Deep-Sea Research 11 (1) 137-141 (1964)

(15) Devereux, R., et al., Development of a Telemetering Oceanographic Buoy, General Dynamics/Convair Progress Report GDC-63-060 under Contract Nonr-3062(00) (Feb 1963)

(16) Uyeda, S.T., Buoy Configuration Resulting From Model Tests and Computer Study, Buoy Technology, Transactions of the 1964 Buoy Technology Symposium, Washington, D.C., 24-25 Mar 1964, Supplement pp. 31-42 (1964)

(17) Saunders, H.E., Hydrodynamics in Ship Design, New York, Society of Naval Architects and Marine Engineers, 2 vols. (1957), vol 2, p. 291 and pp. 418-423

(18) United States Steel Corporation, Columbia-Geneva Steel Division, Wire Rope Handbook, San Francisco, Calif. (1959) 194 pp.

(19) Gaul, R.D., Influence of Vertical Motion on the Savonius Rotor Current Meter, Agricultural and Mechanical College of Texas, Department of Oceanography and Meteorology, Tech. Rept. Ref. No. 63-4T, 1 Feb 1963, 29 pp.

(20) Paquette, R.G., Practical Problems in the Direct Measurement of Ocean Currents, Marine Sciences Instrumentation (Proceedings of the Symposium on Transducers for Oceanic Research, San Diego, California, 8–9 November 1962) New York, Plenum Press (1963), 195 pp., pp. 135–146

Unclassified
Security Classification

DOCUMENT CONTROL DATA - R&D

(Security classification of title, body of abstract and indexing annotation must be entered when the overall report is classified)

1 ORIGINATING ACTIVITY (Corporate author) GM Defense Research Laboratories General Motors Corporation	2a REPORT SECURITY CLASSIFICATION Unclassified 2b GROUP

3 REPORT TITLE

The Dynamics of Simple Deep-Sea Buoy Moorings

4 DESCRIPTIVE NOTES (Type of report and inclusive dates)

Final Report May 1964 — November 1965

5 AUTHOR(S) (Last name, first name, initial)

Paquette, Robert G.

Henderson, Bion E.

6. REPORT DATE	7a TOTAL NO. OF PAGES	7b NO OF REFS
November 1965	190	20

8a. CONTRACT OR GRANT NO. Nonr-4558(00) b. PROJECT NO. NR 083-196 c. d.	9a. ORIGINATOR'S REPORT NUMBER(S) TR65-79 9b. OTHER REPORT NO(S) (Any other numbers that may be assigned this report)

10 AVAILABILITY/LIMITATION NOTICES

11 SUPPLEMENTARY NOTES	12. SPONSORING MILITARY ACTIVITY
	U.S. Navy Office of Naval Research

13. ABSTRACT

The dynamics of buoy mooring ropes under conditions typical of the open sea were simulated in an analog computer. Motions sufficient to cause significant errors in current meters were found in the ropes. Dynamic tensions rising to dangerous values were found in short, taut steel ropes. Lesser tensions were found in nylon ropes. Rope shapes in ocean currents varying with depth also were obtained incidental to the principal study.

DD FORM 1 JAN 64 1473 0101-807-5800

Security Classification

Security Classification

14 KEY WORDS	LINK A		LINK B		LINK C	
	ROLE	WT	ROLE	WT	ROLE	WT
Buoys						
Buoy Dynamics						
Buoy Moorings						
Anchoring						
Mooring Dynamics						
Ocean Currents						
Oceanography						
Computers, Analog						

INSTRUCTIONS

1. ORIGINATING ACTIVITY: Enter the name and address of the contractor, subcontractor, grantee, Department of Defense activity or other organization *(corporate author)* issuing the report.

2a. REPORT SECURITY CLASSIFICATION: Enter the overall security classification of the report. Indicate whether "Restricted Data" is included. Marking is to be in accordance with appropriate security regulations.

2b. GROUP: Automatic downgrading is specified in DoD Directive 5200.10 and Armed Forces Industrial Manual. Enter the group number. Also, when applicable, show that optional markings have been used for Group 3 and Group 4 as authorized.

3. REPORT TITLE: Enter the complete report title in all capital letters. Titles in all cases should be unclassified. If a meaningful title cannot be selected without classification, show title classification in all capitals in parenthesis immediately following the title.

4. DESCRIPTIVE NOTES: If appropriate, enter the type of report, e.g., interim, progress, summary, annual, or final. Give the inclusive dates when a specific reporting period is covered.

5. AUTHOR(S): Enter the name(s) of author(s) as shown on or in the report. Enter last name, first name, middle initial. If military, show rank and branch of service. The name of the principal author is an absolute minimum requirement.

6. REPORT DATE: Enter the date of the report as day, month, year; or month, year. If more than one date appears on the report, use date of publication.

7a. TOTAL NUMBER OF PAGES: The total page count should follow normal pagination procedures, i.e., enter the number of pages containing information.

7b. NUMBER OF REFERENCES: Enter the total number of references cited in the report.

8a. CONTRACT OR GRANT NUMBER: If appropriate, enter the applicable number of the contract or grant under which the report was written.

8b, 8c, & 8d. PROJECT NUMBER: Enter the appropriate military department identification, such as project number, subproject number, system numbers, task number, etc.

9a. ORIGINATOR'S REPORT NUMBER(S): Enter the official report number by which the document will be identified and controlled by the originating activity. This number must be unique to this report.

9b. OTHER REPORT NUMBER(S): If the report has been assigned any other report numbers *(either by the originator or by the sponsor)*, also enter this number(s).

10. AVAILABILITY/LIMITATION NOTICES: Enter any limitations on further dissemination of the report, other than those imposed by security classification, using standard statements such as:

(1) "Qualified requesters may obtain copies of this report from DDC."

(2) "Foreign announcement and dissemination of this report by DDC is not authorized."

(3) "U. S. Government agencies may obtain copies of this report directly from DDC. Other qualified DDC users shall request through ________."

(4) "U. S. military agencies may obtain copies of this report directly from DDC. Other qualified users shall request through ________."

(5) "All distribution of this report is controlled. Qualified DDC users shall request through ________."

If the report has been furnished to the Office of Technical Services, Department of Commerce, for sale to the public, indicate this fact and enter the price, if known.

11. SUPPLEMENTARY NOTES: Use for additional explanatory notes.

12. SPONSORING MILITARY ACTIVITY: Enter the name of the departmental project office or laboratory sponsoring *(paying for)* the research and development. Include address.

13. ABSTRACT: Enter an abstract giving a brief and factual summary of the document indicative of the report, even though it may also appear elsewhere in the body of the technical report. If additional space is required, a continuation sheet shall be attached.

It is highly desirable that the abstract of classified reports be unclassified. Each paragraph of the abstract shall end with an indication of the military security classification of the information in the paragraph, represented as *(TS)*, *(S)*, *(C)*, or *(U)*.

There is no limitation on the length of the abstract. However, the suggested length is from 150 to 225 words.

14. KEY WORDS: Key words are technically meaningful terms or short phrases that characterize a report and may be used as index entries for cataloging the report. Key words must be selected so that no security classification is required. Identifiers, such as equipment model designation, trade name, military project code name, geographic location, may be used as key words but will be followed by an indication of technical context. The assignment of links, roles, and weights is optional.

Security Classification